Proprioceptive hair cells on the neck of the squid *Lolliguncula brevis*: a sense organ in cephalopods for the control of head-to-body position

T. PREUSS[1,3] AND B. U. BUDELMANN[1,2]

[1]*Marine Biomedical Institute, and* [2]*Department of Otolaryngology, University of Texas Medical Branch, Galveston, Texas 77555–1163, U.S.A.*
[3]*Universität Tübingen, Lehrstuhl für Biokybernetik, Auf der Morgenstelle 28, D-72076 Tübingen, Germany*

CONTENTS

SUMMARY

Decapod cephalopods, such as cuttlefishes and squids, have a distinct neck region that allows movements (roll, pitch and yaw) of the head relative to the body. This paper describes the structure, innervation and central pathways of proprioceptive hair cells on the neck of the squid *Lolliguncula brevis* that sense such movements and control head-to-body position.

These hair cells exist on the dorsal side of the neck underneath the nuchal cartilage, close to the animal's midline on either side of the nuchal crest. On each side, the hair cells can be divided into an anterior and a posterior group of 25–35 and 70–80 cells, respectively. An individual hair cell carries up to 300 kinocilia of equal length (about 30 μm), arranged in up to seven rows. The hair cells of the left and right anterior group are morphologically polarized in the medial direction, whereas the hair cells of the left and right posterior group are polarized in the anterior direction. The hair cells are primary sensory cells. They are innervated by a branch of the postorbital nerve and project ipsilaterally into the ventral part of the ventral magnocellular lobe. Efferent synaptic contacts are present at the base of the hair cells.

In behavioural tests the influence of the neck hair cells on head position control was investigated. During imposed body rolls, a unilateral deafferentation of the cells caused an asymmetric change of the compensatory head roll response and elicited a head roll offset to the operated side. Bilateral deafferentation of the cells elicited a downward head pitch offset. This offset was superimposed on the compensatory head pitch response during imposed body pitch.

Phil. Trans. R. Soc. Lond. B (1995) **349**, 153–178
Printed in Great Britain

These morphological and behavioural findings show that the neck hair cells and the associated nuchal cartilage structures of *Lolliguncula brevis* form a neck receptor organ that, together with statocyst and visual inputs, controls the position of the animal's head and body.

1. INTRODUCTION

Decapod cephalopods, such as cuttlefishes and squids, are fast moving, visually oriented predators. They are able to move along and around all three body axes. Such manoeuvrability is made possible by a mobile funnel, through which water jets are expelled during jet propulsion, and by the movement of fins.

In most decapod cephalopods the head is separated from the body by a distinct neck region. This allows the head to be moved (roll, pitch and yaw) relative to the body. Any head movement shifts the sense organs (eyes, statocysts, 'lateral lines', chemoreceptors) of the head and, unique to cephalopods, the arms and tentacles which are attached to the head (for a review on sense organs, see Budelmann (1994)). Clearly, head movements can be used to shift gaze, e.g. during fixation and tracking of prey (Messenger 1968, 1977; Foyle & O'Dor 1988). Head movements are also part of positional reflexes that serve to stabilize the visual image on the retina during body turns and in different body positions (see figure 4 and Budelmann (1975)).

For the control of head and body position with respect to visual cues and gravity, cephalopods have sophisticated visual and equilibrium receptor systems (Young 1960, 1989; Dijkgraaf 1961, 1963; Budelmann 1970, 1975, 1990; Collewijn 1970; Messenger 1970, 1981; Stephens & Young 1982; Budelmann & Young 1984; Budelmann *et al.* 1987). In animals with moveable heads, however, visual and equilibrium information *per se* is not sufficient for a proper control of body posture and movement because the sense organs that monitor the orientation in space (equilibrium receptor systems and eyes) are situated in the head, whereas the motor systems responsible for locomotion and a correct upright posture are situated in the body. Therefore, for proper head and body movements, additional proprioceptive information is necessary that takes into account the position of the head relative to the body (Mittelstaedt 1964; Mergner *et al.* 1983*a*,*b*, 1992; Mittelstaedt & Mittelstaedt 1991). Such proprioceptive information is also essential for an active realignment of the head and body.

In vertebrates, proprioceptive information about head-to-trunk (head-to-body) position is provided by internal joint receptors and muscle spindle organs in the upper neck (McCouch *et al.* 1951; Biemond & De Jong 1969; for reviews, see De Jong & Bles 1986; Taylor 1992). They are involved in neck reflexes, such as the cervico-collic reflex in humans, cats and birds (Mittelstaedt 1964; Roberts 1973; Peterson *et al.* 1981; Bilo & Bilo 1983; Mergner *et al.* 1983*a*,*b*; Taylor & McCloskey 1988; Bilo 1991; Hlavacka *et al.* 1992).

In insects, various types of external and internal proprioceptive neck organs have been described. They consist of cuticular hair sensilla and chordotonal organs (Peters 1962; Thurm 1963; for reviews see Hoffmann 1963, 1964). Behavioural studies in dragonflies, locusts and flies have shown their influence on head position, head–body coordination and flight steering (Mittelstaedt 1950; Haskell 1959; Goodman 1965; Land 1973; Geiger & Poggio 1977; Liske 1977; Horn & Lang 1978; Hengstenberg 1988; Hensler & Robert 1990; Miall 1990; Preuss & Hengstenberg 1990, 1992).

Because most decapod cephalopods are able to move their head relative to the body, it is reasonable to assume that they have some kind of proprioceptor that monitors head-to-body position. However, so far no such receptors have been described, except in a preliminary note (Preuss & Budelmann 1991). The aims of the present study were: (1) to identify possible neck proprioceptors in squid; (2) to describe their structure, innervation and central pathways; and (3) to study their influence on head-to-body position.

2. MATERIALS AND METHODS

(*a*) *Experimental animals*

The common bay squid *Lolliguncula brevis* was used for this study. The animals were caught in the Gulf of Mexico and transported in shipboard seawater containers to the laboratory, where they were maintained in circular tanks (2 m diameter, 80 cm high) in a closed system of recirculating seawater (for details, see Yang *et al.* 1989); 21 animals (males and females; size range between 10 and 60 mm mantle length) were used for the anatomical studies and 39 animals for the behavioural studies (mostly females; size range between 50 and 70 mm mantle length). In some behavioural experiments, the animals were kept individually in smaller tanks (1 m diameter, 50 cm high) for up to two weeks.

(*b*) *Anatomical studies*

The anatomy of the dorsal neck region was examined by light microscopy (LM), scanning electron microscopy (SEM) and transmission electron microscopy (TEM). The animals were killed by an overdose of anaesthesia (magnesium chloride, $MgCl_2 \cdot 6H_2O$ solution (75 g l^{-1}), mixed 1:1 with seawater (Messenger *et al.* 1985)). Isolated head–neck preparations were obtained by cutting through the mantle about 1/3 posterior to the anterior mantle edge. The posterior part of the mantle and the arms were then removed, leaving the head and neck region of the animal intact.

For LM and TEM, six animals (10–30 mm mantle length) were used. The isolated head–neck preparations were fixed in OsO_4 (20 g l^{-1}) (Zetterquist buffer, pH 7.4) for 1 h at 4 °C, dehydrated in graded ethanol solutions and embedded in Epon. For LM, serial sections (3–5 μm) were cut with a glass knife on a LKB 8800 Ultrotome III microtome, stained with toluidine blue and analysed and photographed with a Leitz Othoplan

transmission bright-field photomicroscope or with a Zeiss Axiovert 35 phase-contrast photomicroscope. Ultrathin sections (70–80 nm) were cut with a diamond knife on a LKB 8800 Ultrotome III microtome and viewed with a JEOL 100 CX transmission electron microscope.

For SEM, six animals (10–50 mm mantle length) were used. The isolated head–neck preparations were pinned with fine, insulated insect needles in a Petri dish and fixed in OsO_4 (20 g l^{-1}) (Zetterquist buffer, pH 7.4) for 1 h at 4 °C, or in glutaraldehyde (40 g l^{-1}) (isotonic phosphate buffer, pH 7.3) for 2 h at 4 °C. After fixation, the tissue was dehydrated in graded ethanol solutions, critical-point dried in a Balzers CPD 020 unit, gold–palladium coated with a Hummer II sputter unit (Technics, Alexandria, Virginia, U.S.A.) and viewed with a Topcon DS-130-Dual Stage scanning electron microscope (Pleasanton, California, U.S.A.).

(*c*) *Centrifugal cobalt staining of the postorbital nerve*

Four animals were used for this study. The head–neck preparations were mounted ventral side up in a dish and kept under seawater. The operations were done with the aid of a Wild M5 stereomicroscope and fibre optics illumination. After opening the brain capsule ventrally, all brain tissue was removed close to the point where the postorbital nerve (Young 1976) passes through the orbital cartilage. The left or right postorbital nerve was then carefully dissected from its surrounding tissue and cut close to the cartilage with fine Vannas scissors. The cut end of the nerve was then treated for 1–2 min with distilled water to osmotically open the nerve fibres that were possibly sealed by the cut. Thereafter, the nerve was introduced into the tip of a polyethylene suction electrode of matching size, filled with 1 M $CoCl_2$ solution. Care was taken not to damage the nerve. To prevent leakage of $CoCl_2$ into the surrounding tissue or water, the tip of the electrode was pushed slightly into the opening of the cartilage canal. Co^{2+} ions were injected iontophoretically into the nerve fibres by passing positive current pulses (6 Hz, 100 ms duration, 8 μA) for 15–20 h at a temperature of 4–5 °C.

After iontophoretic injection of the Co^{2+} ions, the tissue was washed with seawater and treated for 2–3 min with a saturated solution of ammonium sulphide in seawater to precipitate the Co^{2+} ions as black cobalt sulphide. After washing with seawater for about 5 min, the tissue was fixed in a formaldehyde–seawater solution (40 g l^{-1}) for one day, dehydrated in graded ethanol and cleared in cedar wood oil. Inspection of the neck region for cobalt-filled cells and the course of stained fibres was done in whole-mount preparations with a Wild M 400 or a Zeiss photomicroscope.

(*d*) *Centripetal cobalt staining of the postorbital nerve*

Five animals were used for this study. The head–neck preparations were mounted dorsal side up in a seawater-filled dish. The branch of the postorbital nerve that innervates the neck hair cells was carefully dissected from its surrounding muscle and connective tissue at the point where it runs close to the surface of the skin of the dorsal side of the neck. After cutting the nerve with fine Vannas scissors, its peripheral end was treated with distilled water and then introduced into the tip of a polyethylene suction electrode. Co^{2+} injection and precipitation was as described above. The brain capsule remained unopened during this procedure. After Co^{2+} injection, the head–neck preparation was fixed in a formaldehyde–seawater solution (40 g l^{-1}) for two days. Thereafter the eyeballs were removed and the remaining tissue dehydrated in graded ethanol solutions and infiltrated with paraffin (2 × 1 h) under vacuum (15 mmHg) in a Fisher histomatic tissue processor. Sagittal or transverse serial sections (30–40 μm) of the brain were cut with a rotary microtome, the sections mounted on gelatin-coated slides and exposed to formalin vapour while drying in an oven at 30 °C for 3–4 h. The paraffin was then removed with xylene and the sections were rehydrated and double-intensified with the use of a modified Timm's sulphide silver method (Budelmann & Young 1984, 1985). After counterstaining with cresyl violet, the sections were dehydrated in graded ethanol solutions and coverslipped with Permount. Sections were viewed with a Leitz transmission bright-field or a Zeiss Axiovert 35 phase-contrast photomicroscope.

(*e*) *Nerve operations in living squid*

Because of the transparency of the squid's body tissue, the branch of the postorbital nerve that innervates the epidermal neck hair cells is, with proper illumination, visible in a living animal. Thus, a selective cut of that nerve branch can easily be performed with fine Vannas scissors. All operations were done in animals anaesthetized for 8–10 min in $MgCl_2 \cdot 6H_2O$ (75 g l^{-1}) mixed 1 : 2 with seawater. During the operation, a stereomicroscope was used and care was taken to avoid damage of the muscles and the surrounding tissue. Unilateral and bilateral nerve cuts were performed. To avoid a side-dependent effect, the unilateral cuts were made alternately on the left and right side in successive experiments. After completion of the operations, the gills of the animals were rinsed with seawater to accelerate the recovery (5–10 min) from anaesthesia. Behavioural tests were begun at least 90 min after the operation to avoid possible long-term effects of the anaesthesia. As a control, sham operations were done in three animals. The skin incision was in the same area and to the same depth as for a nerve cut, but the nerve was left intact.

(*f*) *Statocyst operations in living squid*

To eliminate the sensory input of the equilibrium receptor organs (statocysts), animals were anaesthetized for 15 min with $MgCl_2 \cdot 6H_2O$ (75 g l^{-1}) mixed 1:2 with seawater and then carefully positioned (ventral side up) in a seawater-filled dish with a black wax bottom. Illumination of the head capsule was from below through a small window cut into the wax. The funnel of the animal was bent caudally to allow an unrestricted view onto the statocyst cavities inside the head. Under stereomicroscopical control, the skin and muscle tissue were cut down to the ventral floor of the cranium. While small hooks were used to keep the tissue apart, a small window was cut into the statocyst cavity; this permitted the introduction of the tip of a seawater-filled syringe into the statocyst cavity. The statoliths and statoconial layers were then washed from their sensory epithelia with a gentle jet of seawater. At the end of the experiments, the animals were killed and the statocysts dissected to ensure the success of the operation.

(*g*) *Test apparatus*

A test apparatus was designed to measure head position (HP) and body position (BP) of an animal during imposed rotations around its roll (longitudinal) and pitch (transverse) body axes. The apparatus included an animal holder and a rotation device inside a glass aquarium. The animal holder allowed one to keep an animal in a fixed position relative to the holder, but permitted unrestricted movements of the head and fins (figure 1). To attach the animal to the holder, two small hooks grasped underneath the dorsal anterior edge of the mantle on the left and right side of the animal. The hooks were fixed to the ends of moderately stiff springs to provide some flexibility of the hooks, while prohibiting movements of the animal in anterior direction. Support of the posterior two thirds of the mantle was given by a trough-shaped supporting device. The size and shape of that device could be adjusted to the anatomical contour of the animal's body to provide sufficient lateral support. All parts of the holder were wrapped with layers of Teflon tape, or covered with plasticine, to avoid damage to the delicate skin. Prior to being placed in the holder, the animal was slightly anaesthetized (7.5% $MgCl_2 \cdot 6H_2O$ mixed 1:2 with seawater; induction time 5 min). To allow it to recover from the anaesthesia and to adapt to the holder, the animal was placed into a holding tank for at least 90 min during which it was allowed to swim freely while attached to the holder. To compensate for the weight of the holder, a styrofoam float was attached to it to make it neutrally buoyant.

To impose rotations, the holder was attached to a turning device that allowed full rotations of the animal around its roll and pitch axes. The position of the animal was adjusted such that the axis of rotation was through the animal's mid-longitudinal axis for imposed roll, and through a transverse axis at the level of the anterior end of the dorsal mantle tip for imposed pitch. The angular position of the animal holder with respect to an external reference was measured with a 360° scale attached to the turning device. The whole set-up (turning device with holder and animal) was placed in a glass aquarium (30 × 30 × 80 cm) that was connected to a system of recirculating seawater.

To exclude visual cues, the animal was surrounded by an opaque cylinder (23 cm diameter) that was equally illuminated from the outside by 4 units of fluorescent light; each unit consisted of 4 Philips 40 W tubes, covered with a screen of milky Perspex. The light units were positioned at the top, the bottom and on either side of the aquarium. During most of the experiments, the illumination inside the cylinder was about 2800 Lux. Both ends of the cylinder were covered with black shields; one had a circular hole for the lens of a video camera. Thus, all inevitable contours formed concentric rings around the animal and, therefore, excluded visual positional cues.

(*h*) *Recording and data analysis*

Depending upon the axis of rotation, either a frontal view (during roll) or a lateral view (during pitch) of the animal's head and body was recorded with a video CCD camera (Sony Handycam Hi8). A digital time code (1 s resolution) and a horizontal reference line were included in the video picture. Before each experiment, the 360° scale of the turning device and the position of the animal were calibrated with respect to the horizontal reference line.

For analysis, a video recorder (Sony EV-S900 NTSC) in combination with a video printer (Panasonic AG-EP60) was used that allowed bidirectional single frame transport and a display of digitalized still-video pictures. These were partly enlarged and displayed on a monitor for measurements of head and body positions. Initially, a pivoted Plexiglas disc with fine parallel lines was superimposed on the video picture and the relevant head and body angles were measured (1° accuracy) relative to the horizontal reference line. Later, a single frame analysis was done with a computer supported video analysis system, consisting of a Macintosh Quadra 900 computer, a video capture card and a public domain software program (NIH-Image 1.47). This system allowed measurements of the angular position of the head and body on the computer monitor relative to an 'internal' reference.

The same computer system was used for a morphometric analysis of the enlarged surface outlines of the head–neck region after the micrographs in question were digitalized with a high resolution scanner (Hewlett Packard Scanjet IIc).

(*i*) *Behavioural tests*

The animals were rotated in steps around different body axes. For imposed roll, animals (N = 7) were alternately rotated around their mid-longitudinal axis to the left (−65°) and right (+65°) in five steps. For imposed pitch, animals ($N = 4$) were rotated around a transverse body axis downward (−39°; anterior down) or upward (+39°; anterior up) in three steps. All rotations to any of the imposed positions (roll and

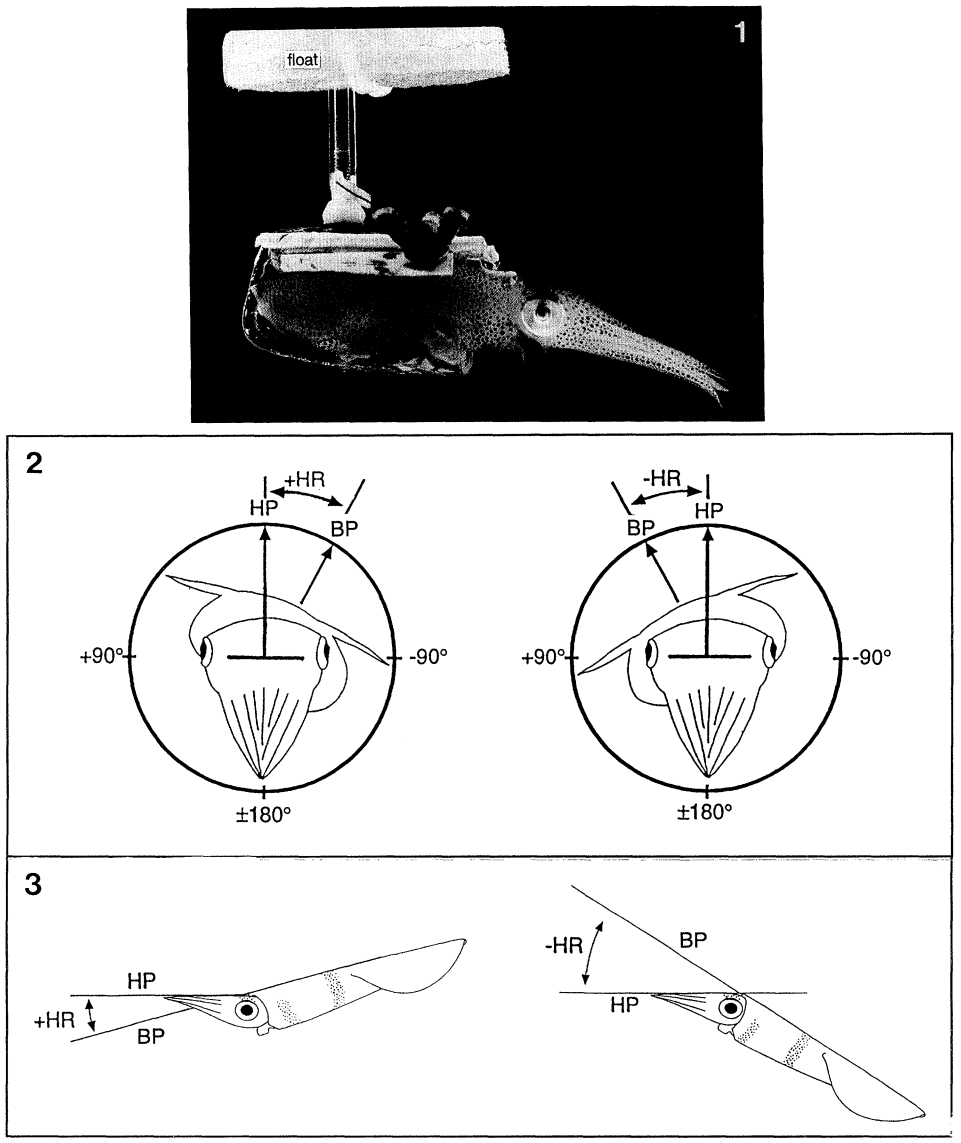

Figure 1. The squid *Lolliguncula brevis* attached to the animal-holder that keeps the animal's body in a fixed position but allows unrestricted movements of the animal's head. During the experiments the holder is connected to a rotation device; in the figure it is made neutrally buoyant by a float to allow the animal to swim 'freely'.

Figures 2 and 3. Illustrations of the head response ($\pm$HR) and the positions of the animal's head (HP) and body (BP) during body roll (figure 2) and body pitch (figure 3). The head response (HR = HP − BP) for roll (figure 2) is the angle between the head and body mid-sagittal planes, and for pitch (figure 3) the angle between the head and body horizontal planes.

pitch) started from a horizontal body position ($_{\text{roll/pitch}}$BP = 0°). In each imposed position, the animals were kept for 20 s and then rotated back to the 0°-body-position for a 20 s intermission.

(*j*) *Measurements of head and body positions*

On the video picture, the head roll position ($_{\text{roll}}$HP) of an animal is indicated by a line at right angles to the connecting line between the centres of the left and right eye when seen from the anterior (figure 2). The body roll position ($_{\text{roll}}$BP) is identical to the roll position of the holder to which the animal is attached. The body roll position is indicated by a reference line on the animal holder that is at right angles to the mid-sagittal plane of the body (figure 2). The head and body roll positions are defined as the angular deviations (of those lines) of the head and body from the vertical. Consequently, $_{\text{roll}}$HP = 0° and $_{\text{roll}}$BP = 0° indicate the position of the head and body during normal orientation. Head and body roll positions to the right of the animal are given as positive $_{\text{roll}}$HP and $_{\text{roll}}$BP values, and head and body roll positions to the left as negative values.

The head pitch position ($_{\text{pitch}}$HP) is indicated by a tangential line to the dorsal crown of the head (figure 3). The body pitch position ($_{\text{pitch}}$BP) is identical to the pitch position of the holder; it is also indicated by a reference line on the holder that is parallel to a longitudinal body axis. The head and body pitch positions are defined as the angular deviations (of those lines) of the head and body from the direction of the absolute horizontal. Head and body downward pitch positions are given as negative $_{\text{pitch}}$HP and $_{\text{pitch}}$BP

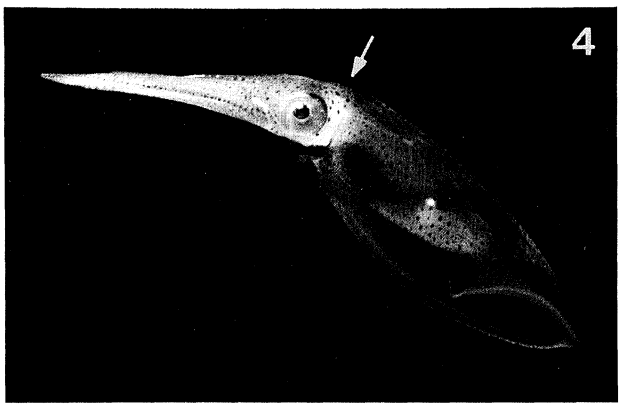

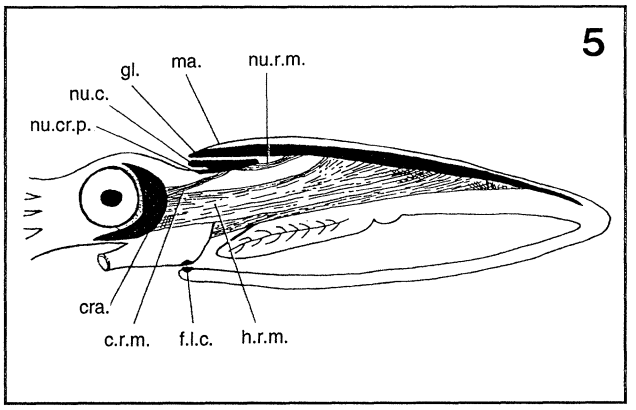

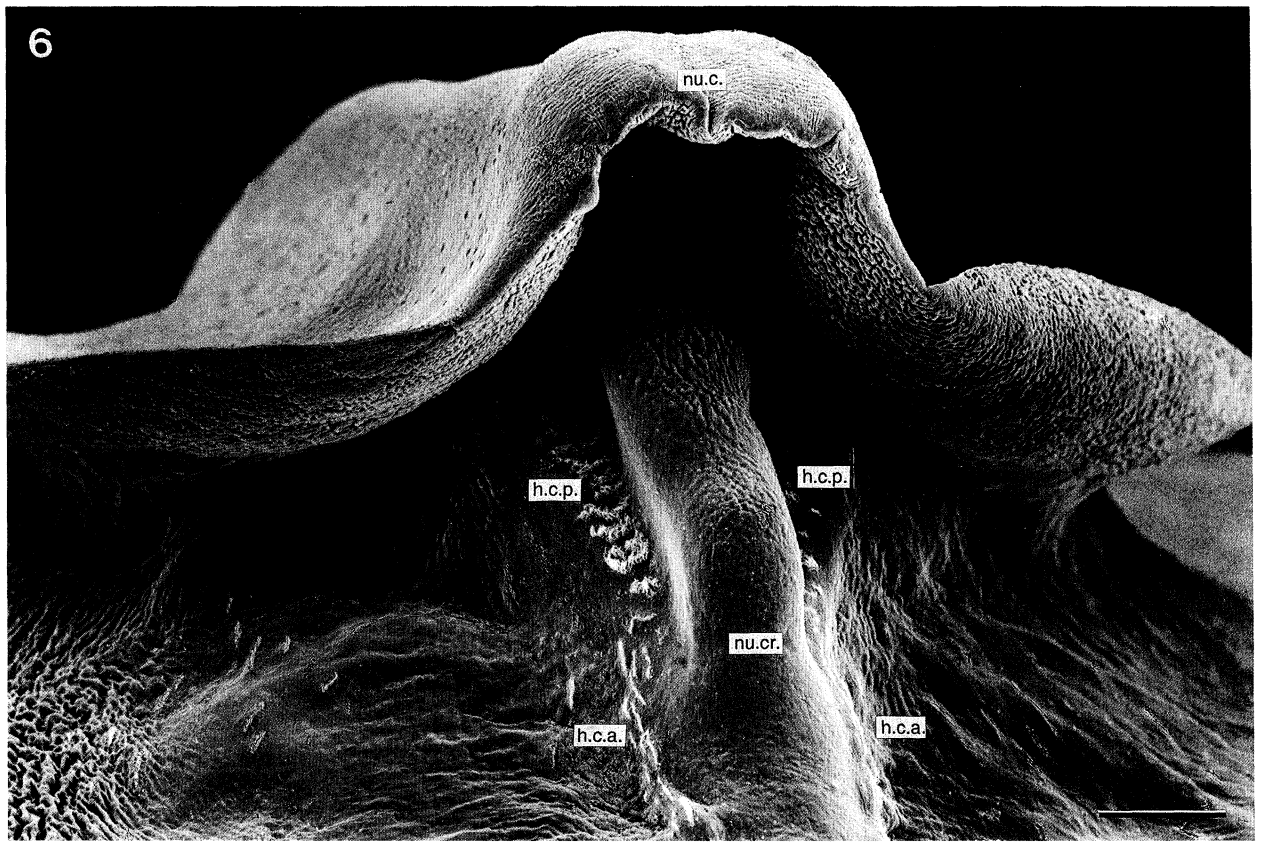

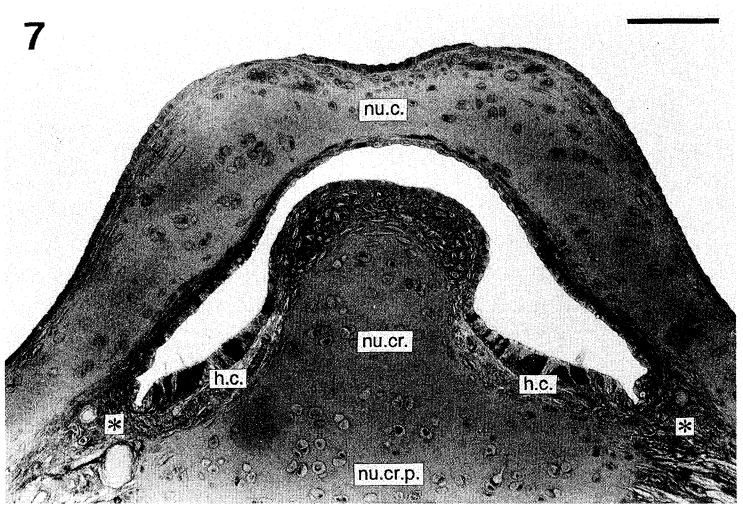

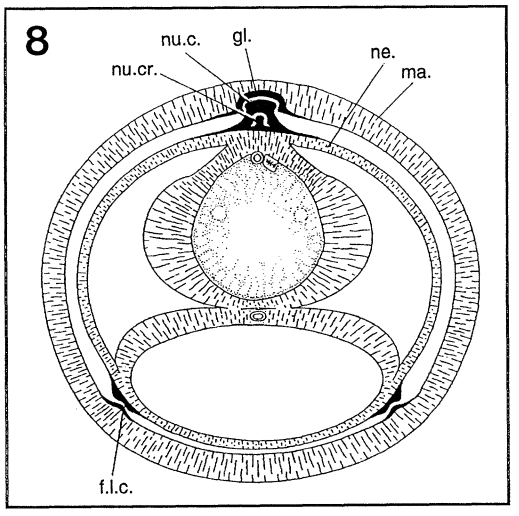

Figure 4. *Lolliguncula brevis* (mantle length 60 mm) during prey fixation. The arrow indicates the location of the neck receptor organ.

Figure 5. Diagram of *Lolliguncula brevis*. Lateral view to show the head–neck cartilages and associated muscles (modified after Wells 1988).

values, and head and body upward pitch positions as positive values. Note that $_{\text{pitch}}$HP and $_{\text{pitch}}$BP values during normal orientation (i.e. in freely moving animals) may differ from 0° (see, for example, body position in figure 4).

For any imposed body position around the roll or pitch axis, the *head response* (HR) of an animal can be described by the compensatory head roll response ($_{\text{roll}}$HR) or compensatory head pitch response ($_{\text{pitch}}$HR), which denote the angle between the animal's head and body (HR = HP − BP). Head roll responses towards the right are given as positive $_{\text{roll}}$HR values, and towards the left as negative values; similarly, head pitch responses in the dorsal direction are given as positive $_{\text{pitch}}$HR values, and in the ventral direction as negative values. Figures 2 and 3 illustrate these relationships.

(*k*) *Database*

Although 39 animals were tested in behavioural experiments, data were evaluated for only those animals (about 80%) with which a complete experimental series was performed. A complete series included experiments with the same animal before (control) and after the operation. Individual experiments of a series were performed at intervals of 1–3 days. Each experiment was done with four to seven animals and was repeated twice for each animal. In each experimental trial, and for any given imposed position, the mean value of seven measurements of the head and body position was calculated. The single measurements were made at 2 s intervals and started not earlier than 3 s after a positional change.

3. RESULTS

(*a*) *Head movements in free-swimming squid*

Under laboratory conditions, a free-swimming *Lolliguncula* keeps its body in an almost horizontal position with the head and body aligned. During interactions with other squids, however, such as chasing, mating, or during predatory behaviour, head-to-body movements occur. Most frequently, head movements around a pitch (transverse) axis were seen. For example, when a squid hovers on a spot or swims very slowly head-first near a prey, the body is often pitched, whereas the head and arms remain horizontal (figure 4). Such a head-to-body movement is obviously part of a positional head–eye reflex to stabilize the field of view. In other situations, however, the animals keep the head aligned with the body during upward or downward body pitch, i.e. no compensatory head responses occur.

Head turns around a yaw (vertical) axis were seen regularly, when a squid turned towards an object of interest, e.g. during predatory behaviour (see also Messenger 1968; Foyle & O'Dor 1988). Head yaw turns were often accompanied by yaw turns of the body. Changes of yaw position, however, do not change the orientation of the head or body with respect to gravity and therefore no obvious statocyst-controlled compensatory head–eye reflexes were seen.

Head and body movements around a roll (longitudinal) axis are rare, or are more rigidly controlled. Such movements were seen in slow-motion videos of fast swimming squids, e.g. during chromatophore display in courtship behaviour the body was rolled towards a rival, whereas the head remained horizontal.

These observations demonstrate that *Lolliguncula* is able to move its head relative to the body around all three major body axes (pitch, yaw and roll). The angular range of head movements was measured on photographs of free-swimming squid and on still-video pictures taken during the behavioural experiments. The range is about ±20° for head yaw and about ±30° for head roll; it is asymmetric (presumably because of morphological constraints) for head pitch: +20° for head upward pitch and about −30° for head downward pitch.

In addition to head pitch, yaw and roll movements, linear head movements along the body length axis were seen. These piston-like head movements occurred during breathing and during head retraction immediately before jetting.

(*b*) *Anatomy of the neck receptor organ*

(i) *The head–neck skeleton and muscle systems*

The head–neck skeleton system of squids consists of two main parts: (1) the cranial cartilage (cephalic cartilage; Williams 1909) which encloses the brain; and (2) the nuchal cartilage, an elongated, trough-shaped cartilaginous plate that lies on the dorsal side of the neck underneath the skin (figures 5–8). In addition, the gladius (pen), a feather-shaped plate of chitin, extends dorsally from the anterior to the posterior end of the mantle (figure 5). At its anterior end, a grooved ventral surface interlocks with the dorsal surface of the nuchal cartilage (figure 8). Both plates match exactly with their surface contours and form a 'sliding joint' (Williams 1909) that provides some freedom for movement of the head relative to the body.

The present analysis of the external anatomy showed that an additional cartilaginous plate exists underneath the anterior end of the nuchal cartilage, *the nuchal crest plate* (figures 5, 7, 16, 17 and 20). It has an oval base (length 1.5 mm, width 0.7 mm), from which a cartilaginous ridge, the *nuchal crest*, arises medially (figures 6–8 and 12). The nuchal crest fits into a notch on the ventral surface of the nuchal cartilage (figures 6–8).

Figure 6. The dorsal neck region (nuchal cartilage complex) with the neck receptor organ of *Lolliguncula brevis* (the mantle is removed). The anterior and posterior hair cell groups of the neck receptor organ are situated on either side of the nuchal crest; they are covered by the nuchal cartilage. (Note that the anterior edge of the nuchal cartilage is bent upwards owing to fixation). Scale bar 100 μm.

Figure 7. Transverse section of the nuchal cartilage complex (the mantle is removed). The asterisks (*) indicate the lateral connective tissue connections between the nuchal crest plate and the nuchal cartilage. Scale bar 100 μm.

Figure 8. Diagram of a transverse section through the neck region of *Lolliguncula brevis* (modified after Mangold *et al.* 1989).

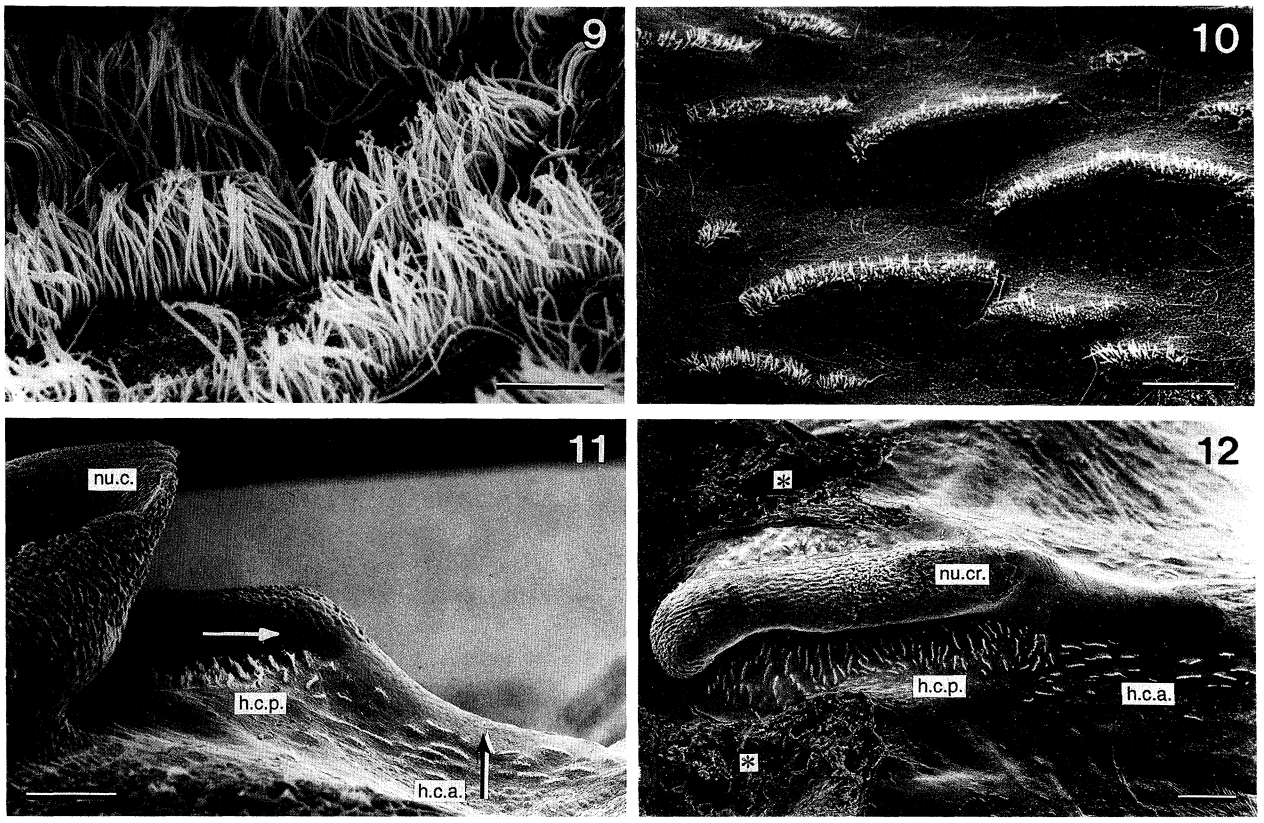

Figure 9. Ciliary bundles of the hair cells of the neck receptor organ with up to 300 kinocilia per cell. Scale bar 10 μm.

Figure 10. Variations in size of the ciliary bundles of the hair cells. (Note that in this preparation the kinocilia are broken off, presumably during the SEM preparation procedure). Scale bar 20 μm.

Figure 11. Direction of morphological polarization of the hair cells of the neck receptor organ (lateral view of the right side; anterior is to the right). The hair cells of the anterior group are polarized in the medial direction and the hair cells of the posterior group in the anterior direction (arrows). Scale bar 100 μm.

Figure 12. Anterior and posterior hair cell groups of the neck receptor organ; dorsal view of the nuchal crest plate (the nuchal cartilage is removed). The asterisks (*) indicate the areas where the connection between the nuchal crest plate and the nuchal cartilage was cut. Scale bar 100 μm.

The lateral edges and the posterior end of the nuchal crest plate are connected to the overlying nuchal cartilage by connective tissue (figures 7 and 16). The ventral surface of the nuchal crest plate is attached to the dorsal side of the neck (figure 7).

In squids the head muscle system is well developed (Williams 1909). On either side, a strong head retractor muscle is attached to the posterior part of the cranial cartilage and the ventral surface of the gladius (figure 5). In addition, an indirect head retractor muscle system operates via the nuchal cartilage. It has two parts: (1) the cephalic retractor muscle (m. retractor capitis anterior (Young 1938)), which is attached to the anterior edge of the nuchal cartilage and the posterior part of the cranial cartilage, and (2) the nuchal cartilage retractor muscle, which is attached to the posterior edge of the nuchal cartilage and the ventral surface of the gladius (figure 5). The head retractor and nuchal cartilage retractor muscles also serve to fasten the head to the mantle.

(ii) *Location and arrangement of the epidermal neck hair cells*

Epidermal hair cells are present on the dorsal side of the neck, located between the nuchal cartilage and the nuchal crest plate. They lie close to the animal's midline on either side (left and right) of the nuchal crest (figures 6, 7 and 18). The cells are arranged in an anterior group of 25–35 hair cells and a posterior group of 70–80 hair cells, giving a total of about 110 hair cells on each side (figures 6, 11 and 12). In the anterior group, the hair cells are arranged in 4–5 rows of 7–9 hair cells each; in the posterior group, they are arranged in 35–40 rows of 2–3 hair cells each (figures 6, 11 and 12).

Individual hair cells carry between 30 and 300 kinocilia; these are arranged in elongated ciliary bundles (figure 9). The hair cells do not carry stereovilli (stereocilia). The length of the long axis of a ciliary bundle varies considerably (10–40 μm) between individual hair cells in the anterior and the posterior hair cell groups (figure 10). The length of an individual cilium is about 30 μm; this is less than the distance between the surface of the hair cell epithelium and the overlying nuchal cartilage in the posterior group (40–50 μm (figures 16 and 17), but see Discussion). Measurements on transverse and sagittal sections (e.g. figures 7 and 16) of the surface lengths of the hair cell epithelium and the opposite nuchal cartilage give identical values for both surface outlines.

In each hair cell group, the arrangement of the

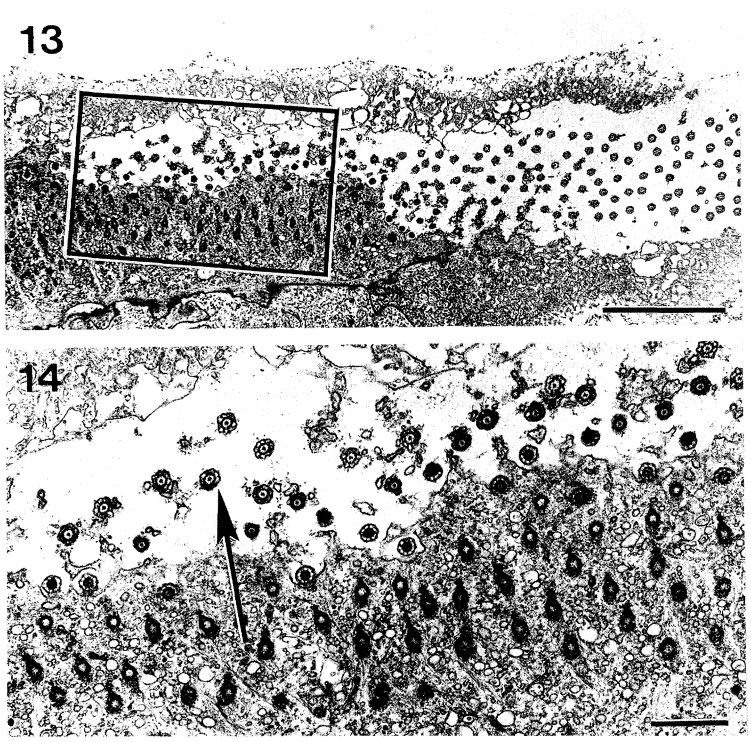

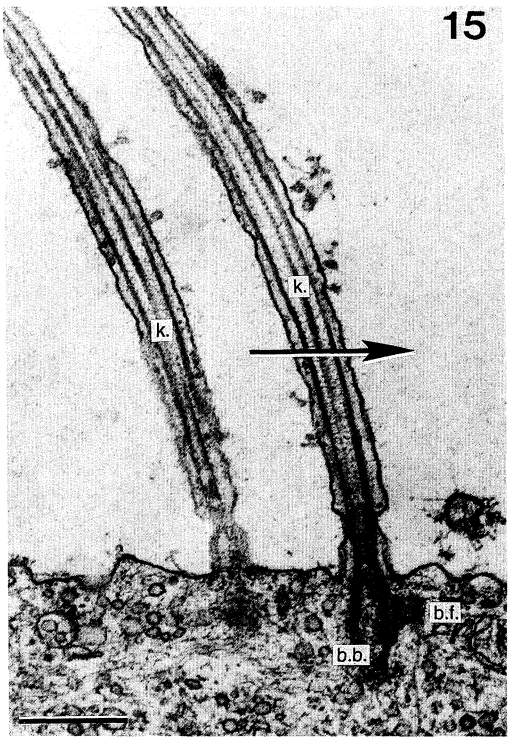

Figures 13 and 14. Cross sections through the distal part and kinocilia of a hair cell of the posterior hair cell group. Figure 14 is a magnification of the area outlined in figure 13. Note the uniform orientation of the basal feet, which defines the direction (arrow) of morphological polarization. Scale bars 5 μm (figure 13) and 1 μm (figure 14).

Figure 15. Transverse section through the elongated kinociliary group of a neck hair cell to show the inclination of the cilia towards the surface of the epithelium and the orientation of their basal feet. The arrow indicates the direction of morphological polarization of the cilia and thus that of the hair cell. Scale bar 0.5 μm.

ciliary bundles is strictly organized (figures 6, 10, 11 and 12). In the anterior group, the long axes of the elongated ciliary bundles are all oriented parallel to the long axis of the nuchal crest and, thus, parallel to the longitudinal axis of the body (figures 6, 11 and 12). In the posterior group, the long axes of the ciliary bundles are all oriented at right angles to the long axis of the nuchal crest and thus parallel to the transverse axis of the body (figures 6, 11 and 12).

(iii) *Morphological polarization of the epidermal neck hair cells*

Each kinocilium within the ciliary group contains $9\times2+2$ internal tubuli (figures 14 and 15), and is morphologically polarized, e.g. by a basal foot attached to its basal body about 0.2 μm below the cell surface (figure 15). The basal feet of all kinocilia of one hair cell point in the same direction and thus morphologically polarize the hair cell in just one direction. This direction of polarization is always at right angles to the long axis of the elongated ciliary bundles (figures 13 and 14). Such a morphological polarization is well known in invertebrate and vertebrate mechanoreceptive hair cells; it correlates with a physiological polarization (see Discussion).

The patterns of morphological polarization of the left and right anterior and posterior hair cell group were analysed in transverse, sagittal and tangential sections at electron microscopical level. The basal feet of the cilia of all anterior hair cells face in the medial direction, i.e. towards the nuchal crest (figure 11); with respect to the left and right anterior hair cell group, the directions of polarization are opposed. The basal feet of the cilia of all posterior hair cells face in the anterior direction, i.e. towards the animal's head (figure 11); with respect to the left and right posterior group, the directions of polarization are the same.

(iv) *Ultrastructure of the neck hair cell epithelium*

The neck region underneath the nuchal cartilage reveals ultrastructural differences between its anterior and posterior parts and, specifically, between the anterior and posterior hair cell groups (table 1). Therefore both regions will be described separately.

Anterior neck region and anterior hair cells

Sections through the region of the anterior hair cells show a single-layer epithelium with three cell types: hair cells, supporting cells and mucus cells (figure 19). The anterior hair cells have a globular shape in transverse sections (height about 20 μm, width about 30 μm), with a small apical area and a much larger basal area in direct contact with the underlying connective tissue (figures 19, 21 and 22). An axon (about 4 μm in diameter) arises from the base of each hair cell and extends into the underlying connective tissue, where it runs immediately below and parallel to the hair cell epithelium (figure 21). The presence of an axon classifies the hair cells as primary sensory cells.

On the apical side, kinocilia extend from the surface of the hair cells. They are of equal length and are arranged in 5–7 rows (figures 13 and 14). Their morphological polarization is in a medial direction (see

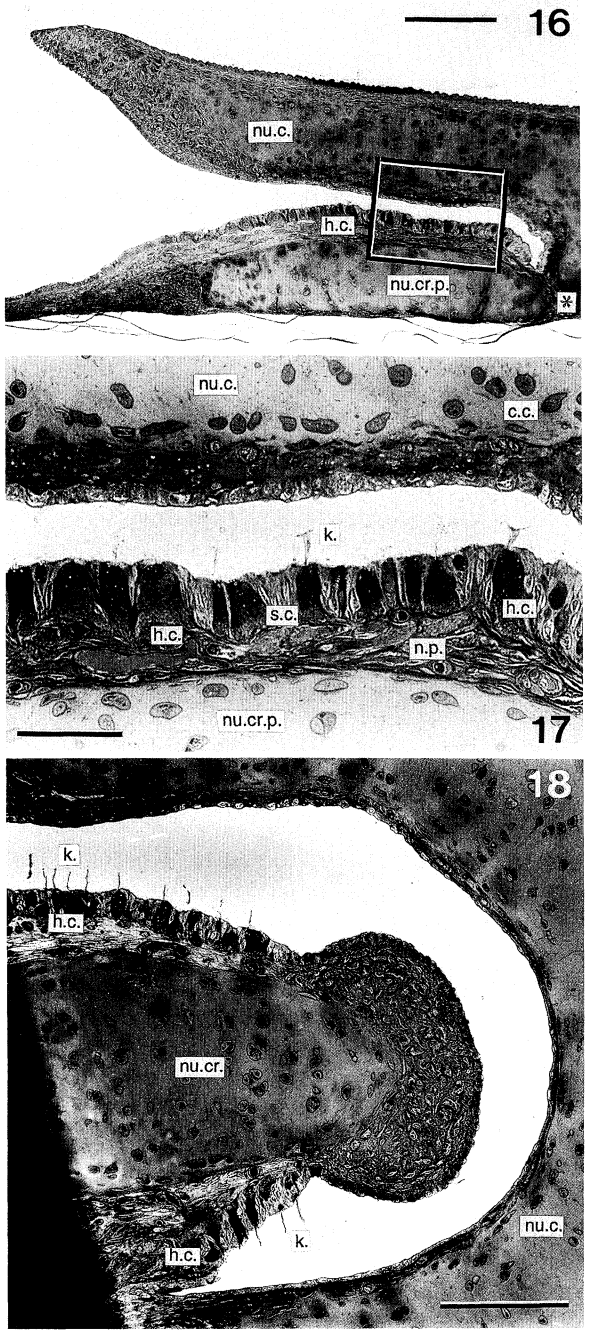

Figure 16. Sagittal section through the neck receptor organ (lateral to the nuchal crest) to show the location of the hair cell epithelium between the nuchal cartilage and the nuchal crest plate. Note that the increasing distance between the anterior part (to the left) of the nuchal cartilage and the epithelium is a fixation artefact. Scale bar 200 μm.

Figure 17. Magnification of the area outlined in the figure 16. Note that in unfixed tissue the tips of the cilia most likely are in contact with the overlying nuchal cartilage. Scale bar 50 μm.

Figure 18. Horizontal section (slightly oblique) through the posterior part of the nuchal crest and nuchal crest plate to show the parallel arrangement of the ciliary bundles of the posterior neck hair cells of the left and right side (posterior is to the top). Scale bar 100 μm.

above). From the basal body of each kinocilium numerous rootlets radiate into the cell (figures 22 and 24).

The anterior hair cells are laterally surrounded by supporting cells of irregular shape; their number is much larger than that of the hair cells. All along the length of the contacting membranes of the supporting cells and the hair cells, many well-developed interdigitations exist (figure 22). Apically, the supporting cells bear short microvilli (figures 21, 22 and 24). Large mucus-secreting gland cells are scattered between the hair and supporting cells (figure 19). The number of mucus cells increases laterally with increasing distance from the crest. In that region, hair cells are rare and a well-developed basal lamina separates the epithelium from the underlying connective tissue; in the region where the hair cells exist, the basal lamina is only poorly developed. The tissue underneath the epithelium includes the axons of the hair cells, a layer of collagenous connective tissue, muscle fibres interspersed with collagenous fibres, and some blood vessels (figures 19, 21 and 22).

Posterior neck region and posterior hair cells

Sections through the region of the posterior hair cells also show a single-layer epithelium with hair cells and supporting cells, but only a few mucus cells. In contrast to the anterior hair cell epithelium, it rests on a cartilaginous plate (nuchal crest plate; figures 16, 17 and 20). In transverse sections, the posterior hair cells are slender (height about 35 μm, width about 20 μm; figures 17 and 20). At their base an axon arises, indicating that the hair cells are primary sensory cells. All axons run in a thin layer of connective tissue between the epithelium and the nuchal crest plate immediately below and parallel to the hair cell epithelium (figures 17 and 20); this layer includes collagenous fibres and blood vessels.

On the apical side, kinocilia extend from the surface of the hair cells. They are of equal length (about 30 μm; figures 9 and 17) and arranged in five to seven rows; their morphological polarization, however, is in the anterior direction (see above). From their basal bodies rootlets radiate into the cell (figure 23). Some hair cells contain a large number of mitochondria.

The posterior hair cells are laterally surrounded by slender supporting cells, which often have an electron-dense cytoplasm (figure 20). All cells are mechanically stabilized by interdigitations at the apical region of the cells (figure 23). A dense microvillar border covers the apical cell surface of the supporting cells (figure 20).

(v) *Efferent endings in contact with the neck hair cells*

At the base of the anterior and the posterior neck hair cells efferent profiles are present that make synaptic contacts with the hair cells (figures 21, 24 and 25). The synapses are characterized by parallel, electron-dense membranes that are separated by a synaptic cleft. The cleft is 25 nm wide and contains electron-dense cleft material. The profiles are filled with round, clear vesicles (about 10 nm in diameter) and occasionally with mitochondria (figures 25 and 26).

Table 1. *Morphological differences between the anterior and posterior hair cell groups of the neck receptor organ of* Lolliguncula brevis

	anterior hair cells	posterior hair cells
number	25–35	70–80
arrangement	in 4–5 parallel rows with 7–9 hair cells each	in 35–40 parallel rows with 2–3 hair cells each
polarization	ciliary group oriented longitudinally; polarization is in medial direction	ciliary group oriented transversely; polarization is in anterior direction
shape	voluminous, more wide than high	slender, more high than wide
support	connective tissue and many supporting cells	cartilage of nuchal crest plate and supporting cells
interdigitation of hair cells and neighbouring cells	from apical to proximal	mostly apical
rootlets	numerous	numerous
afferent innervation	primary sensory cell with axon	primary sensory cell with axon
efferent innervation	present at base of hair cell	present at base of hair cell

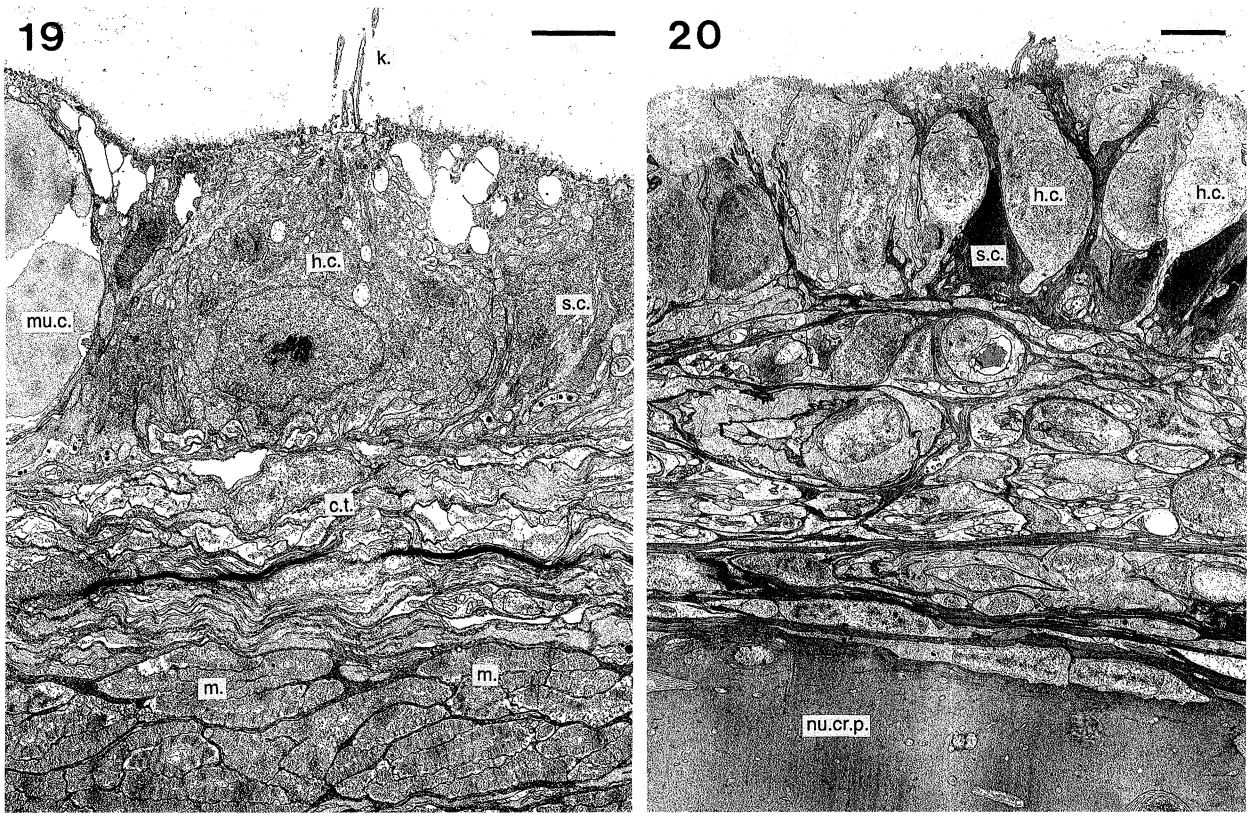

Figure 19. Transverse section through the epidermis of the anterior hair cell group, showing the epithelium with hair cells, mucus cells and supporting cells. Note the thick layers of connective tissue and muscle fibres below the epithelium. Scale bar 5 μm.

Figure 20. Transverse section through the epidermis of the posterior hair cell group, showing the epithelium with hair cells and supporting cells. Note the cartilage of the nuchal crest plate below the epithelium. Scale bar 10 μm.

(vi) *Innervation of the neck hair cells*

After centrifugal cobalt staining of the branch of the postorbital nerve that innervates the neck hair cells, an anterior and a posterior group of cell bodies are stained close to the nuchal crest (figure 27). These cells, almost certainly, are the hair cells of the anterior and posterior hair cell group for the following two reasons: (1) the stained cells and the hair cells in the anterior and posterior group coincide in number and location; and (2) from LM and TEM studies, no other sensory cells are known in those locations that might be innervated via that branch of the postorbital nerve.

The stained branch of the postorbital nerve splits into a large (130 μm × 25 μm) and a small bundle (80 μm × 15 μm). The large bundle innervates the posterior and the small bundle the anterior group of hair cells (figures 27 and 28). Both bundles include large (2–5 μm) and small (0.1–0.3 μm) nerve fibres (figures 29 and 30). The large bundle contains about 70 and the small bundle about 30 large fibres; each

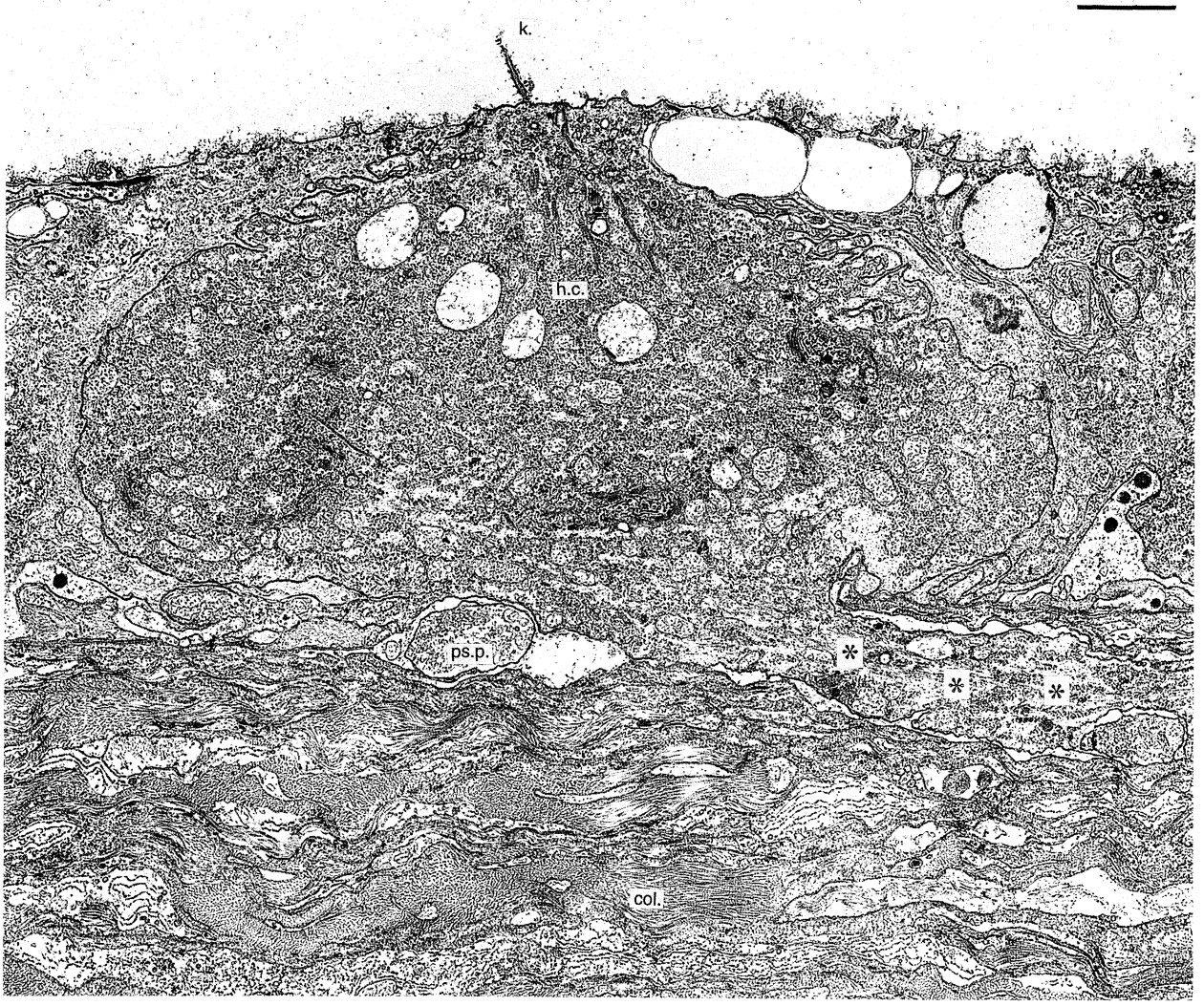

Figure 21. Transverse section through a hair cell of the anterior hair cell group. Note the axon leaving the hair cell (asterisks) and a large presynaptic profile below the hair cell. Scale bar 3 μm.

large fibre is surrounded by a glial cell and contains mitochondria at its periphery (figure 29). The number of large fibres corresponds with the number of hair cells found in the posterior (70–80) and anterior (25–35) hair cell groups (figures 12 and 28). The small fibres are packed in clusters of up to 30 fibres and are wrapped in a single glial cell (figure 30). The small fibres, most probably, belong to the efferent profiles that synapse onto the hair cells and therefore are part of the efferent innervation.

(vii) *Central projection of the neck hair cells*

The squid brain surrounds the oesophagus (figure 31) and is subdivided into supra-, peri- and sub-oesophageal masses; these are further divided into 38 distinct lobes (Young 1976, 1977, 1979).

Centripetal cobalt staining was used to analyse the central pathways of the afferent and efferent fibres of the branch of the postorbital nerve that innervates the epidermal neck hair cells. The stained fibres pass through the cranial cartilage postero-dorsally and continue to the sub-oesophageal mass of the brain (figure 31). They enter the brain between the posterior pedal and the palliovisceral lobes and run straight down to the ventral part of ventral magnocellular lobe (figure 32); there they terminate in fine arborizations throughout the neuropil. All fibres are varicose and fine and are most probably afferent in nature (figure 33). No stained cell bodies were seen in the ventral magnocellular lobe, nor were any stained fibres seen crossing to the contralateral magnocellular lobe or to any other contralateral part of the brain. Also, no stained cell bodies of efferent fibres were found anywhere in the brain (but see Discussion).

(*c*) *Behaviour*

(i) *Theoretical background*

The morphological data described above allow three hypotheses to be made concerning the function of the neck hair cells (see also Discussion).

Hypothesis I. The location of the neck hair cells between the nuchal cartilage and the nuchal crest plate (figures 7, 16 and 17) predicts that: *the neck hair cells are stimulated by the overlying nuchal cartilage during head-to-body movements.*

Hypothesis II. The pattern of morphological polarization of the neck hair cells (figure 11), together with the assumption that the morphological

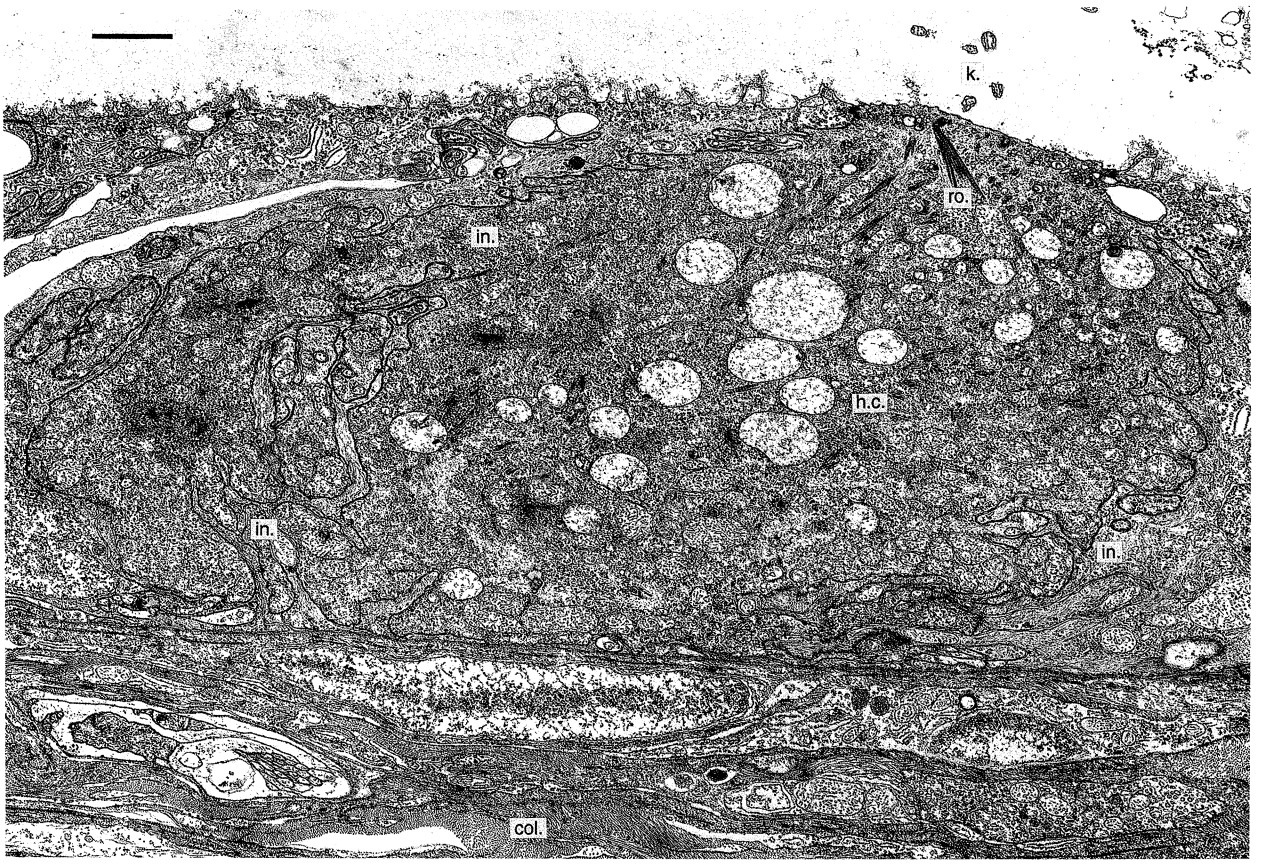

Figure 22. Transverse section through a hair cell of the anterior hair cell group, showing the well-developed interdigitations with the neighbouring supporting cells. Scale bar 2 μm.

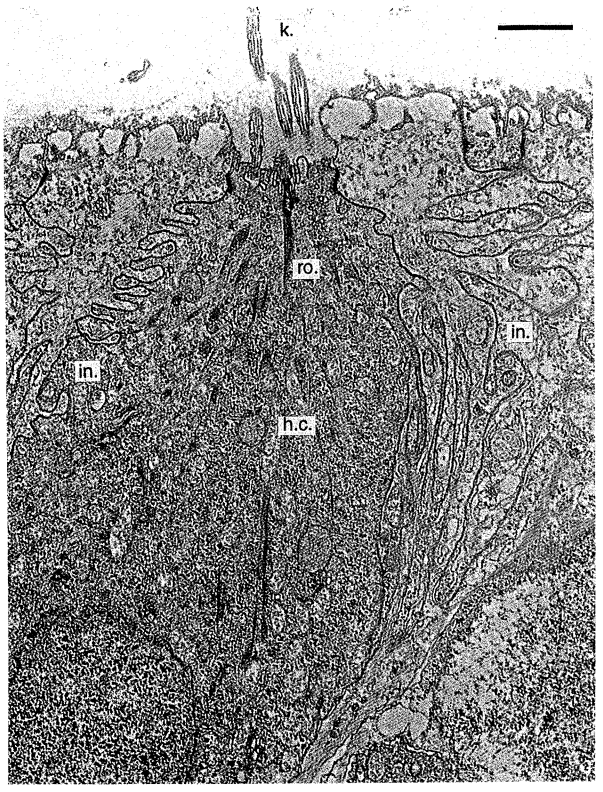

Figure 23. Transverse section through the distal parts of hair and supporting cells of the posterior hair cell group, showing their heavy interdigitations. Scale bar 1 μm.

polarization of the hair cells coincides with a physiological polarization (see Budelmann & Williamson 1994), predict that: (i) *the two anterior groups of hair cells (which are arranged at right angles to the roll plane and are polarized in the medial direction) are adequately stimulated by head roll movements*; *and* (ii) *the two posterior groups of hair cells (which are arranged at right angles to the pitch plane and are polarized in the anterior direction) are adequately stimulated by head pitch movements.*

Hypothesis III. The arrangement of the neck hair cells on either side of the nuchal crest predicts that: (i) *head roll movements cause an asymmetric stimulation of the neck hair cells on the left and the right side, and* (ii) *head pitch movements cause a symmetric stimulation of the neck hair cells on the left and the right side.*

These three hypotheses were tested in behavioural experiments, in which the sensory input from the neck hair cells was eliminated by unilateral and bilateral cutting of the branch of the postorbital nerve that innervates the neck hair cells.

(ii) *Neck hair cell influence on head roll position*

Bimodal interaction of statocyst and neck hair cell inputs

The head roll response of *Lolliguncula* ($N = 7$) was analysed during imposed body roll to the left and right (see Materials and methods).

Intact animals responded to a given body roll position with a compensatory head roll response in a direction opposite to the direction of the imposed body roll (figure 34). The amplitude of the response changed

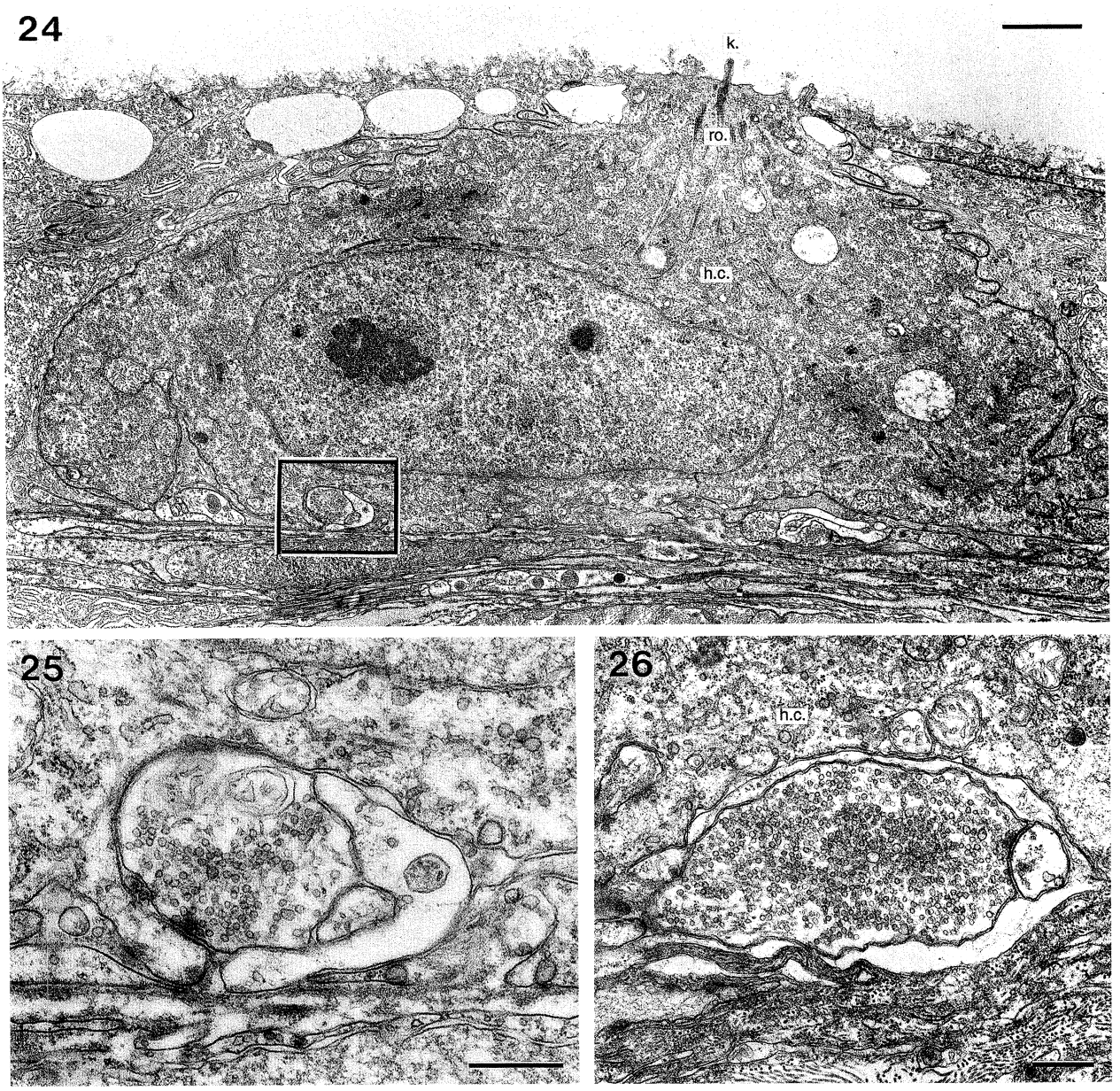

Figures 24–26. Efferent innervation of the hair cells of the neck receptor organ. Transverse section through a hair cell of the anterior hair cell group (figure 24), with a vesicle-filled efferent profile at its base that makes synaptic contact with the hair cell (figure 25; higher magnification of the area outline in figure 24). Figure 26 shows a large efferent profile with a uniform population of small, clear synaptic vesicles. Scale bars 2 μm (figure 24) and 0.5 μm (figures 25 and 26).

with increasing body roll position in a sinusoidal-like manner with an average maximum $_{roll}HR$ of $\pm 22°$ at $_{roll}BP = \pm 65°$; individual animals showed a maximum $_{roll}HR$ of $\pm 30°$. The compensatory head roll response was symmetric for turns to the left and to the right side (figure 34).

The compensatory head roll response of intact animals reached no distinct peak within the tested range of body roll positions (figure 34). Because the positions were limited to a maximum $_{roll}BP$ of $\pm 65°$ (because of an increasing excitement of the animals at larger body roll positions that made it difficult to measure head positions), it is reasonable to predict that the amplitude of the compensatory head roll response reaches its maximum at $_{roll}BP > \pm 65°$, presumably at $_{roll}BP = \pm 90°$.

To test for an influence of the neck hair cells on the compensatory head roll response, the postorbital nerve was unilaterally cut in the same animal group. The cuts were alternated between the left and right sides to prevent a lateral bias of the operation. For analysis and illustration of the results, however, all data for the unilaterally right-operated animals were converted (by a change of sign) into data for unilaterally left-operated animals to allow further processing of all the data combined.

Imposed body rolls of unilaterally operated animals to the operated (left) and unoperated (right) side had two effects on the compensatory head roll response: (1) a small overall offset (*ca.* 3°) to the operated side, and (2) for body roll to the operated side, a reduction of the head roll amplitude at body roll positions larger than about $-39°$. The latter effect was significant ($p < 0.05$; *t*-test for paired samples) at $_{roll}BP = \pm 65°$ for

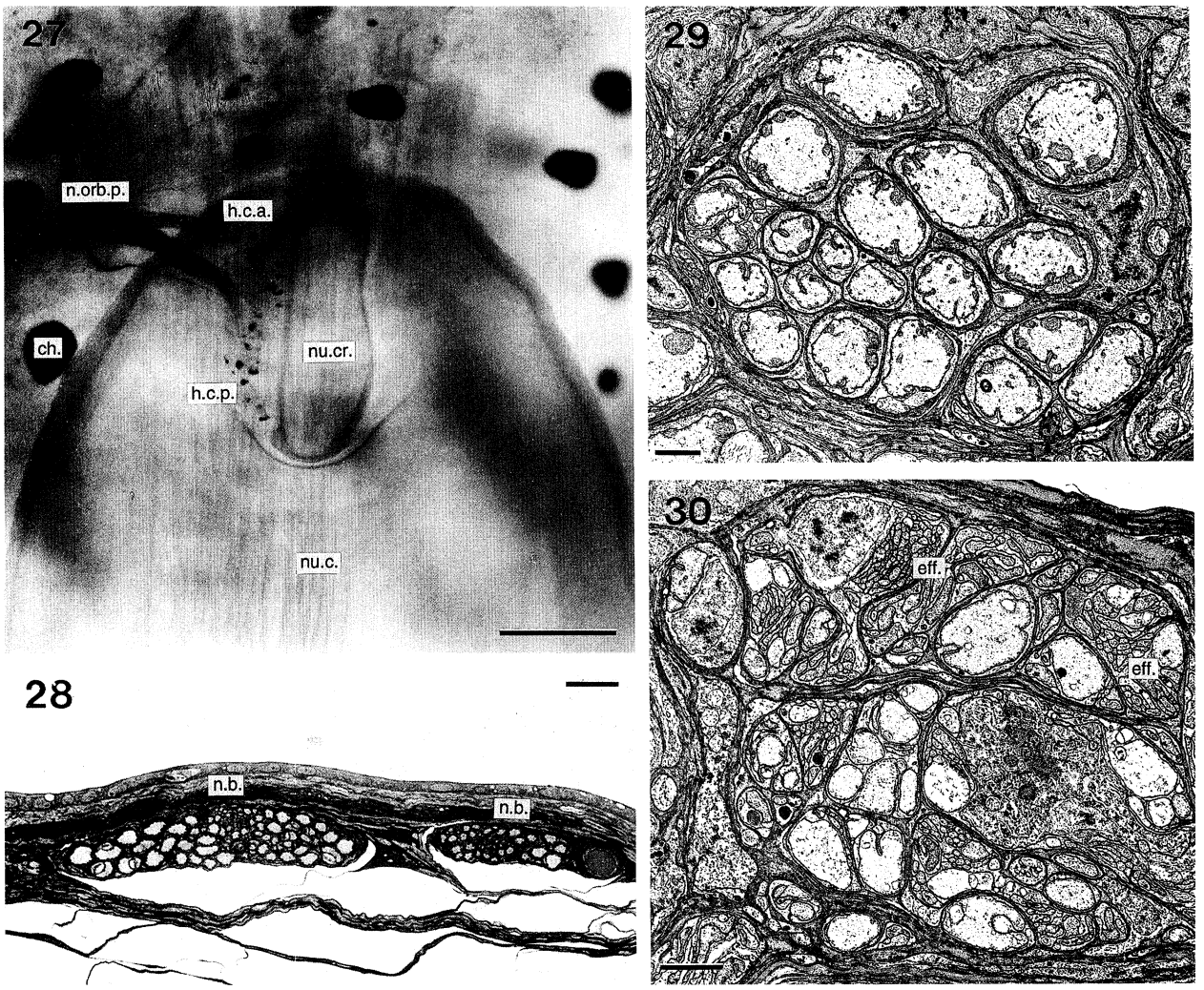

Figure 27. Innervation of the neck hair cells of the neck receptor organ. Dorsal view of the neck region after centrifugal cobalt staining of the left postorbital nerve. The branch that innervates the hair cells divides into two smaller bundles: one innervates the cells of the anterior hair cell groups, and the other those of the posterior groups. Whole mount preparation; anterior is top of page. Scale bar 100 μm.

Figures 28–30. Cross sections at light (figure 28) and electron microscopical level (figures 29 and 30) of the branch of the postorbital nerve that innervates the neck hair cells. Sections were taken at the point where the branch has separated into two smaller bundles. Note the bundles of fine, presumably efferent, fibres (figure 30). Scale bars 20 μm (figure 28) and 2 μm (figures 29 and 30).

turns to the operated side ($_{roll}HR = 13° \pm 2.7°$ s.e.m.), compared with the unoperated side ($_{roll}HR = 23° \pm 0.6°$ s.e.m.) (figure 34).

After bilateral operations (i.e. after an additional cut of the postorbital nerve on the unoperated side), the asymmetric effects on the compensatory head roll response were no longer seen (figure 34). This can be taken as proof that the asymmetry seen in unilaterally operated animals was due to an asymmetric sensory input from the neck hair cells. Bilaterally operated animals showed no differences in the compensatory head roll response between body roll to the left and to the right side (figure 34). The head roll amplitude at $_{roll}BP = \pm 65°$ was slightly reduced compared with intact animals (figure 34).

Gain of the compensatory head roll response

Complete compensation of an imposed body roll requires a compensatory head roll response of equal size and opposite sign, i.e. a gain of 1 for any elicited head roll ($G = {}_{roll}HR/{}_{roll}BP$). Under the experimental conditions, however, intact animals compensate for less than 50 % of the imposed body roll (figure 35). Over the whole range of imposed body roll positions the gain of the compensatory head roll response varied between $G = 0.5$ and $G = 0.38$; it declined with increasing body roll positions (figure 35).

In intact animals, the gain of the compensatory head roll response was similar for body roll to the left and to the right side; the data were therefore averaged and shown as a single gain curve. In contrast, in unilaterally operated animals the gain was different for body roll to the operated and unoperated side (figure 35). When rolled to the operated side, the compensation was about 20–30 % of the imposed body roll. The gain was larger at smaller body roll positions ($G = 0.32$ at $_{roll}BP = 13°$) and declined with increasing body roll ($G = 0.2$ at $_{roll}BP = 65°$ (figure 35)). In contrast, when unilaterally operated animals were rolled to the unoperated side, the compensation was 40–60 % of the

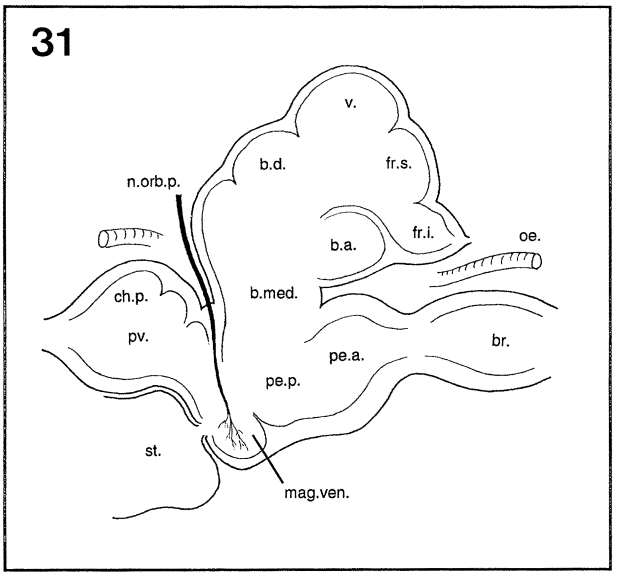

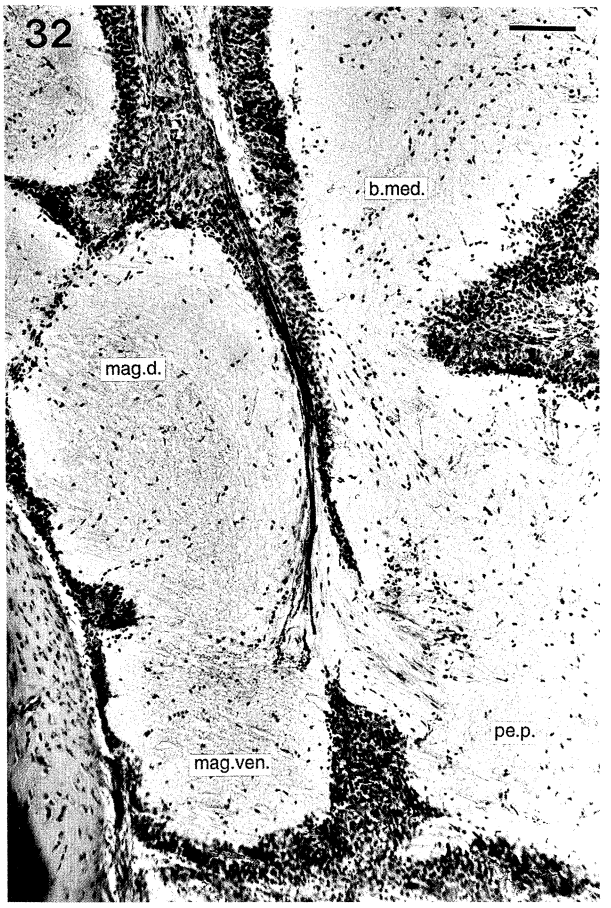

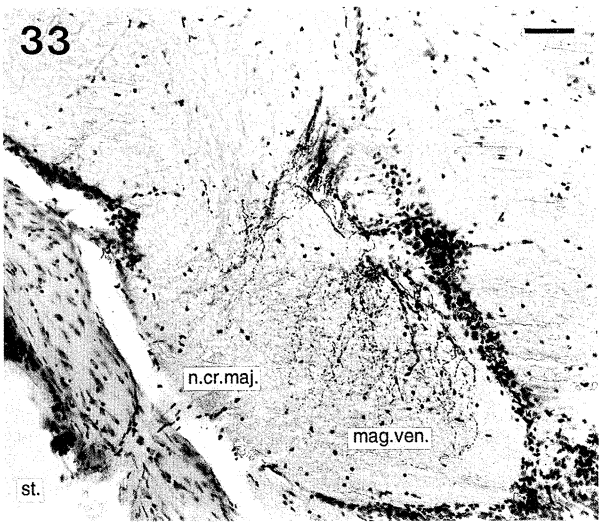

Figure 31. Central projection of the hair cells of the neck receptor organ. Diagram of a sagittal section of the brain of *Lolliguncula brevis*, illustrating the pathway of the hair cells' afferent fibres. The origin of the efferent fibres is still unknown.

Figures 32 and 33. Centripetal cobalt fillings of the branch of the postorbital nerve that innervates the hair cells of the neck receptor organ. Sagittal section of the part of the ventral sub-oesophageal lobes, showing fine afferent fibres running to, and terminating in, the ventral magnocellular lobe. Note the entry of the large crista nerve of the statocyst into that lobe. Scale bars 100 μm (figure 32) and 50 μm (figure 33).

imposed body roll positions (figure 35). The gain was larger at smaller body roll ($G = 0.62$ at $_{\text{roll}}\text{BP} = 13°$) and declined with increasing body roll ($G = 0.37$ at $_{\text{roll}}\text{BP} = 65°$ (figure 35)).

Exclusive influence of the neck hair cell input on head roll position

The above results show an influence of the neck hair cells on head roll without visual cues (see Materials and methods) but with a positional input from the statocysts. To analyse the exclusive effect of the neck hair cells on head roll, experiments were performed with animals ($N = 4$) that had the statocysts bilaterally destroyed, in combination with a unilateral elimination of the neck hair cell input.

Bilateral destruction of the statocysts abolished the compensatory head roll response (figure 36). The head

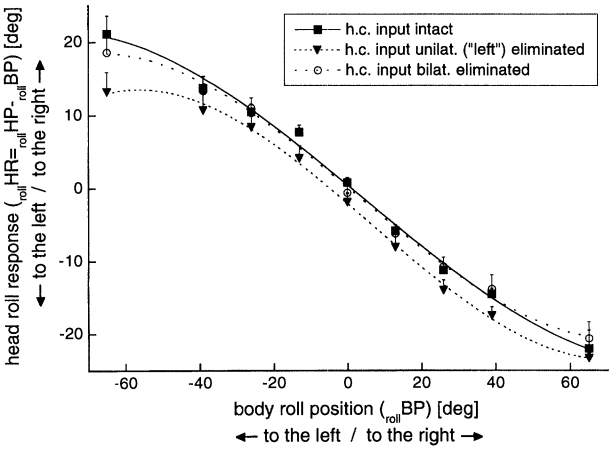

Figure 34. Influence of the neck receptor organ on compensatory head roll of *Lolliguncula*. Averaged data ($N = 7$; means ± s.e.m.) of the compensatory head roll response to imposed body roll positions of intact animals and of animals after unilateral and bilateral elimination of the sensory input of the hair cells of the neck receptor organ. Note that in unilaterally operated animals body rolls to the left are equal to body rolls to the operated side.

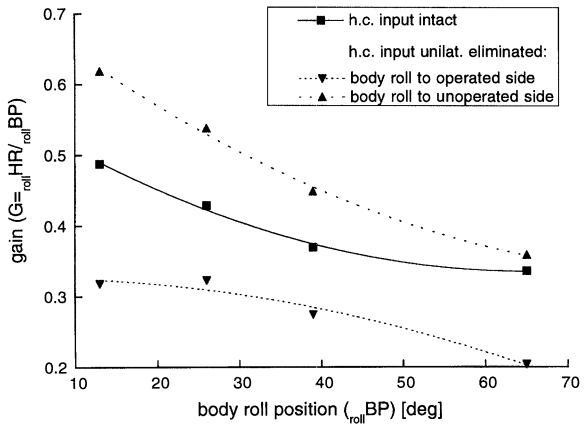

Figure 35. Gain of the compensatory head roll response of *Lolliguncula* to imposed body roll positions. Averaged data from animals ($N = 7$) before and after unilateral elimination of the hair cells of the neck receptor organ.

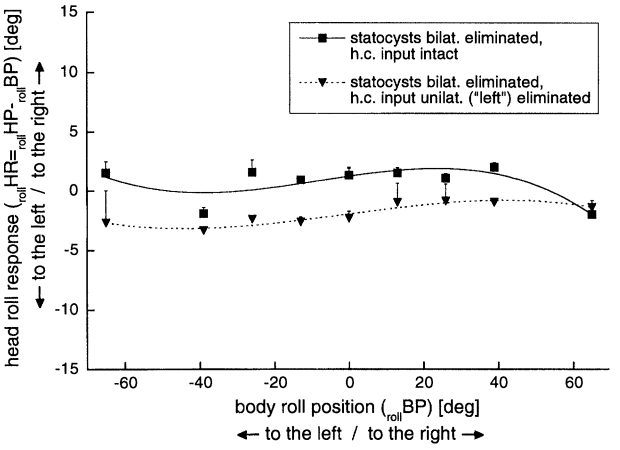

Figure 36. Influence of the neck receptor organ on the head roll response of *Lolliguncula* after elimination of the sensory input from the statocysts. Averaged data from animals ($N = 4$; means ± s.e.m.) before and after additional unilateral elimination of the sensory input of the hair cells of the neck receptor organ.

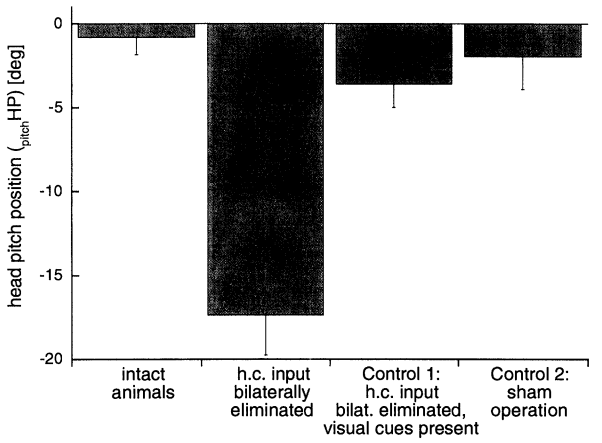

Figure 37. Influence of the neck receptor organ on the head pitch position of *Lolliguncula*. Averaged data ($N = 4$; means ± s.e.m.) of the head pitch position before (intact animals) and after bilateral elimination of the sensory input of the hair cells of the neck receptor organ. Control 1 ($N = 3$; means ± s.e.m.), visual cues (horizontal black stripes) present; control 2 ($N = 3$; means ± s.e.m.), sham operation.

remained aligned with the body ($_{roll}$HR ≈ 0) over the whole range of imposed body roll positions. This indicates that the previously shown compensatory head roll response was driven by the sensory input from the statocysts (figures 34 and 36). After an additional unilateral elimination of the neck hair cell input, a head roll offset occurred towards the operated side (figure 36). The offset was small but consistent over the whole range of imposed body roll (−3° ± 0.5° s.e.m.; figure 36).

(iii) *Neck hair cell influence on head pitch position*

Evoked head pitch with the body in normal position ($_{pitch}$BP = 0°)

In the visually homogeneous surroundings of the experimental set-up, intact animals ($N = 4$) with the body in normal position ($_{pitch}$BP = 0°) keep the head closely aligned to the body and thus to the horizon ($_{pitch}$HP ≈ 0° (figure 37)). Bilateral elimination of the sensory input from the neck hair cells elicits a distinct head pitch offset of −17.4° ± 2.4° s.e.m. ($P < 0.01$; *t*-test for paired samples (figure 37)). The head pitch offset remained for at least 20 min; it was as large as −33° in individual animals and seems to be close to the anatomical limit for such a head movement.

To prove that the operated animals were still able to compensate for the head pitch offset and to exclude the possibility that the neck muscles had been damaged during the operations, a horizontal black and white stripe pattern (spatial wavelength $\lambda = 30°$) was presented to each animal in its frontal visual field. The pattern was arranged such that one of the black stripes was at the same height as the body of the animal. With such a visual cue, the head pitch offset was largely reduced, i.e. the head was kept almost horizontal, aligned with the body and parallel to the stripe pattern (figure 37). Also, after sham operations ($N = 3$) no

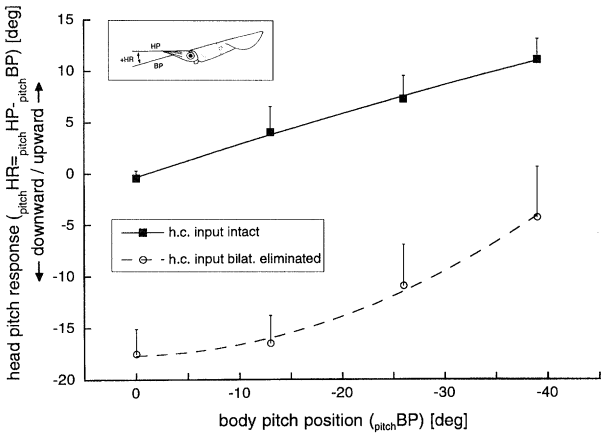

Figure 38. Influence of the neck receptor organ on the compensatory head pitch response of *Lolliguncula*. Averaged data ($N = 4$; means ± s.e.m.) of the head pitch response to imposed downward body pitch positions.

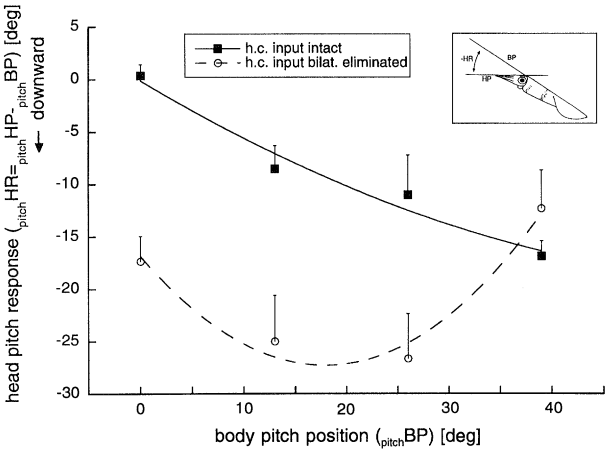

Figure 39. Influence of the neck receptor organ on the compensatory head pitch response of *Lolliguncula*. Averaged data ($N = 4$; means ± s.e.m.) of the head pitch response to imposed upward body positions.

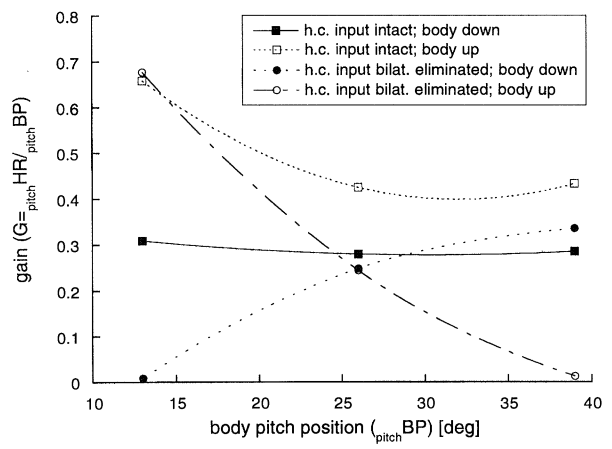

Figure 40. Gain of the compensatory head pitch response of *Lolliguncula* to imposed upward and downward body pitch positions. Averaged data from animals ($N = 4$) before and after bilateral elimination of the sensory input of the hair cells of the neck receptor organ.

head pitch offset occurred (figure 37). These results show that the head pitch offset of animals whose neck hair cells had been operated on bilaterally was not caused by a damage of neck muscles and can be compensated for by visual cues.

Head pitch to imposed body pitch

The influence of the neck hair cell input on head pitch was analysed during imposed downward and upward pitch on the body. Since the responses were different, they are presented separately.

Head pitch to imposed body downward pitch. In intact animals ($N = 4$) a downward body pitch caused a compensatory upward head pitch response; the head pitch compensated for about 30 % of the imposed body pitch displacements (figure 38). Within the tested range of 0–39° body pitch, the amplitude of the compensatory head pitch increased steadily with increasing body pitch (maximum $_{pitch}$HR = +11.1° ± 2° s.e.m. at $_{pitch}$BP = −39°). Body pitch positions larger than 39° were not used because the animals became too excited and measurements of head position were difficult to perform. Bilateral elimination of the neck hair cell input caused two changes of the compensatory head pitch response. The first was a downward pitch offset of about 17° over the whole range of imposed downward body pitch positions, with the compensatory upward head pitch response superimposed on the head pitch offset; the second was a change in the nature of the compensatory head pitch response compared with that of intact animals: below a body downward pitch of −13° no obvious compensatory head pitch response occurred, but for larger body pitch positions ($_{pitch}$BP > −13°) the compensatory response increased, as indicated by the larger slope (figure 38). The amplitude of the compensatory head pitch, calculated to the head offset as new baseline, increased steadily with increasing body pitch position with a maximum $_{pitch}$HR of +13° ± 4.7° s.e.m. at $_{pitch}$BP = −39°. This maximum response was 17 % larger than in intact animals.

Head pitch to imposed body upward pitch. In intact animals ($N = 4$), an upward body pitch caused a compensatory downward head pitch response; the head pitch compensated for about 50–60 % of the imposed upward body pitch (figure 39). The amplitude of compensatory head pitch increased steadily with increasing body pitch (maximum $_{pitch}$HR = −17° ± 1.5° s.e.m. at $_{pitch}$BP = +39° (figure 39)). The magnitude of the response during upward body pitch was about 25 % larger than the response during downward body pitch (compare figures 38 and 39). Bilateral elimination of the neck hair cell input elicited the same downward head pitch offset of 17°, but only at upward body pitch positions below $_{pitch}$BP = 26°; over this range, a superimposed downward compensatory head pitch was seen as well (figure 39). The amplitude of compensatory head pitch, calculated with the head offset as new baseline, showed a steady increase with increasing body pitch positions up to +13°, but then remained rather stable for body pitch positions up to $_{pitch}$BP = +26° ($_{pitch}$HR = −9.4° ± 4.3° s.e.m. at $_{pitch}$BP = +26°). For a body pitch position larger than +26°, however, the direction of the head pitch response reversed; this head upward movement was seen in all animals tested ($N = 4$).

Gain of the compensatory head pitch response

Because of the head pitch offset after bilateral elimination of the neck hair cell input, the gain of the head pitch response of operated animals was calculated to the head pitch offset as new baseline ($G = ({}_{\text{pitch}}\text{HR} - 17.4°)/ {}_{\text{pitch}}\text{BP}$). During imposed downward body pitch, intact animals showed an almost constant head pitch response gain ($G \approx 0.3$) over the whole range of downward body pitch positions (figure 40). After bilateral elimination of the neck hair cell input the gain was close to zero for small downward body pitch positions (${}_{\text{pitch}}\text{BP} = 13°$), but increased to a maximum of $G \approx 0.34$ at ${}_{\text{pitch}}\text{BP} = 39°$ (figure 40). During imposed upward body pitch, intact animals showed the highest response gain ($G \approx 0.7$) at small upward body pitch positions (${}_{\text{pitch}}\text{BP} = 13°$); it decreased at larger body pitch positions (${}_{\text{pitch}}\text{BP} = 39°$) to $G \approx 0.45$ (figure 40). After bilateral elimination of the neck hair cell input the gain was the same ($G \approx 0.7$) as in intact animals at small upward body pitch positions (${}_{\text{pitch}}\text{BP} = 13°$), but it declined at larger pitch positions (${}_{\text{pitch}}\text{BP} = 40°$) to $G \approx 0$ (figure 40).

4. DISCUSSION

(*a*) *Anatomical data*

The present study shows that epidermal hair cells exist in the nuchal cartilage complex of the neck of the squid *Lolliguncula brevis*. According to their structure, these cells, together with the associated cartilages of the nuchal cartilage complex, form a *neck receptor organ* that monitors head-to-body positions and head-to-body movements around roll and pitch axes. The following four criteria support the idea that the hair cells are mechanoreceptors with a proprioceptive function: (1) their afferent and efferent innervation, (2) their central projection, (3) their ultrastructure and morphological polarization, and (4) their specific location on the neck.

(i) *Afferent innervation*

According to the cobalt staining experiments, the cells in the anterior and posterior hair cell groups are innervated by a branch of the postorbital nerve (figure 27). Before this branch reaches the two groups of hair cells, it divides into two smaller bundles; this emphasizes the separation of the hair cells into two groups with different functional characteristics (see below). Previous cobalt staining experiments in cephalopods did not give any evidence for trans-neuronal staining (Budelmann & Young 1984, 1985; Budelmann *et al.* 1987); therefore the staining of the somata of the hair cells via the postorbital nerve and the presence of an axon leaving the hair cells (figure 21) shows that the neck hair cells are primary sensory cells. Furthermore, in the large and small bundles of the postorbital nerve, the number of fibres with a diameter larger than 2 μm corresponds well with the number of hair cells in the posterior and anterior hair cell groups, respectively; this indicates that the large-diameter fibres are the axons of the neck hair cells.

(ii) *Efferent innervation*

There are a number of small vesicle-filled profiles in the nerve plexus underneath the hair cell epithelium; some form efferent synapses with the neck hair cells (figures 21 and 24–26). In addition, a large number of fine, presumably efferent, fibres were found in the nerve bundles that innervate the neck hair cells (figure 30). These are strong indications that the neck hair cells are under efferent control, similar to the mechano-sensitive hair cells in the maculae and cristae of the cephalopod statocysts (see, for example, Colmers 1977, 1981; Budelmann *et al.* 1987). An efferent innervation of the neck hair cells, for example, would allow a feedback or a feedforward regulation of the hair cells' sensitivity, i.e. it could keep the cells in their best operating range. A similar function has been proposed for the efferent innervation of the statocyst hair cells of cephalopods (Williamson 1985, 1989; Williamson & Budelmann 1985) and other molluscs (Wolff 1970; Janse *et al.* 1988), as well as for vertebrate vestibular hair cells (Dieringer *et al.* 1977; Goldberg & Fernandez 1980).

In cephalopods, different types of synaptic vesicle have been described with respect to size and shape; they are most probably associated with different types of transmitters (Ducros 1979, Budelmann & Bonn 1982; Auerbach & Budelmann 1986, Williamson 1989; Tu & Budelmann 1994). Because the vesicles in the efferent profiles of the neck receptor organ are small, round and clear, they are presumably cholinergic and may have an inhibitory effect on the neck hair cells.

(iii) *Central projection*

The anterior and posterior neck hair cells project ipsilaterally to one brain area only: the ventral part of the ventral magnocellular lobe (figures 31–33). This area also receives direct input from the statocysts and the optic lobes (Young 1976). It seems likely, therefore, that in the ventral part of the ventral magnocellular lobe the statocyst and the visual information about head position in space, as well as the information about head-to-body position, are integrated for proper postural control. Further inputs into the magnocellular lobe are from the arm and funnel nerves (Young 1976), suggesting that the head-to-body position is also an integrative part of the system that coordinates the movements of the arms and funnel.

In decapods, the ventral magnocellular lobe is considered an intermediate motor centre with direct and indirect connections to several effector systems (Young 1939, 1976; Boycott 1961; Messenger 1983). In squids, it contains the first-order giant cells that mediate jet-propulsion and send fibres into the palliovisceral lobe, which is a motor centre for head retraction (Boycott 1961; Young 1976). This connection could be the pathway through which the neck receptor organ is involved in the control of the head retraction reflex that accompanies jet propulsion (T. Preuss, unpublished results).

Some output fibres from the magnocellular lobe project to higher motor centres in the supra-oesophageal part of the brain, such as the anterior and

median basal lobes (Young 1977). When electrically stimulated, these higher centres cause fin, funnel and head movements (Boycott 1961; Chichery 1983; Messenger 1983). It is therefore possible that the neck receptor organ influences the head-to-body positions and movements via this pathway.

The cobalt staining did not reveal the central origin (somata) of the efferent fibres, most probably because of the limitations of the cobalt staining technique when applied to small-diameter fibres (see Budelmann & Young 1984). Also, the cobalt staining gave no evidence of direct projections to the contralateral side of the brain; whether indirect connections exist via interneurons remains to be seen.

(iv) *Ultrastructure and morphological polarization*

The neck hair cells demonstrate several morphological features that indicate their mechanosensory function. Each hair cell is morphologically polarized by a uniform orientation of the basal feet on the basal bodies of its kinocilia. The direction of polarization is always at a right angle to the long axis of its ciliary group (figures 13 and 14); this is similar to the situation in the hair cells of the cephalopod statocyst and lateral line organs (Barber 1968; Budelmann *et al.* 1973, 1991; Budelmann 1979, 1988) and it is comparable to the situation in the hair cells of the vertebrate vestibular and lateral line systems (Flock 1971; Lowenstein 1974; Platt 1977). In vertebrate hair cells, a morphological polarization has a well-known physiological correlate (see, for example, Flock 1971; Jakobs & Hudspeth 1990), and this has recently been demonstrated for the hair cells in the statocyst of cephalopods as well (Budelmann & Williamson 1994): shear (deflection) of the cilia in the direction of their basal feet causes maximal excitation of the hair cells, and maximal inhibition when shear occurs in the opposite direction. By analogy with those results, the neck hair cells of *Lolliguncula* are almost certainly directionally sensitive mechanoreceptors.

In addition, the fact that the neck hair cells are located either on collagenous connective tissue or on a solid cartilaginous plate and are interlocked in a framework of supporting cells favours their mechanosensory function. Such support against lateral and vertical displacements is especially important for mechanosensory cells in the skin of soft-bodied animals to operate with any degree of precision. Furthermore, the cilia have well-developed rootlets originating from the basal bodies; this is characteristic of mechanoreceptive hair cells.

(v) *Location*

The neck hair cells are located between the nuchal cartilage and the nuchal crest plate. In squids, this is a strategic place for monitoring head-to-body movements because it is the only place where a defined (but limited) relative movement occurs between stiff structures that serve as a 'skeletal reference'. In addition, the concentration of polarized hair cells on the nuchal crest plate indicates their specific function. Concentrations of superficial proprioceptors that are stimulated by other body parts or contact sclerites are well known in arthropods and can be compared with vertebrate joint receptors (for references, see Introduction).

(*b*) *Function of the neck receptor organ*

(i) *The cartilaginous structures*

Besides their likely function as a 'skeletal reference', the nuchal cartilage and nuchal crest plate probably also serve to ensure a certain distance between the hair cell epithelium and the ventral surface of the nuchal cartilage; this distance is crucial for the stimulation of the hair cells (see below). Furthermore, because the surface contours of the hair cell epithelium and the overlying nuchal cartilage match, it is reasonable to assume that in a living animal the distance between the hair cell epithelium and the nuchal cartilage is not wider than the length of the cilia, to allow a proper mechanical contact of the tips of the cilia with the overlying nuchal cartilage. Such a contact, unless extremely firm, is difficult to see in LM, TEM and SEM preparations because of the differential shrinkage of the tissues during fixation.

(ii) *Stimulation of the neck receptor organ*

The connection between the nuchal cartilage and the nuchal crest plate allows some movement between these structures when the head is moved relative to the body. Such movements may be somewhat confined to medial and lateral pivoting movements over the top of the crest during head roll, and to shifts along the crest in anterior and posterior direction during head pitch. Strong support for this idea comes from the fact that for each of the two directions of movement (roll and pitch) a group of neck hair cells exists with matching polarization. According to this polarization, for any given angle of tilt the hair cells of the left and right anterior hair cell groups will be maximally stimulated during head roll, while the hair cells of the left and right posterior hair cell groups will be maximally stimulated during head pitch. The correspondence between stimulus direction and direction of sensitivity of the neck hair cells resembles the similar match known in the semicircular canals of vertebrates, in the statocyst canals of crustaceans, and in the proprioceptive neck organs (prosternal organs) of insects, where attitude specific motions of the auxiliary structures (cupula or contact sclerites) and the pattern of polarization of the receptors (hair cells or hair sensilla) coincide (Lowenstein 1974; Sandeman 1975; Preuss & Hengstenberg 1992).

The kinematics of the neck receptor organ of *Lolliguncula* during head movements is difficult to clarify satisfactorily through morphological studies because of fixation and dehydration artifacts, but electrophysiological recordings from the nerve that innervates the organ (the postorbital nerve) should clarify at least some points.

(*c*) *Proprioception in soft-bodied animals*

In vertebrates and arthropods, proprioceptive control of joints and jointed body parts depends on parallel sensory input from two kinds of proprioceptors: (1) the

joint receptors (vertebrates) and hair plate sensilla (arthropods), which provide information about the position of a joint (skeletal reference), and (2) the muscle spindle and tendon organs (vertebrates) and chordotonal organs (arthropods), which provide information about the force (strain) in the connecting muscles and tendons. These inputs together encode the position of a joint, as well as the direction and velocity of its movement.

In cephalopods, mechanosensitive strain (muscle) receptors associated with mantle and fin movements have been described in octopus, cuttlefish and squid (Alexandrowicz 1960; Gray 1960; Graziadei 1964*a*,*b*; Boyle 1976; Kier *et al.* 1985). There is little or no evidence, however, on whether or how the information gained by these receptors is used centrally (Gray 1960; Rowell 1966; Boyle 1976, 1986). Owing to the lack of an articulated skeleton, soft-bodied animals in general seem to have no equivalent of the 'skeletal reference' of vertebrates and arthropods (Laverack 1968, 1976; Dorsett 1976; Wells 1976; Boyle 1986). The neck receptor organ of *Lolliguncula brevis* can be considered the first exception to this rule. Similar organs seem to exist in the squids *Sepioteuthis lessoniana* and *Loligo opalescens* (T. Preuss, unpublished results).

(*d*) *Behavioural experiments*

As predicted from the gross morphology and ultrastructure, the behavioural experiments support the idea that the neck receptor organ of *Lolliguncula* has a proprioceptive function in head-to-body coordination during roll and pitch (see also §3(c)(i)).

(i) *Head roll*

In cephalopods, as well as in many other animals, compensatory head roll responses are known to be controlled by mechanosensory input from the equilibrium receptor organs (statocysts and otolith organs) (for further references, see Holst (1950) and Budelmann (1970)). The present experiments gave similar results for *Lolliguncula*. (1) During imposed body roll the compensatory head roll response is sinusoidal (as is common for compensatory responses that are driven by equilibrium receptor organs); and (2) after bilateral elimination of the statocysts the compensatory head roll response is destroyed.

Animals with the neck receptor organ unilaterally destroyed (but with the statocysts intact) show clear asymmetries of their compensatory head roll responses: (1) a reduced amplitude and a roughly 50% reduced gain, when the body was rolled to the operated, compared with the unoperated, side and (2) a head roll offset to the operated side. These asymmetries disappeared when the remaining intact neck receptor organ was also destroyed. The asymmetry in the compensatory head roll response indicates the presence of an asymmetric head roll command that is caused by a proprioceptive signal from the neck receptor organ.

These findings indicate that at least two mechanosensory inputs influence the head roll position in squid: (1) a statocyst signal that stabilizes the head with respect to gravity; and (2) a proprioceptive neck receptor organ signal that stabilizes the head with respect to the body. The two signals oppose each other during imposed body roll and ultimately lead to a head roll position that reflects an equilibrium between both head roll commands. Such an antagonistic interaction will enable an animal to realign head and body for any given head-to-body roll movement. In contrast, in the normal position, the two signals can assist each other for stabilizing the head and body roll position.

Similar interactions are also known in vertebrates for vestibular and proprioceptive neck reflexes (Mittelstaedt 1964; Peterson *et al.* 1981; Mergner *et al.* 1983*a*,*b*, 1992; Hlavacka *et al.* 1992), and can be compared with the interactions between the mechanosensory inputs from statocysts and leg proprioceptors found in crustaceans (Schöne & Neil 1977; Schöne *et al.* 1983).

In *Lolliguncula*, further evidence for an influence of the neck receptor organ on head roll comes from experiments that have shown that there exists a multimodal interaction of visual, statocyst and neck receptor organ inputs on the head roll position (Preuss & Budelmann 1995). The present behavioural and anatomical findings also indicate a possible central interaction of signals from the eyes, statocysts and the neck receptor organ for the control of head position. Such a interaction has been proposed for most animals that are able to move their head relative to the body (Mittelstaedt 1950, 1964; Roberts 1973; Mergner *et al.* 1981, 1992; Mittelstaedt & Mittelstaedt 1991).

(ii) *Head pitch*

In *Lolliguncula*, a bilateral elimination of the neck hair cell input caused a large head pitch offset (figures 37–39) and thereby demonstrates the importance of the proprioceptive input from the neck receptor organ for the control of head pitch. The offset also shows that the neck receptor organ influences the tonus of the head muscles, as has been shown, for example, for proprioceptive neck organs in insects (Shepheard 1974; Preuss & Hengstenberg 1992). In cephalopods, this influence could be due to a tonic discharge of neck hair cells that are stimulated when the head and body are aligned, i.e. that are in mechanical contact with the nuchal cartilage, or to a spontaneous activity of the neck hair cells. Such a permanent level of baseline activity is required for a bidirectionally sensitive mechanoreceptor and has been demonstrated electrophysiologically, for example, in afferent statocyst fibres of cephalopods (Budelmann 1976) and crustaceans (Cohen 1955, 1960; Knox 1970), and in insect neck proprioceptive afferents (Haskell 1960; Liske 1989).

The head pitch offset was large for animals with intact statocysts. Obviously, the input from the statocysts (which are located in the head) is not sufficient for a proper compensation of the head offset; or, conversely, the neck receptor organ plays a dominant role in the control of head pitch. Another explanation might be that head pitch is not rigidly linked to the absolute horizon and is thus not stabilized by the statocysts in this particular position. In fact,

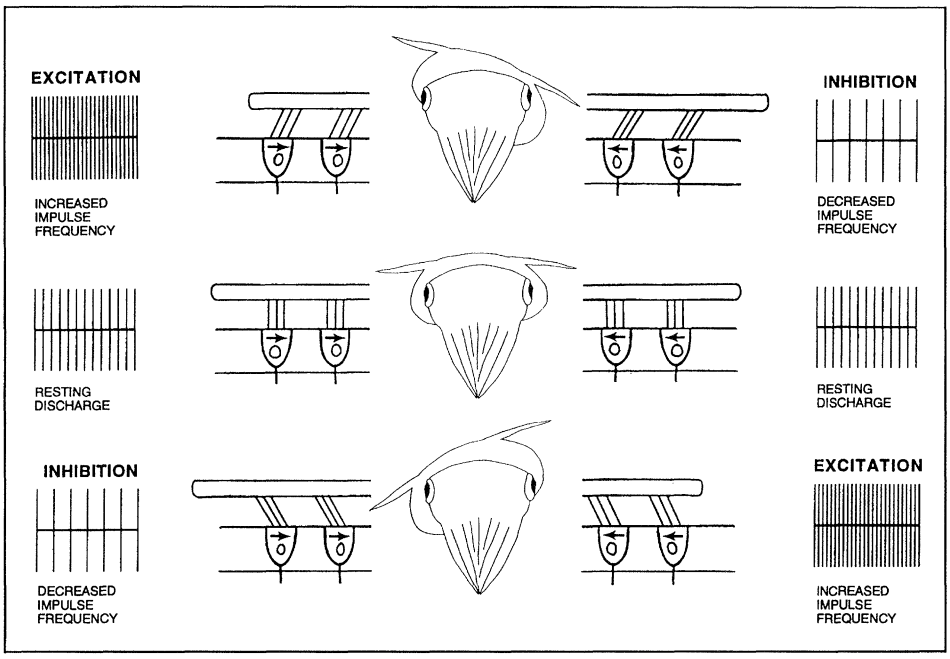

Figure 41. Diagrammatic illustration of the influence (excitation/inhibition) of head-to-body roll on the impulse frequency of the anterior hair cells of the neck receptor organ of *Lolliguncula*. The two diagrams to the left and right of the animal illustrate (1) the deflection of the cilia of the hair cells, caused by the movement of the nuchal cartilage relative to the hair cell epithelium, and (2) the presumed impulse frequency of the hair cells of the anterior hair cell group on that side (the arrows inside the hair cells indicate their direction of morphological polarization). Top row, imposed body roll to the left; middle row, normal body position; bottom row, imposed body roll to the right.

steady, simultaneous head and body pitch positions are frequently seen in free-swimming squid; they are part of normal squid behaviour (Moynihan & Rodaniche 1982).

The variability in head pitch position contrasts the rigidly controlled head roll position and seems to counteract the effort of stabilizing the visual image on the retina. The large compensatory counter-rolling of the eyes ($\pm 45°$) that decapod cephalopods show when pitched, however, may account for proper compensation (Budelmann 1975, 1990). The variability in head pitch could also indicate that stabilization is essential only in some situations; such plasticity is known, for example, in head control systems of insects (Wolf & Heisenberg 1980; Hengstenberg *et al.* 1986).

The amount of compensatory eye movements during head roll is not known, but owing to anatomical constraints it is certainly limited (Budelmann & Young 1993). Consequently, to achieve a proper visual stabilization during roll, a rigidly controlled head roll position is essential.

In *Lolliguncula*, a statocyst-driven compensatory head pitch occurs during imposed downward and upward body pitch. The downward head pitch offset of animals with the neck receptor organ bilaterally destroyed was therefore superimposed on the statocyst-controlled compensatory head pitch (figures 38 and 39); this, in turn, suggests a continuous input of the neck receptor organ into the system that controls head pitch. The additive interaction (with respect to the behavioural output) of the statocyst and neck receptor organ inputs may suggest that an elimination of the neck receptor organ causes a central 'error position signal' that is added to the positional signal from the statocysts. Such a linear interaction of proprioceptive and equilibrium receptor inputs was originally suggested by Mittelstaedt (1964) and has been shown in invertebrates and vertebrates (Peterson *et al.* 1981; Horn 1983; Mergner *et al.* 1983*b*).

In the present experiments, the largest head pitch response of $-33°$ was seen during imposed upward pitch in animals deprived of their neck receptor organs. This might be close to the anatomical limit for head downward pitch and could explain why a further upward body pitch caused the head pitch response to reverse direction.

(*e*) *Control of head yaw by the neck receptor organ?*

The distribution and polarization pattern of the hair cells within the neck receptor organ do not include hair cells that are strategically placed for a control of head-to-body movements in the yaw plane. Nevertheless, such yaw movements could be sensed via an interaction (differential signal) of the left and right groups of hair cells. Preliminary experiments with optokinetically induced head yaw in intact and unilaterally operated animals, however, have given no clear evidence that the neck receptor organ controls head yaw, but further experiments are necessary to clarify this point.

(*f*) *Interaction of the left and right hair cell groups of the neck receptor organ*

The neck receptor organ consists of a left and right anterior group of hair cells with opposing (medial) directions of polarization, and a left and right posterior group of hair cells with identical (anterior) directions

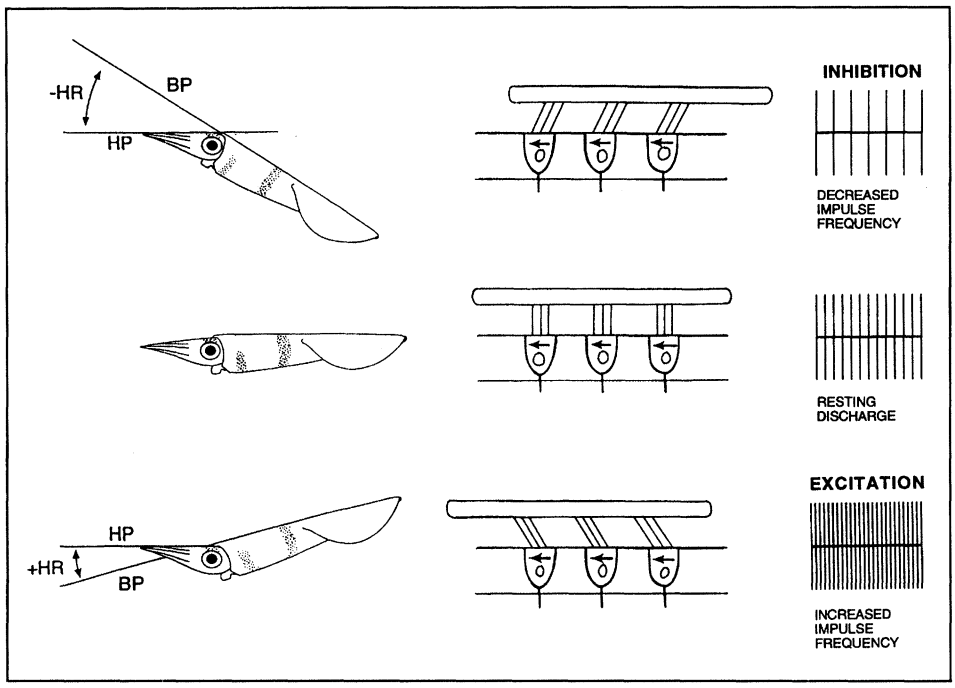

Figure 42. Diagrammatic illustration of the influence (excitation/inhibition) of head-to-body pitch on the impulse frequency of the posterior hair cells of the neck receptor organ of *Lolliguncula*. The two diagrams to the right of the animal illustrate (1) the deflection of the cilia of the hair cells, caused by the movement of the nuchal cartilage relative to the hair cell epithelium, and (2) the presumed impulse frequency of the hair cells of the left and right posterior hair cell groups (the arrows inside the hair cells indicate their direction of morphological polarization). Top row, imposed body upward pitch; middle row, normal body position; bottom row, imposed body downward pitch.

of polarization (figure 11). According to the likely kinematics of the neck receptor organ, any head-to-body roll should stimulate the anterior hair cells in such a way that the discharge activities increase in one group and simultaneously decrease in the other (figure 41). A central integration of these two activities will then produce a differential signal that encodes the direction, as well as the magnitude of the head-to-body roll, and ultimately causes the realignment of the head and body (neck-reflex). A neutral head roll position is achieved by a balance between the activities of the left and right anterior hair cell groups, and those of the left and right head muscle systems that are involved in head roll. Head-to-body pitch, on the other hand, will cause an identical increase, or decrease, in the activity of the left and right posterior hair cell groups (figure 42). Therefore during pitch the activity of either organ, or their central summation, includes the signal that encodes the direction and the magnitude of the head-to-body pitch, and ultimately causes the realignment of the head and body.

This work was supported by German LGFG and DAAD funds (T.P.) and in part by NIH grant (EY 08312–02/05; B.U.B.). Additional support was provided by the Marine Medicine Budget of the Marine Biomedical Institute of the University of Texas Medical Branch at Galveston. Animals were provided through NIH grants RR 01024 and RR 04226 (Dr Roger T. Hanlon). The authors thank Matthew S. Dobbins for assistance with TEM and photography, and Carrie O'Farrell and Vijay K. Ravula for help with some behavioural experiments and data analyses. The Schriners Burns Institute kindly allowed the use of their scanning electron microscope. T.P. thanks Professor D. Varjú (Tübingen) for additional support and advice with the project and H. Neumeister for her help with the drawings, helpful discussions and encouragement.

REFERENCES

Alexandrowicz, J. S. 1960 A muscle receptor organ in *Eledone cirrosa*. *J. mar. biol. Ass. U.K.* **39**, 419–431.

Auerbach, B. & Budelmann, B. U. 1986 Evidence for acetylcholine as a neurotransmitter in the statocyst of *Octopus vulgaris*. *Cell Tiss. Res.* **243**, 429–436.

Barber, V. C. 1968 The structure of mollusc statocysts with particular reference to cephalopods. *Symp. zool. Soc. Lond.* **23**, 37–62.

Biemond, A. & De Jong, J. M. B. V. 1969 On cervical nystagmus and related disorders. *Brain* **92**, 437–458.

Bilo, D. 1991 Integration opto- und mechanosensorischer Afferenzen bei der Flugsteuerung der Haustaube (*Columbia livia* var. *domestica*). *Zool. Jb. Physiol.* **95**, 325–330.

Bilo, D. & Bilo, A. 1983 Neck flexion related activity of flight control muscles in the flow-stimulated pigeon. *J. comp. Physiol.* A **153**, 111–122.

Boycott, B. B. 1961 The functional organization of the brain of the cuttlefish *Sepia officinalis*. *Proc. R. Soc. Lond.* B **153**, 503–534.

Boyle, P. R. 1976 Receptor units responding to movement in the octopus mantle. *J. exp. Biol.* **65**, 1–9.

Boyle, P. R. 1986 Neural control of cephalopod behavior. In *The Mollusca*, vol. 9 (*Neurobiology and behavior*, part 2) (ed. A. O. D. Willows), pp. 1–99. Orlando, Florida: Academic Press.

Budelmann, B. U. 1970 Die Arbeitsweise der Statolithenorgane von *Octopus vulgaris*. *Z. vergl. Physiol.* **70**, 278–312.

Budelmann, B. U. 1975 Gravity receptor function in cephalopods with particular reference to *Sepia officinalis*. *Fortschr. Zool.* **23**, 84–98.

Budelmann, B. U. 1976 Equilibrium receptor systems in molluscs. In *Structure and function of proprioceptors in the invertebrates* (ed. P. J. Mill), pp. 529–566. London: Chapman & Hall.

Budelmann, B. U. 1979 Hair cell polarization in the gravity receptor system of the statocysts of the cephalopods *Sepia officinalis* and *Loligo vulgaris*. *Brain Res.* **160**, 261–270.

Budelmann, B. U. 1988 Morphological diversity of equilibrium receptor systems in aquatic invertebrates. In *Sensory biology of aquatic animals* (ed. J. Atema, R. R. Fay, A. N. Popper & W. N. Tavolga), pp. 757–782. New York: Springer-Verlag.

Budelmann, B. U. 1990 The statocysts of squid. In *Squid as experimental animals* (ed. D. L. Gilbert, W. J. Adelman & J. M. Arnold), pp. 421–439. New York: Plenum Press.

Budelmann, B. U. 1994 Cephalopod sense organs, nerves and the brain: adaptations for high performance and life style. *Mar. Fresh Behav. Physiol.* **25**, 13–33.

Budelmann, B. U. & Bonn, U. 1982 Histochemical evidence for catecholamines as neurotransmitters in the statocyst of *Octopus vulgaris*. *Cell Tiss. Res.* **227**, 475–483.

Budelmann, B. U. & Williamson, R. 1994 Directional sensitivity of hair cell afferents in the *Octopus* statocyst. *J. exp. Biol.* **187**, 245–259.

Budelmann, B. U. & Young, J. Z. 1984 The statocyst–oculomotor system of *Octopus vulgaris*: extraocular eye muscles, eye muscle nerves, statocyst nerves, and the oculomotor centre in the central nervous system. *Phil. Trans. R. Soc. Lond.* B **306**, 159–189.

Budelmann, B. U. & Young, J. Z. 1985 Central pathways of the nerves of the arms and mantle of *Octopus*. *Phil. Trans. R. Soc. Lond.* B **310**, 109–122.

Budelmann, B. U. & Young, J. Z. 1993 The oculomotor system of decapod cephalopods: eye muscles, eye nerves, and the oculomotor neurons in the central nervous system. *Phil. Trans. R. Soc. Lond.* B **340**, 93–125.

Budelmann, B. U., Barber, V. C. & West, S. 1973 Scanning electron microscopical studies of the arrangements and numbers of hair cells in the statocysts of *Octopus vulgaris*. *Sepia officinalis* and *Loligo vulgaris*. *Brain Res.* **56**, 25–41.

Budelmann, B. U., Sachse, M. & Staudigl, M. 1987 The angular acceleration receptor system of *Octopus vulgaris*: morphometry, ultrastructure, and neuronal and synaptic organization. *Phil. Trans. R. Soc. Lond.* B **315**, 305–343.

Budelmann, B. U., Riese, U. & Bleckmann, H. 1991 Structure, function, biological significance of the cuttlefish 'lateral lines'. In *The cuttlefish* (ed. E. Boucaud-Camou), pp. 201–209. Caen: Centre de Publications de l'Université.

Chichery, R. 1983 Motor and behavioural responses obtained by electrical stimulation of peduncle and basal lobes: the control of the visual-static centres on oculomotor reactions and locomotion in the cuttlefish, *Sepia officinalis*. *Fortschr. Zool.* **28**, 231–240.

Cohen, M. J. 1955 The function of the receptors in the statocyst of the lobster *Homarus americanus*. *J. Physiol., Lond.* **130**, 9–34.

Cohen, M. J. 1960 The response pattern of single receptors in the crustacean statocyst. *Proc. R. Soc. Lond.* B **152**, 30–49.

Collewijn, H. 1970 Oculomotor reactions in the cuttlefish *Sepia officinalis*. *J. exp. Biol.* **52**, 369–384.

Colmers, W. F. 1977 Neuronal and synaptic organization in the gravity receptor system of the statocyst of *Octopus vulgaris*. *Cell Tiss. Res.* **185**, 491–503.

Colmers, W. F. 1981 Afferent synaptic connections between hair cells and the somata of intramacular neurons in the gravity receptor system of the statocyst of *Octopus vulgaris*. *J. comp. Neurol.* **197**, 385–394.

De Jong, J. M. B. V. & Bles, W. 1986 Cervical dizziness and ataxia. In *Disorders of posture and gait* (ed. W. Bles & T. Brandt), pp. 185–206. Amsterdam: Elsevier.

Dieringer, N., Blanks, R. H. I. & Precht, W. 1977 Cat efferent vestibular system: weak suppression of primary afferent activity. *Neurosci. Lett.* **5**, 285–290.

Dijkgraaf, S. 1961 The statocyst of *Octopus vulgaris* as a rotation receptor. *Pubblns Staz. Zool. Napoli* **32**, 64–87.

Dijkgraaf, S. 1963 Nystagmus and related phenomena in *Sepia officinalis*. *Experientia* **19**, 29–30.

Dorsett, D. A. 1976 The structure and function of proprioceptors in soft-bodied invertebrates. In *Structure and function of proprioceptors in the invertebrates* (ed. P. J. Mill), pp. 443–484. London: Chapman & Hall.

Ducros, C. 1979 Synapses of cephalopods. *Int. Rev. Cytol.* **56**, 1–22.

Flock, Å. 1971 Sensory transduction in hair cells. In *Handbook of sensory physiology: principles of receptor physiology*, vol. 1 (ed. W. R. Lowenstein), pp. 396–441. Berlin, Heidelberg and New York: Springer-Verlag.

Foyle, T. P. & O'Dor, R. K. 1988 Predatory strategies of squid (*Illex illecebrosus*) attacking small and large fish. *Mar. Behav. Physiol.* **13**, 155–168.

Geiger, G. & Poggio, T. 1977 On head and body movements of flying flies. *Biol. Cybern.* **25**, 177–180.

Goldberg, J. M. & Fernandez, C. 1980 Efferent vestibular system in the squirrel monkey: anatomical location and influence on afferent activity. *J. Neurophysiol.* **43**, 986–1025.

Goodman, L. J. 1965 The role of certain optomotor reactions in regulating stability in the rolling plane during flight in the desert locust *Schistocerca gregaria*. *J. exp. Biol.* **42**, 385–407.

Gray, J. A. B. 1960 Mechanically excitable receptor units in the mantle of the *Octopus* and their connections. *J. Physiol., Lond.* **153**, 573–582.

Graziadei, P. 1964*a* Receptors in the sucker of the cuttlefish. *Nature, Lond.* **203**, 384–386.

Graziadei, P. 1964*b* Muscle receptors in cephalopods. *Proc. R. Soc. Lond.* B **161**, 392–402.

Haskell, P. T. 1959 Hair receptors in locust. Function of certain prothoracic hair receptors in the desert locust. *Nature, Lond.* **183**, 1107.

Haskell, P. T. 1960 The sensory equipment of the migratory *locust*. *Symp. zool. Soc. Lond.* **3**, 1–23.

Hengstenberg, R. 1988 Mechanosensory control of compensatory head roll during flight in the blowfly *Calliphora erythrocephala* Meig. *J. comp. Physiol.* A **163**, 151–165.

Hengstenberg, R., Sandeman, D. C. & Hengstenberg, B. 1986 Compensatory head roll in the blowfly *Calliphora* during flight. *Proc. R. Soc. Lond.* B **227**, 455–482.

Hensler, K. & Robert, D. 1990 Compensatory head rolling during corrective flight steering in locusts. *J. comp. Physiol.* A **166**, 685–693.

Hlavacka, F., Mergner, T. & Schweigart, G. 1992 Interaction of vestibular and proprioceptive inputs for human self-motion perception. *Neurosci. Lett.* **138**, 161–164.

Hoffmann, C. 1963 Vergleichende Physiologie der mechanischen Sinne. *Fortschr. Zool.* **16**, 268–332.

Hoffmann, C. 1964 Bau und Vorkommen von proprioceptiven Sinnesorganen bei den Arthropoden. *Ergebn. Biol.* **27**, 1–38.

Holst, E. von 1950 Die Arbeitsweise des Statolithenapparates bei Fischen. *Z. vergl. Physiol.* **32**, 60–120.

Horn, E. 1983 Behavioural reactions in bimodal fields of stimulus in insects with special reference to flies, *Calliphora erythrocephala*. *Fortschr. Zool.* **28**, 179–196.

Horn, E. & Lang, H. G. 1978 Positional head reflexes and the role of the prosternal organ in the walking fly, *Calliphora erythrocephala*. *J. comp. Physiol.* A **126**, 137–146.

Jakobs, R. A. & Hudspeth, A. J. 1990 Ultrastructural

correlates of mechanoelectrical transduction in hair cells of the bullfrog's internal ear. *Cold Spring Harb. Symp. quant. Biol.* **55**, 547–561.

Janse, C., van der Wilt, G. J., van der Roest, M. & Pieneman, A. W. 1988 Intracellularly recorded responses to tilt and efferent input of statocyst sensory cells in the pulmonate snail *Lymnea stagnalis*. *Comp. Biochem. Physiol.* **90A**, 269–278.

Kier, W. M., Messenger, J. B. & Miyan, J. A. 1985 Mechanoreceptors in the fins of the cuttlefish, *Sepia officinalis*. *J. exp. Biol.* **119**, 369–373.

Knox, C. K. 1970 Signal transmission in random spike trains with applications to the statocyst neurons of the lobster. *Kybernetik* **7**, 167–174.

Land, M. F. 1973 Head movement of flies during visually guided flight. *Nature, Lond.* **243**, 299–300.

Laverack, M. S. 1968 On the receptors of marine invertebrates. *Ann. Rev. Oceanogr. mar. Biol.* **6**, 249–324.

Laverack, M. S. 1976 External proprioceptors. In *Structure and function of proprioceptors in the invertebrates* (ed. P. J. Mill), pp. 1–63. London: Chapman & Hall.

Liske, E. 1977 The influence of head position on the flight behaviour of the fly *Calliphora erythrocephala*. *J. Insect Physiol.* **23**, 375–379.

Liske, E. 1989 Neck hair plate sensilla of the praying mantis: central projections of the afferent neurons and their physiological responses to imposed head movement in the yaw plane. *J. Insect Physiol.* **35**, 677–687.

Lowenstein, O. E. 1974 Comparative morphology and physiology. In *Vestibular system*, part 1 (*Basic mechanisms*) (ed. H. H. Kornhuber), pp. 75–120. Berlin, Heidelberg and New York: Springer-Verlag.

Mangold, K., Bidder, A. M. & Portmann, A. 1989 Organisation générale des céphalopodes. In *Traité de zoologie. anatomie, systématique, biologie*, thome V (*Céphalopodes*) (ed. P. P. Grassé), pp. 7–69. Paris: Masson.

McCouch, G. P., Deering, I. D. & Ling, T. H. 1951 Location of receptors for tonic neck reflexes. *J. Neurophysiol.* **14**, 191–195.

Mergner, T., Deecke, L. & Becker, W. 1981 Patterns of vestibular and neck responses and their interaction: A comparison between cat cortical neurons and human psychophysics. *Ann. N.Y. Acad. Sci.* **374**, 361–372.

Mergner, T., Deecke, L., Becker, W. & Kornhuber, H. H. 1983*a* Vestibular-proprioceptive interactions: neurophysiology and psychophysics. *Fortschr. Zool.* **28**, 241–252.

Mergner, T., Nardi, G. L., Becker, W. & Deecke, L. 1983*b* The role of canal–neck interaction for the perception of horizontal trunk and head rotation. *Expl Brain Res.* **49**, 198–208.

Mergner, T., Rottler, G., Kimmig, H. & Becker, W. 1992 Role of vestibular and neck inputs for the perception of object motion in space. *Expl Brain Res.* **89**, 655–668.

Messenger, J. B. 1968 The visual attack of the cuttlefish, *Sepia officinalis*. *Anim. Behav.* **16**, 342–357.

Messenger, J. B. 1970 Optomotor responses and nystagmus in intact, blinded and statocystless cuttlefish (*Sepia officinalis* L.). *J. exp. Biol.* **53**, 789–796.

Messenger, J. B. 1977 Prey-capture and learning in the cuttlefish, *Sepia*. *Symp. zool. Soc. Lond.* **38**, 347–376.

Messenger, J. B. 1981 Comparative physiology of vision in molluscs. In *Handbook of sensory physiology*, vol. VII/6 C (*Vision in invertebrates*) (ed. H. Autrum), pp. 93–200. Berlin, Heidelberg and New York: Springer-Verlag.

Messenger, J. B. 1983 Multimodal convergence and the regulation of motor programs in cephalopods. *Fortschr. Zool.* **28**, 77–98.

Messenger, J. B., Nixon, M. & Ryan, K. P. 1985 Magnesium chloride as an anaesthetic for cephalopods. *Comp. Biochem. Physiol.* **82**, 203–205.

Miall, R. C. 1990 Visual control of steering in locust flight: the effects of head movement on responses to roll stimuli. *J. comp. Physiol.* A **166**, 735–744.

Mittelstaedt, H. 1950 Physiologie des Gleichgewichtssinnes bei fliegenden Libellen. *Z. vergl. Physiol.* **32**, 422–463.

Mittelstaedt, H. 1964 Basic control patterns of orientational homeostasis. *Symp. Soc. exp. Biol.* **18**, 365–385.

Mittelstaedt, H. & Mittelstaedt, M. L. 1991 From interdependent to independent control of head and trunk. In *The head–neck sensory motor system* (ed. A. Bertholz, W. Graf & P. P. Vidal), pp. 369–373. New York: Oxford University Press.

Moynihan, M. & Rodaniche, A. F. 1982 The behavior and natural history of the Caribbean reef squid *Sepioteuthis sepioidea*. *Adv. Ethol.* **25**, 1–150.

Peters, W. 1962 Die Proprioreзeptiven Organe am Prosternum und an den Labellen von *Calliphora erythrocephala* Mg. *Z. Morph. Ökol. Tiere* **51**, 211–226.

Peterson, B. W., Bilotto, G., Goldberg, J. & Wilson, V. J. 1981 Dynamics of vestibulo-ocular, vestibulo-collic, and cervico-collic reflexes. *Ann. N.Y. Acad. Sci.* **374**, 395–402.

Platt, C. 1977 Hair cell distribution and orientation in goldfish otolith organs. *J. comp. Neurol.* **172**, 283–298.

Preuss, T. & Budelmann, B. U. 1991 A new sense organ in cephalopods: sensory hair cells on the neck of the squid *Lolliguncula brevis*. *Soc. Neurosci. Abstr.* **17**, 1403.

Preuss, T. & Budelmann, B. U. 1995 A dorsal light response in a squid. *J. exp. Biol.* **198**, 1157–1159.

Preuss, T. & Hengstenberg, R. 1990 The influence of neck sense organs on head position in the blowfly *Calliphora erythrocephala* M. In *Brain, perception, cognition* (ed. N. Elsner & G. Roth), p. 123. Stuttgart: Thieme.

Preuss, T. & Hengstenberg, R. 1992 Structure and kinematics of the prosternal organs and their influence on head position in the blowfly *Calliphora erythrocephala* Meig. *J. comp. Physiol.* A **171**, 483–493.

Roberts, T. D. M. 1973 Reflex balance. *Nature, Lond.* **244**, 156–158.

Rowell, C. H. F. 1966 Activity of interneurones in the arm of octopus in response to tactile stimulation. *J. exp. Biol.* **44**, 589–605.

Sandeman, D. C. 1975 Dynamic receptors in the statocysts of crabs. *Fortschr. Zool.* **23**, 185–191.

Schöne, H. & Neil, D. M. 1977 The integration of leg position-receptors and their interaction with statocyst inputs in spiny lobsters. (Reactions of *Palinurus vulgaris* to substrate tilt, III.) *Mar. Behav. Physiol.* **5**, 45–59.

Schöne, H., Neil, D. M., Scapini, F. & Dreissmann, G. 1983 Interaction of substrate, gravity and visual cues in the control of compensatory eye responses in the spiny lobster *Palinurus vulgaris*. *J. comp. Physiol.* A **150**, 23–30.

Shepheard, P. 1974 Control of head movements in the locust, *Schistocerca gregaria*. *J. exp. Biol.* **60**, 735–767.

Stephens, P. R. & Young, J. Z. 1982 The statocyst of the squid *Loligo*. *J. Zool., Lond.* **197**, 241–266.

Taylor, J. 1992 Perception of the orientation of the head on the body in man. In *The head–neck sensory motor system* (ed. A. Bertholz, W. Graf & P. P. Vidal), pp. 488–490. Oxford and New York: University Press.

Taylor, J. L. & McCloskey, D. I. 1988 Proprioception in the neck. *Expl Brain Res.* **70**, 351–360.

Thurm, U. 1963 Die Beziehung zwischen mechanischen Reizgrössen und stationären Erregungszuständen bei Borstenfeld Sensillen von Bienen. *Z. vergl. Physiol.* **46**, 351–382.

Tu, Y. & Budelmann, B. U. 1994 The effect of L-glutamate on the afferent resting activity in the cephalopod statocyst. *Brain Res.* **642**, 47–58.

Wells, M. J. 1976 Proprioception and learning. In *Structure*

and function of proprioceptors in the invertebrates (ed. P. J. Mill), pp. 567–604. London: Chapman & Hall.

Wells, M. J. 1988 The mantle muscle and mantle cavity of cephalopods. In *The Mollusca*, vol. 11 (*Form and function*) (ed. E. R. Trueman & M. R. Clarke), pp. 287–300. San Diego: Academic Press.

Williams, L. W. 1909 *The anatomy of the common squid* Loligo pealii, *Lesueur*. Leiden: E. J. Brill.

Williamson, R. 1985 Efferent influences on the afferent activity from the octopus angular acceleration receptor system. *J. exp. Biol.* **119**, 251–264.

Williamson, R. 1989 Secondary hair cells and afferent neurons of the squid statocyst receive both inhibitory and excitatory efferent inputs. *J. comp. Physiol.* A **165**, 847–860.

Williamson, R. & Budelmann, B. U. 1985 An angular acceleration receptor system of dual sensitivity in the statocyst of *Octopus vulgaris*. *Experientia* **41**, 1321–1322.

Wolf, R. & Heisenberg, M. 1980 On the fine structure of yaw torque in visual field organization of *Drosophila melanogaster*. 2. A temporally and spatially weighting function for the visual field (visual attention). *J. comp. Physiol.* A **140**, 69–80.

Wolff, H. G. 1970 Efferente Aktivität in den Statonerven einiger Landpulmonaten (Gastropoda). *Z. vergl. Physiol.* **70**, 401–409.

Yang, W. T., Hanlon, R. T., Lee, P. G. & Turk, P. E. 1989 Design and function of closed seawater systems for culturing loliginid squids. *Aquacul. Engng* **8**, 47–65.

Young, J. Z. 1938 The functioning of the giant nerve fibres of the squid. *J. exp. Biol.* **15**, 170–185.

Young, J. Z. 1939 Fused neurons and synaptic contacts in the giant nerve fibres of cephalopods. *Phil. Trans. R. Soc. Lond.* B **229**, 465–503.

Young, J. Z. 1960 The statocysts of *Octopus vulgaris*. *Proc. R. Soc. Lond.* B **152**, 3–29.

Young, J. Z. 1976 The nervous system of *Loligo*. II. Suboesophageal centres. *Phil. Trans. R. Soc. Lond.* B **274**, 101–166.

Young, J. Z. 1977 The nervous system of *Loligo*. III. Higher motor centres: the suboesophageal lobes. *Phil. Trans. R. Soc. Lond.* B **276**, 351–398.

Young, J. Z. 1979 The nervous system of *Loligo*. V. The vertical lobe complex. *Phil. Trans. R. Soc. Lond.* B **285**, 311–354.

Young, J. Z. 1989 The angular acceleration receptor system of diverse cephalopods. *Phil. Trans. R. Soc. Lond.* B **325**, 189–237.

Received 12 December 1994, accepted 6 February 1995

ABBREVIATIONS USED IN FIGURES

b.a.	anterior basal lobe
b.b.	basal body
b.d.	dorsal basal lobe
b.f.	basal foot
b.med.	median basal lobe
BP	body position
br.	brachial lobe
c.c.	cartilage cell(s)
ch.	chromatophore
ch.p.	posterior chromatophore lobe
col.	collagen
cra.	cranium
c.r.m.	cephalic retractor muscle
c.t.	connective tissue
eff.	efferent
f.l.c.	funnel locking cartilage
fr.i.	inferior frontal lobe
fr.s.	superior frontal lobe
gl.	gladius
h.c.	hair cells
h.c.a.	anterior hair cells
h.c.p.	posterior hair cells
h.r.m.	head retractor muscle
HP	head position
HR	head response
in.	interdigitation
k.	kinocilium
m.	muscle (fibre)
ma.	mantle
mag.d.	dorsal magnocellular lobe
mag.ven.	ventral magnocellular lobe
mu.c.	mucus cell
n.b.	nerve bundle
n.cr.maj.	nervus crista major
ne.	neck
n.orb.p.	nervus postorbitalis
np.	nerve plexus
nu.c.	nuchal cartilage
nu.cr.	nuchal crest
nu.cr.p.	nuchal crest plate
nu.r.m.	nuchal retractor muscle
oe.	oesophagus
pe.a.	anterior pedal lobe
pe.p.	posterior pedal lobe
ps.p.	presynaptic profile
pv.	palliovisceral lobe
ro.	rootlet
s.c.	supporting cell
st.	statocyst
v.	vertical lobe

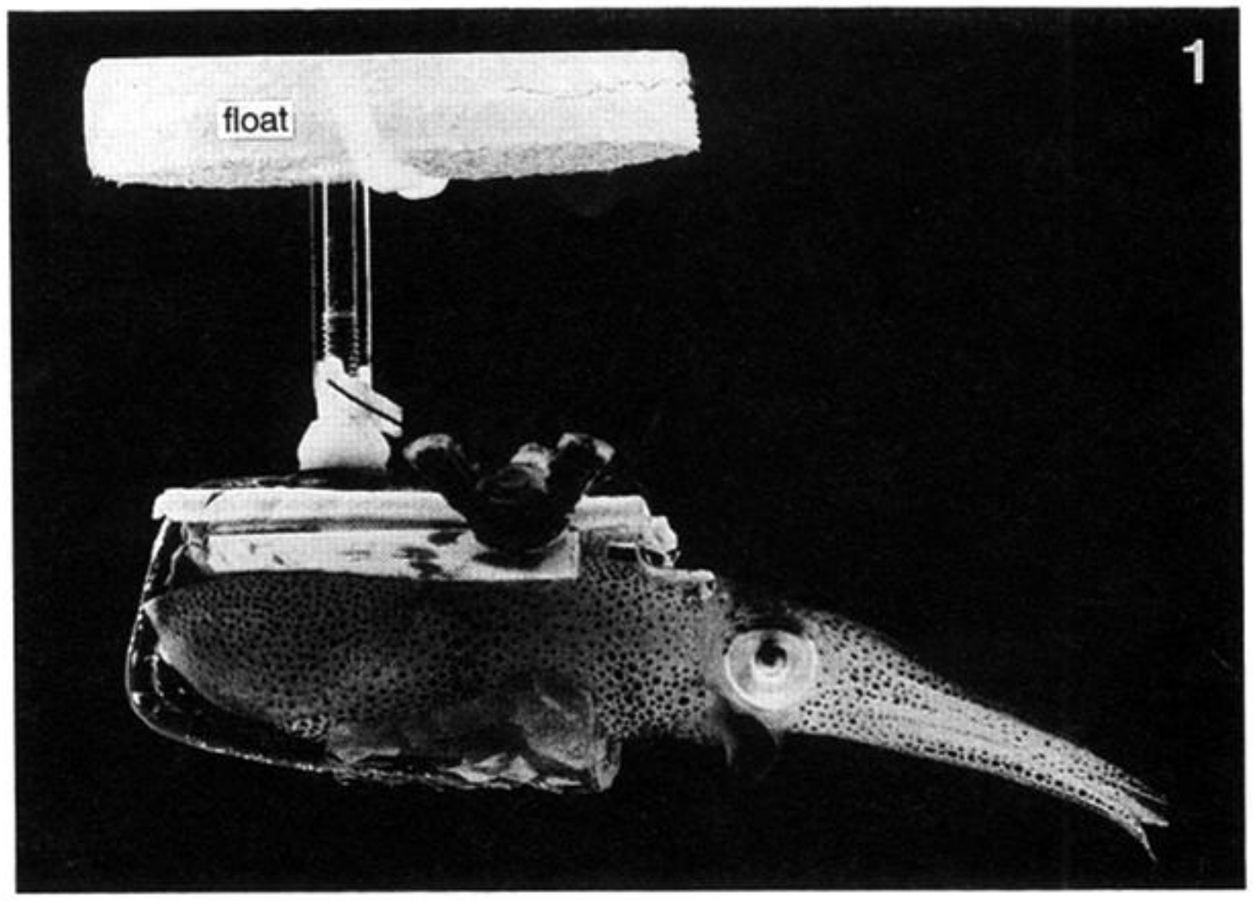

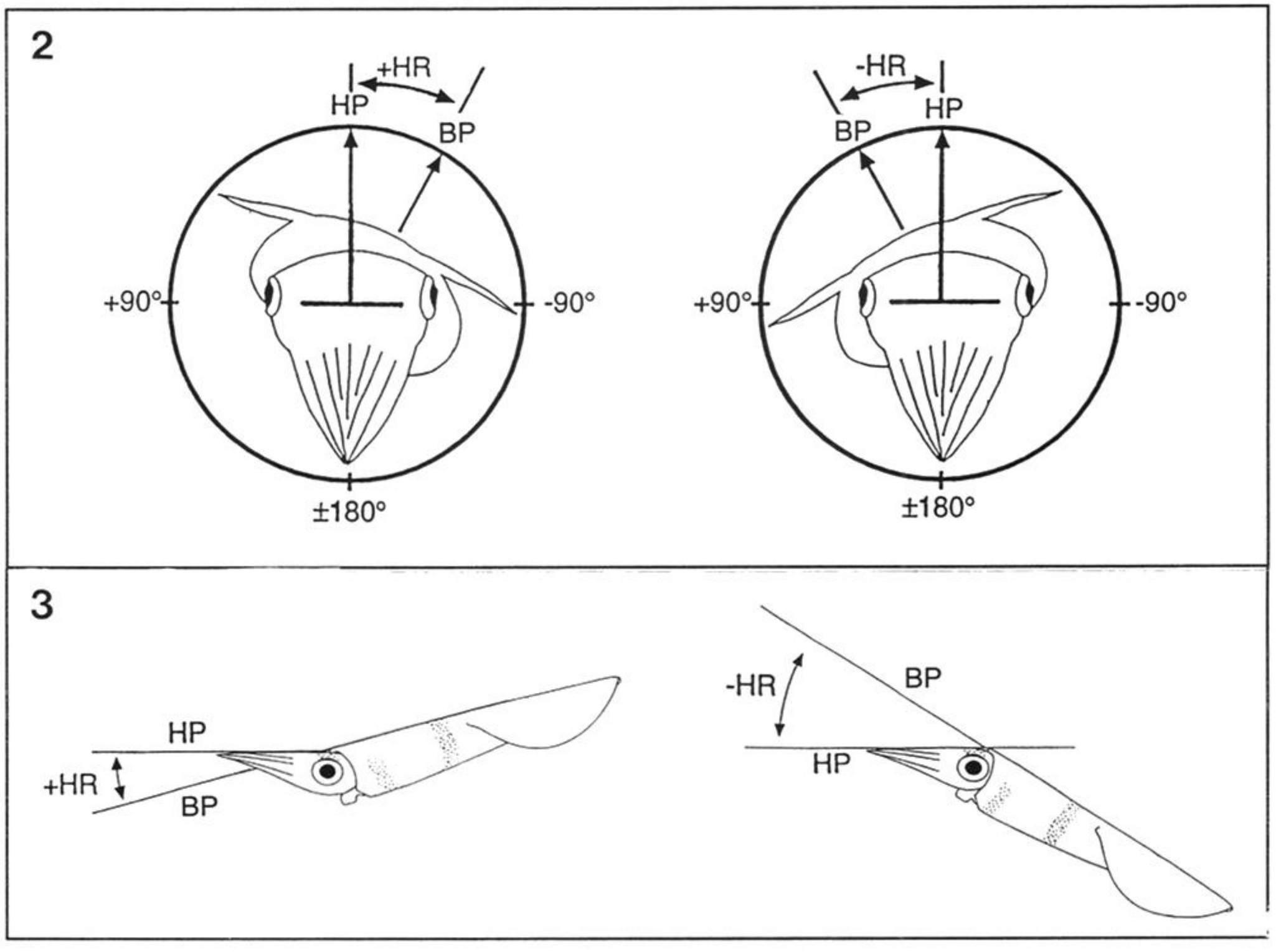

Figure 1. The squid *Lolliguncula brevis* attached to the animal-holder that keeps the animal's body in a fixed position but allows unrestricted movements of the animal's head. During the experiments the holder is connected to a rotation device; in the figure it is made neutrally buoyant by a float to allow the animal to swim 'freely'.

Figures 2 and 3. Illustrations of the head response ($\pm$HR) and the positions of the animal's head (HP) and body (BP) during body roll (figure 2) and body pitch (figure 3). The head response (HR = HP − BP) for roll (figure 2) is the angle between the head and body mid-sagittal planes, and for pitch (figure 3) the angle between the head and body horizontal planes.

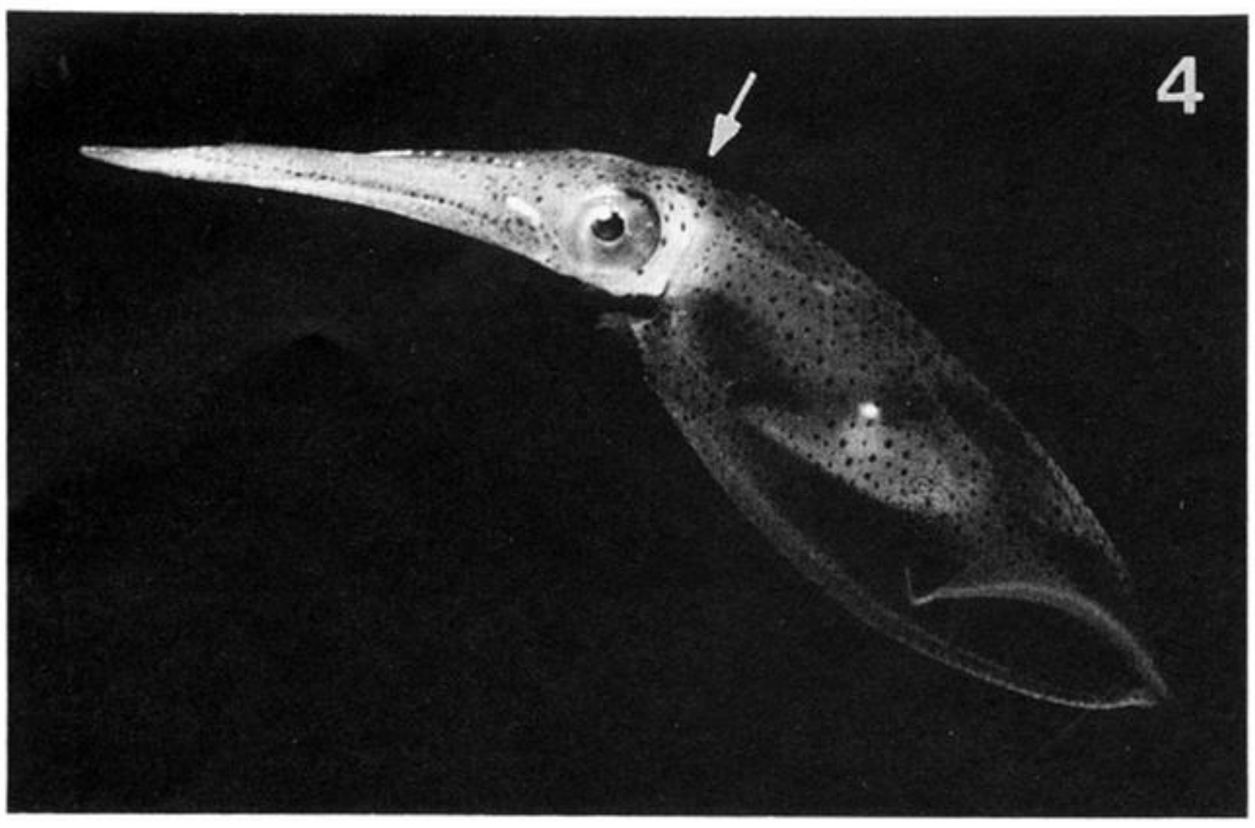

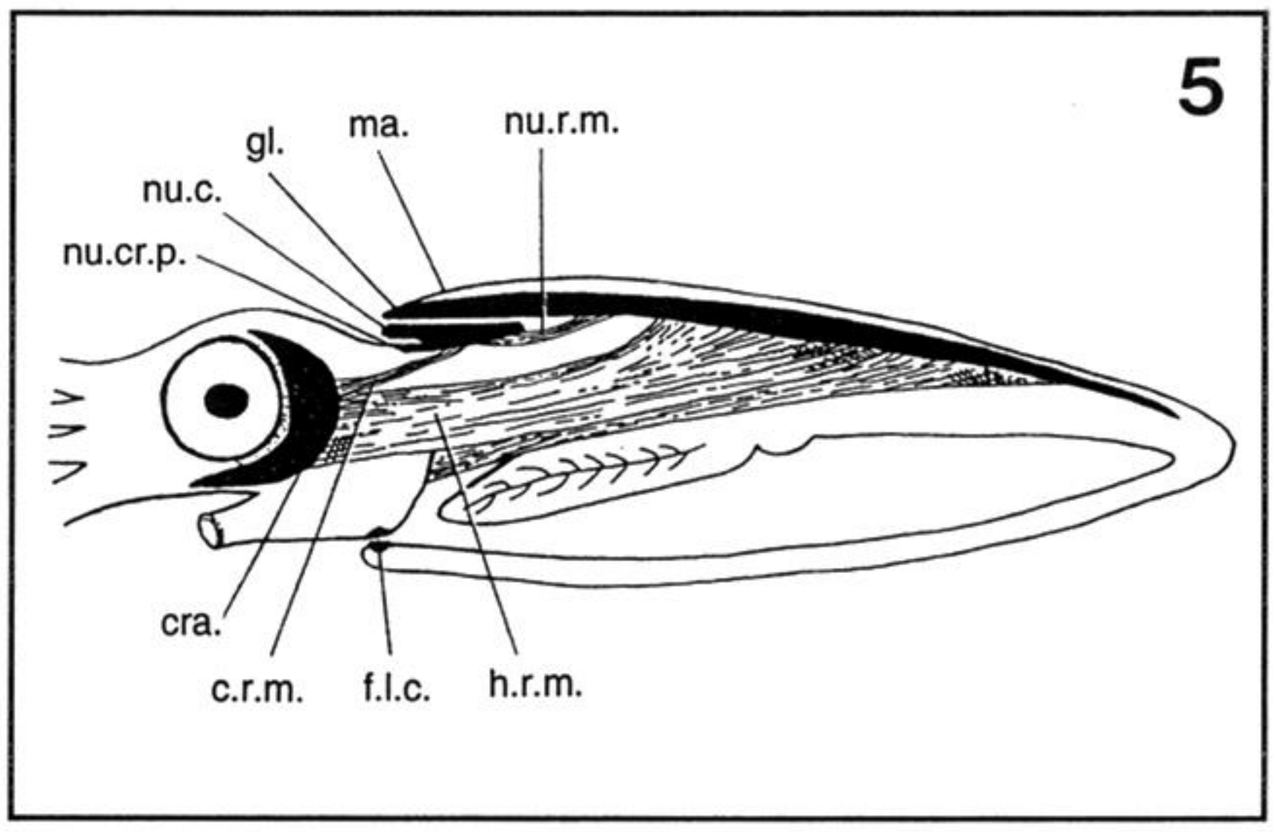

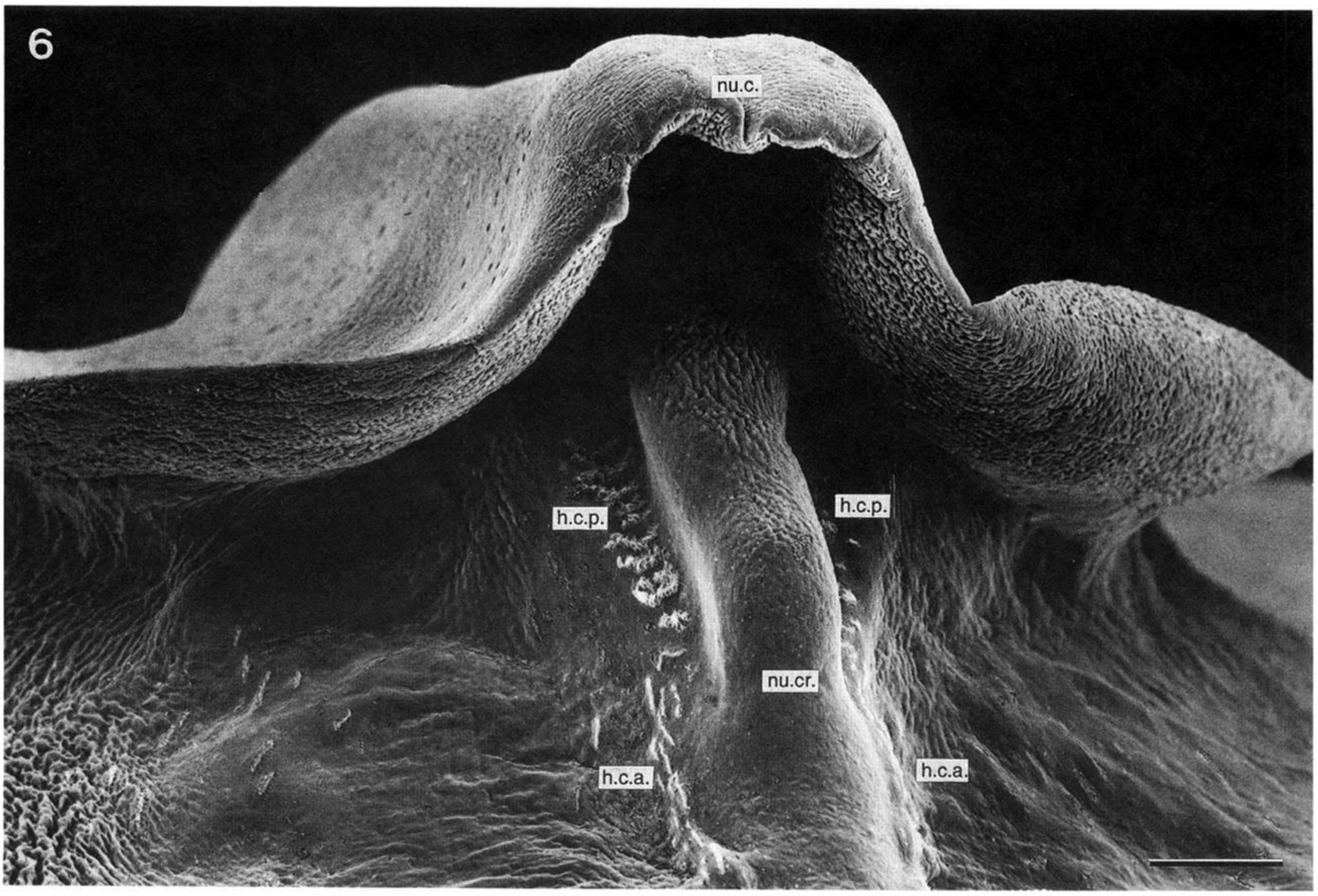

Figure 4. *Lolliguncula brevis* (mantle length 60 mm) during prey fixation. The arrow indicates the location of the neck receptor organ.

Figure 5. Diagram of *Lolliguncula brevis*. Lateral view to show the head–neck cartilages and associated muscles (modified after Wells 1988).

Figure 6. The dorsal neck region (nuchal cartilage complex) with the neck receptor organ of *Lolliguncula brevis* (the mantle is removed). The anterior and posterior hair cell groups of the neck receptor organ are situated on either side of the nuchal crest; they are covered by the nuchal cartilage. (Note that the anterior edge of the nuchal cartilage is bent upwards owing to fixation). Scale bar 100 μm.

Figure 7. Transverse section of the nuchal cartilage complex (the mantle is removed). The asterisks (*) indicate the lateral connective tissue connections between the nuchal crest plate and the nuchal cartilage. Scale bar 100 μm.

Figure 8. Diagram of a transverse section through the neck region of *Lolliguncula brevis* (modified after Mangold *et al.* 1989).

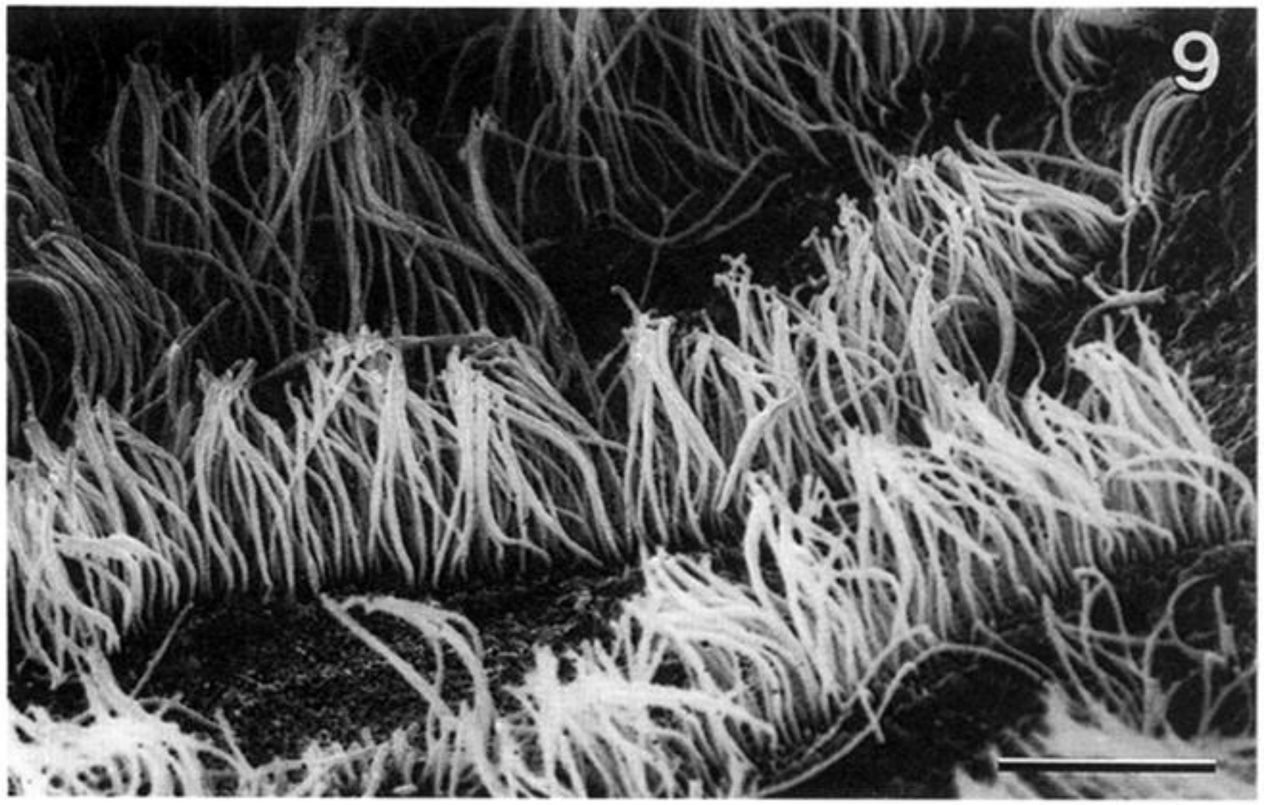

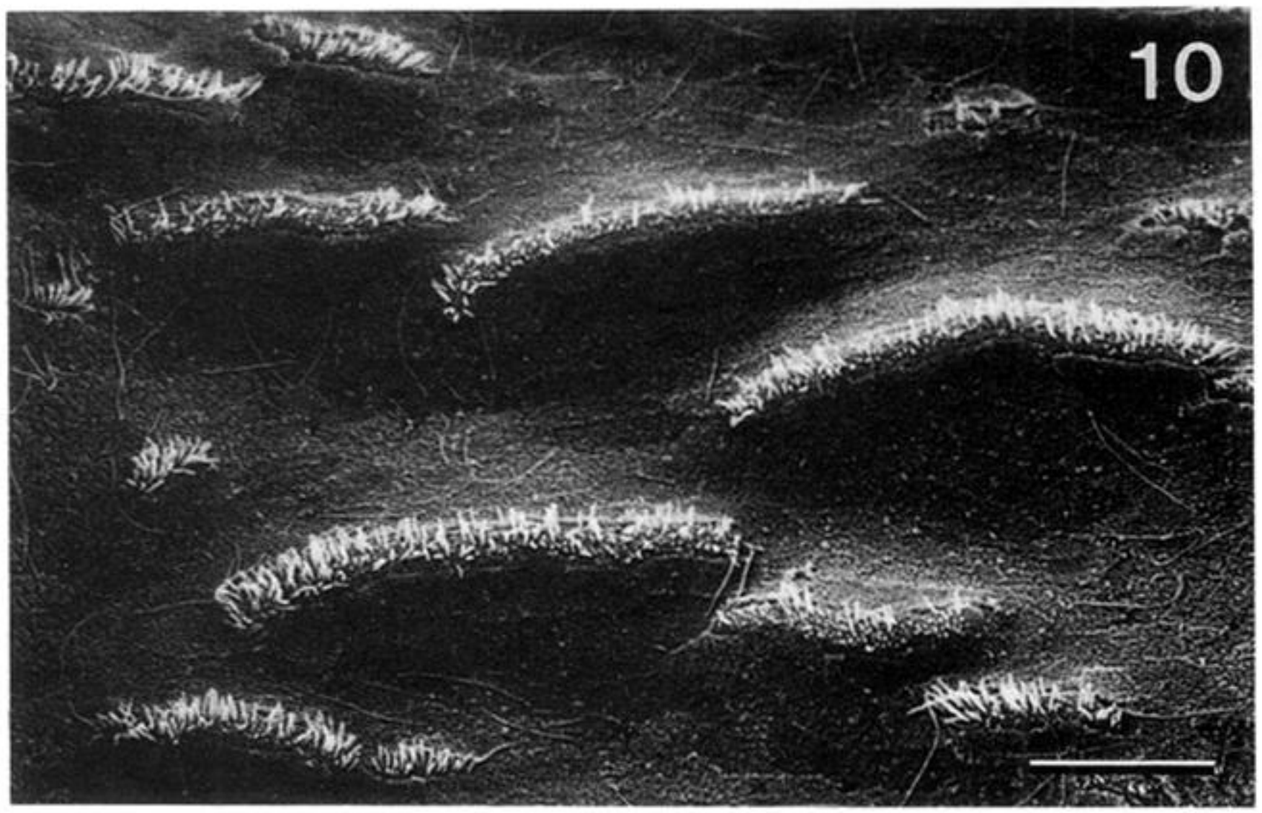

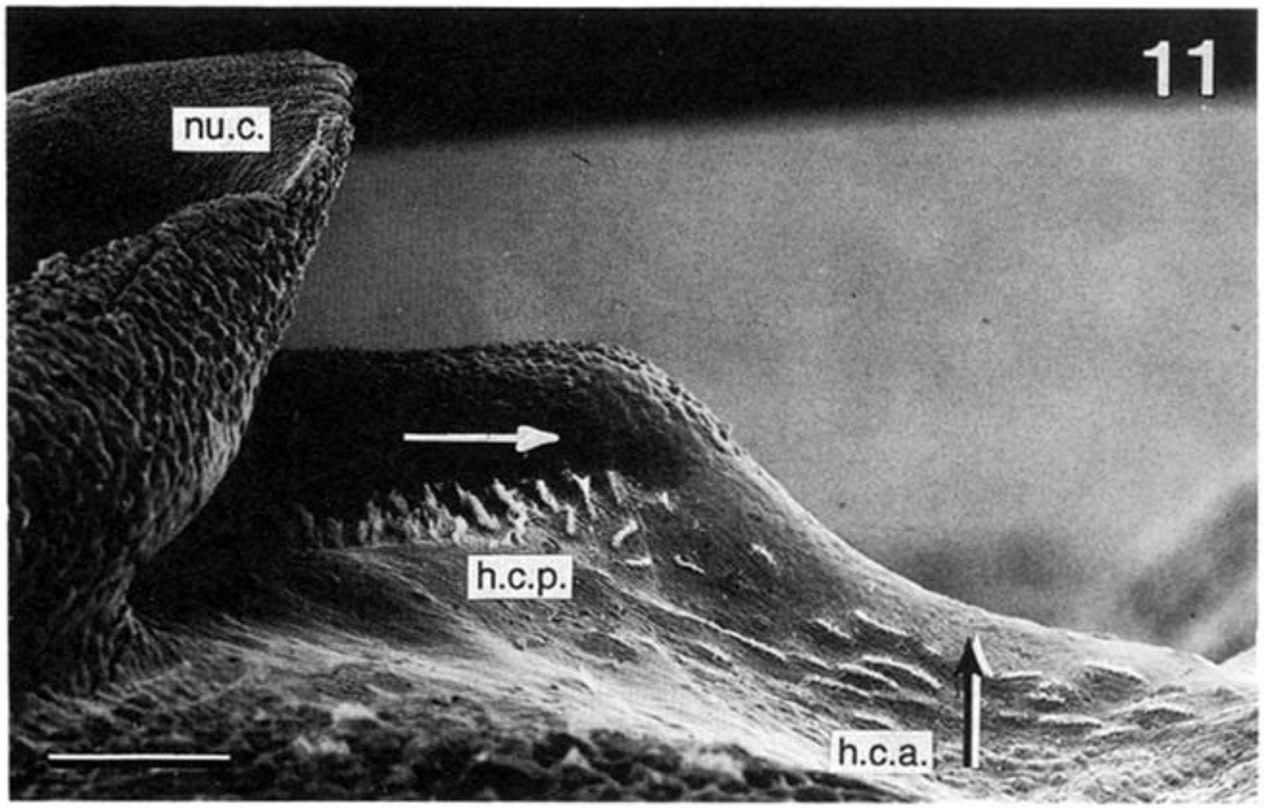

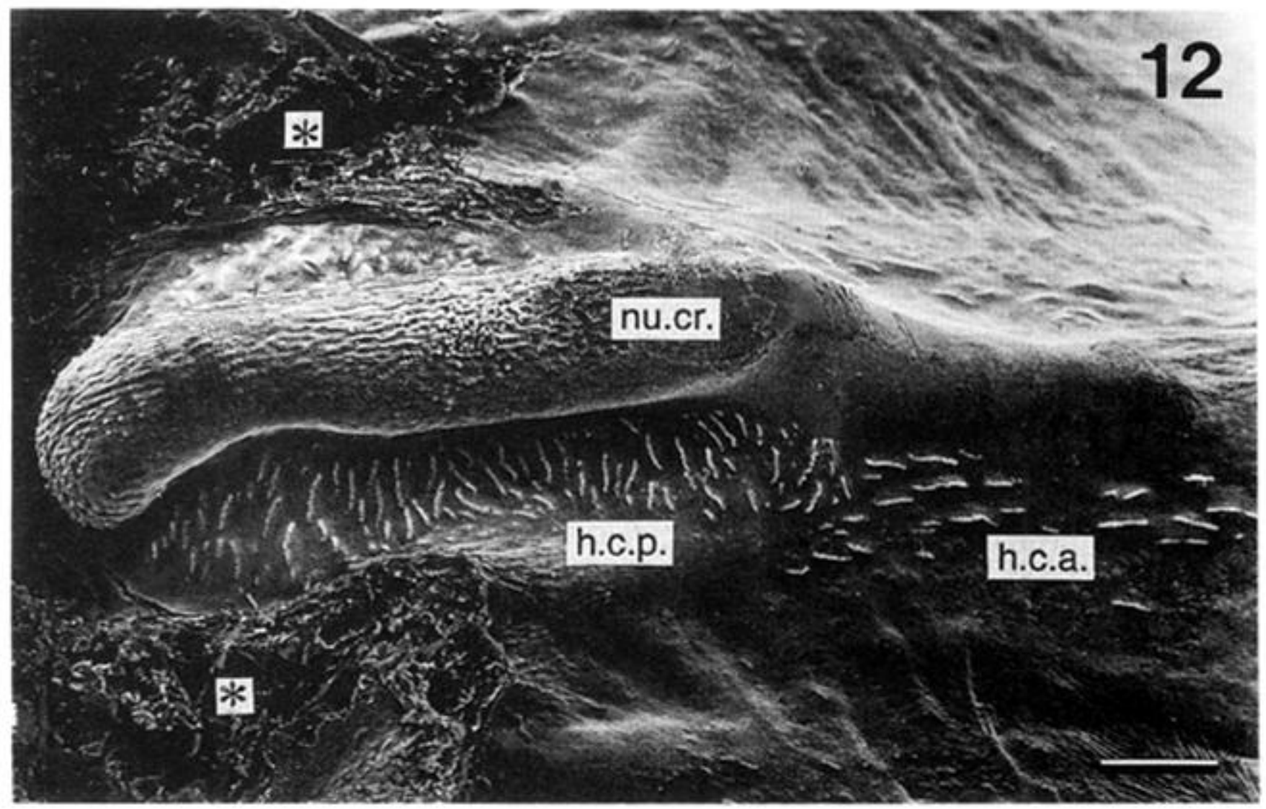

Figure 9. Ciliary bundles of the hair cells of the neck receptor organ with up to 300 kinocilia per cell. Scale bar 10 µm.

Figure 10. Variations in size of the ciliary bundles of the hair cells. (Note that in this preparation the kinocilia are broken off, presumably during the SEM preparation procedure). Scale bar 20 µm.

Figure 11. Direction of morphological polarization of the hair cells of the neck receptor organ (lateral view of the right side; anterior is to the right). The hair cells of the anterior group are polarized in the medial direction and the hair cells of the posterior group in the anterior direction (arrows). Scale bar 100 µm.

Figure 12. Anterior and posterior hair cell groups of the neck receptor organ; dorsal view of the nuchal crest plate (the nuchal cartilage is removed). The asterisks (*) indicate the areas where the connection between the nuchal crest plate and the nuchal cartilage was cut. Scale bar 100 µm.

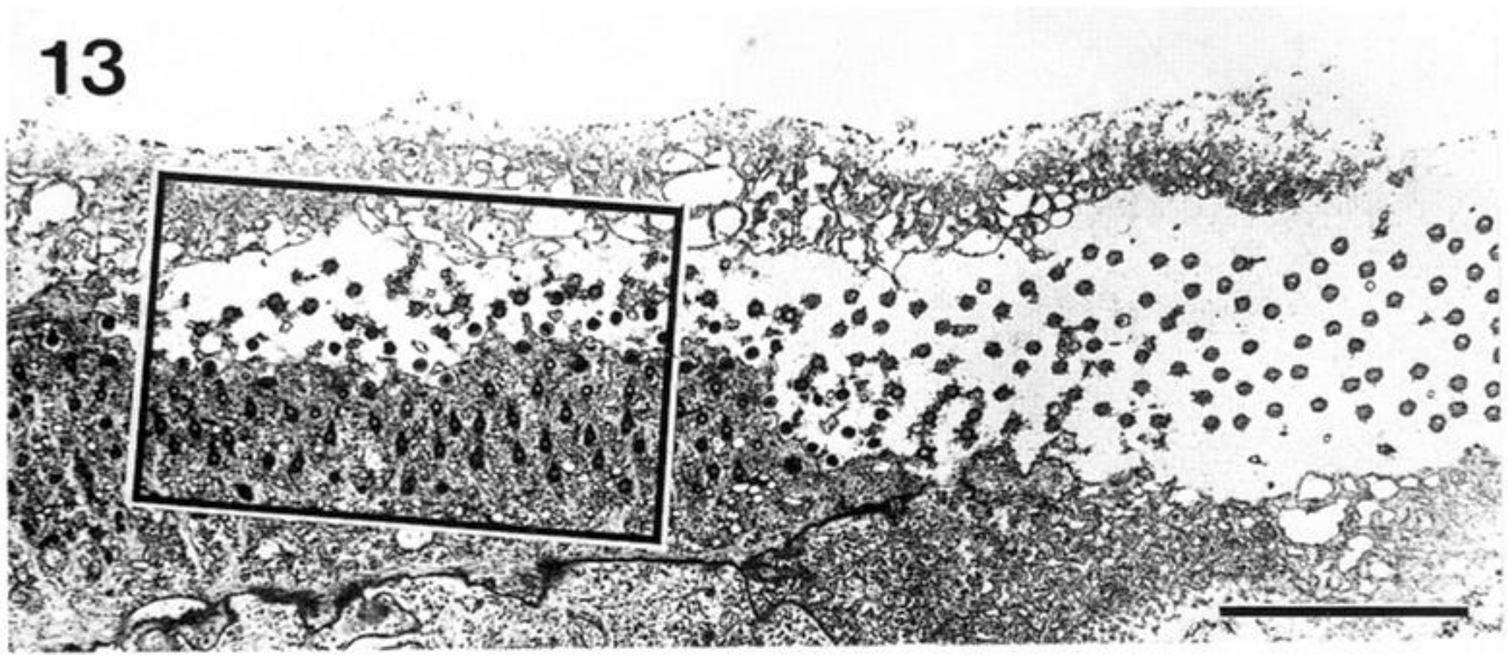

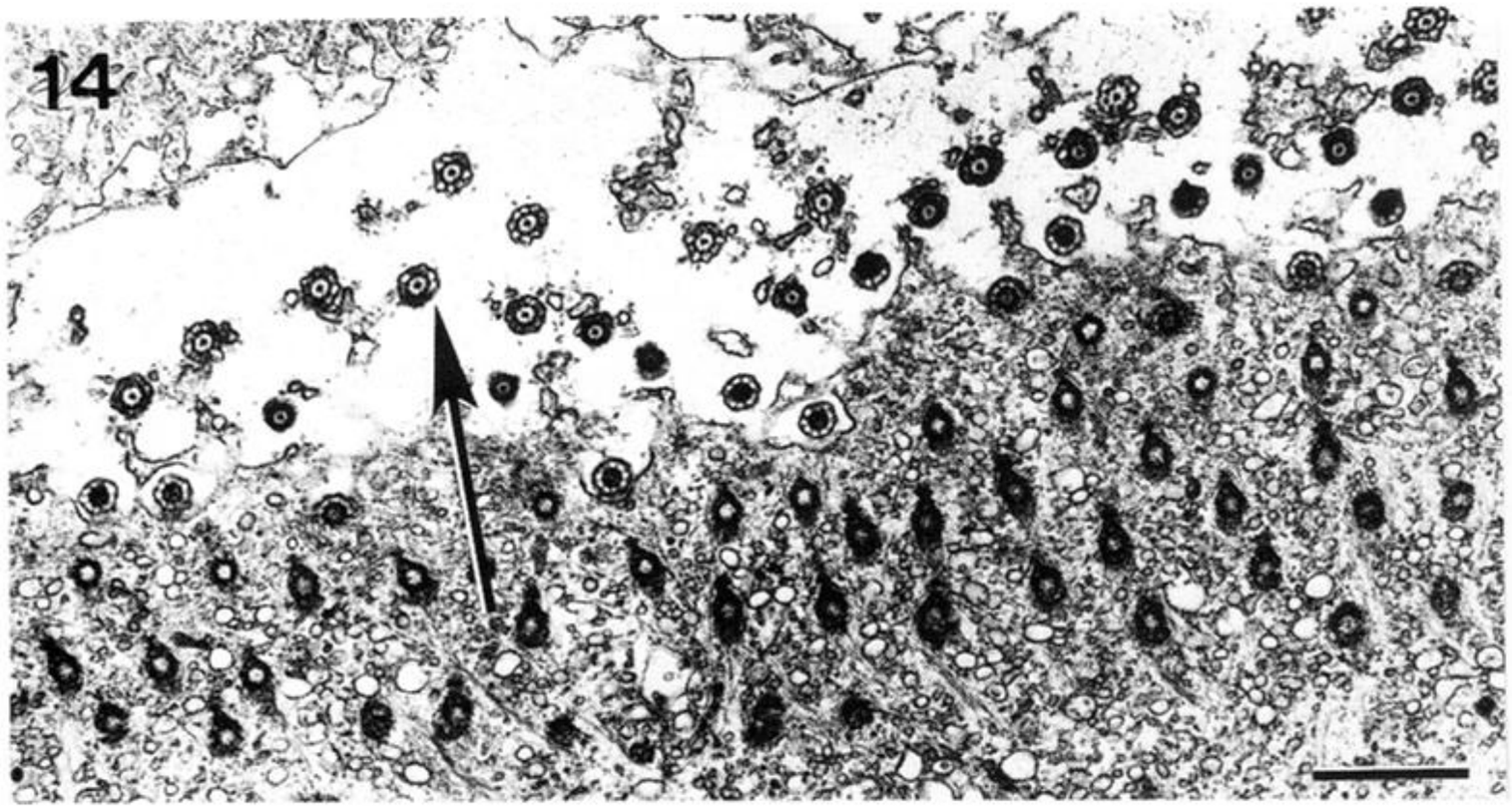

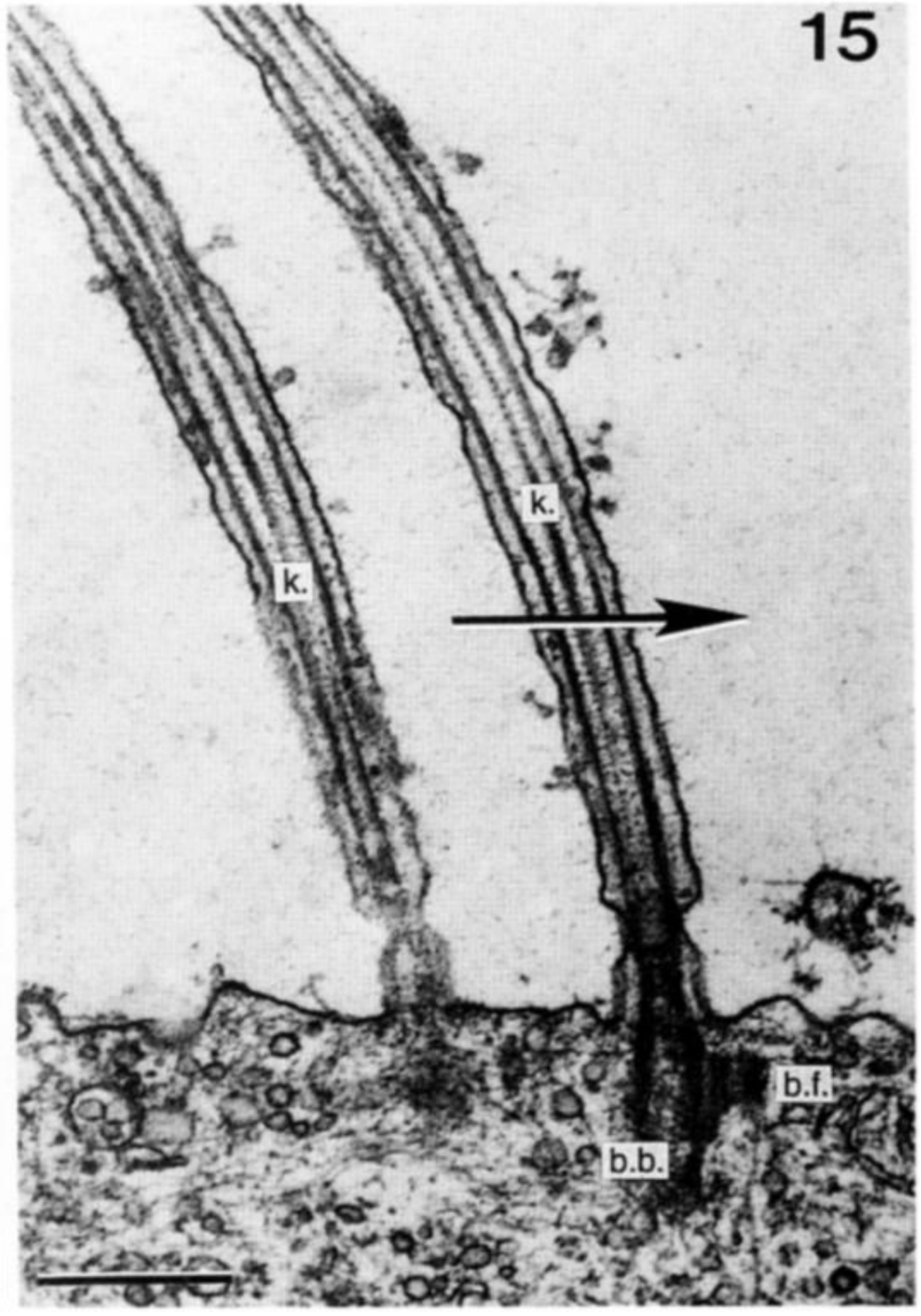

Figures 13 and 14. Cross sections through the distal part and kinocilia of a hair cell of the posterior hair cell group. Figure 14 is a magnification of the area outlined in figure 13. Note the uniform orientation of the basal feet, which defines the direction (arrow) of morphological polarization. Scale bars 5 μm (figure 13) and 1 μm (figure 14).

Figure 15. Transverse section through the elongated kinociliary group of a neck hair cell to show the inclination of the cilia towards the surface of the epithelium and the orientation of their basal feet. The arrow indicates the direction of morphological polarization of the cilia and thus that of the hair cell. Scale bar 0.5 μm.

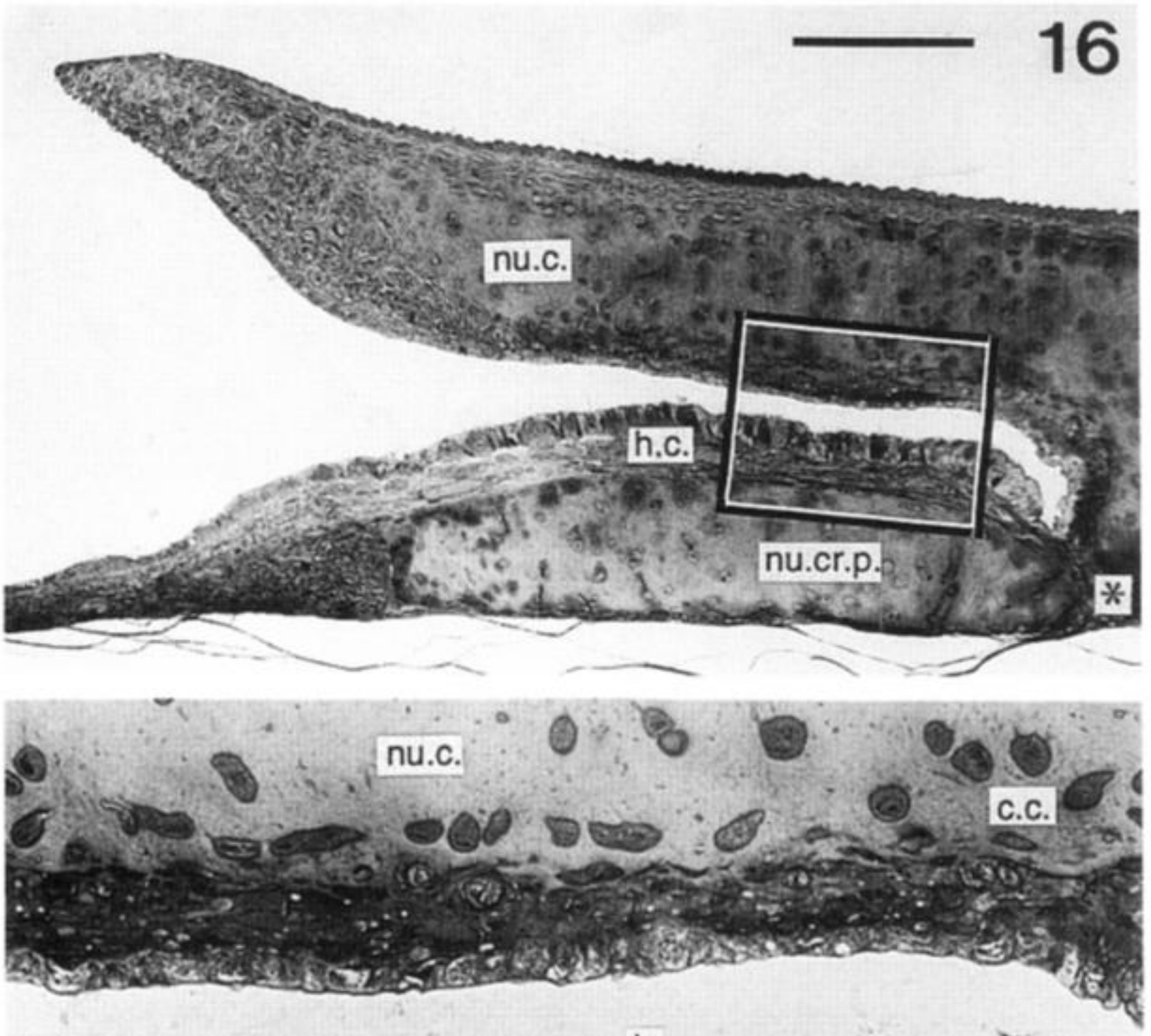

Figure 16. Sagittal section through the neck receptor organ (lateral to the nuchal crest) to show the location of the hair cell epithelium between the nuchal cartilage and the nuchal crest plate. Note that the increasing distance between the anterior part (to the left) of the nuchal cartilage and the epithelium is a fixation artefact. Scale bar 200 µm.

Figure 17. Magnification of the area outlined in the figure 16. Note that in unfixed tissue the tips of the cilia most likely are in contact with the overlying nuchal cartilage. Scale bar 50 µm.

Figure 18. Horizontal section (slightly oblique) through the posterior part of the nuchal crest and nuchal crest plate to show the parallel arrangement of the ciliary bundles of the posterior neck hair cells of the left and right side (posterior is to the top). Scale bar 100 µm.

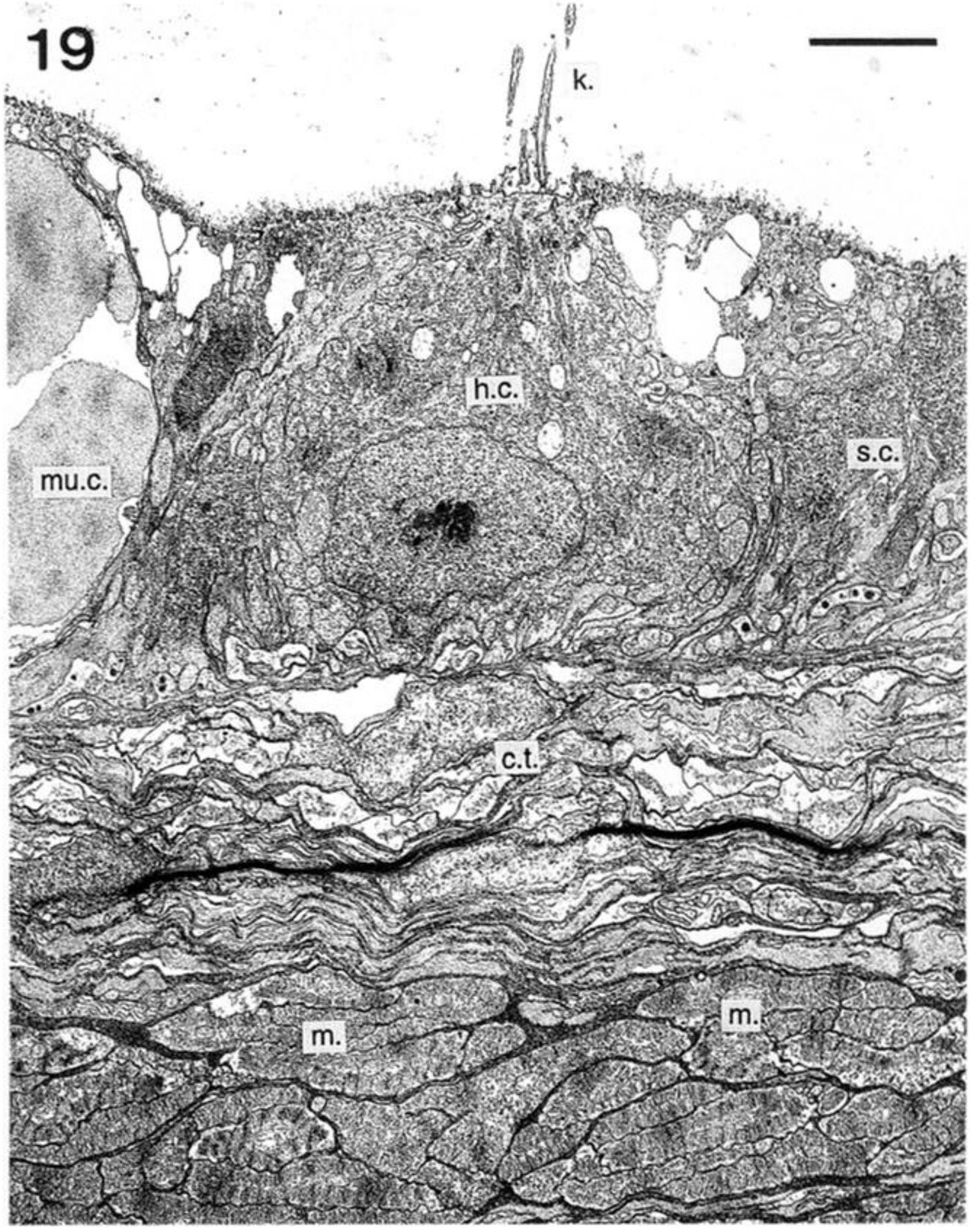

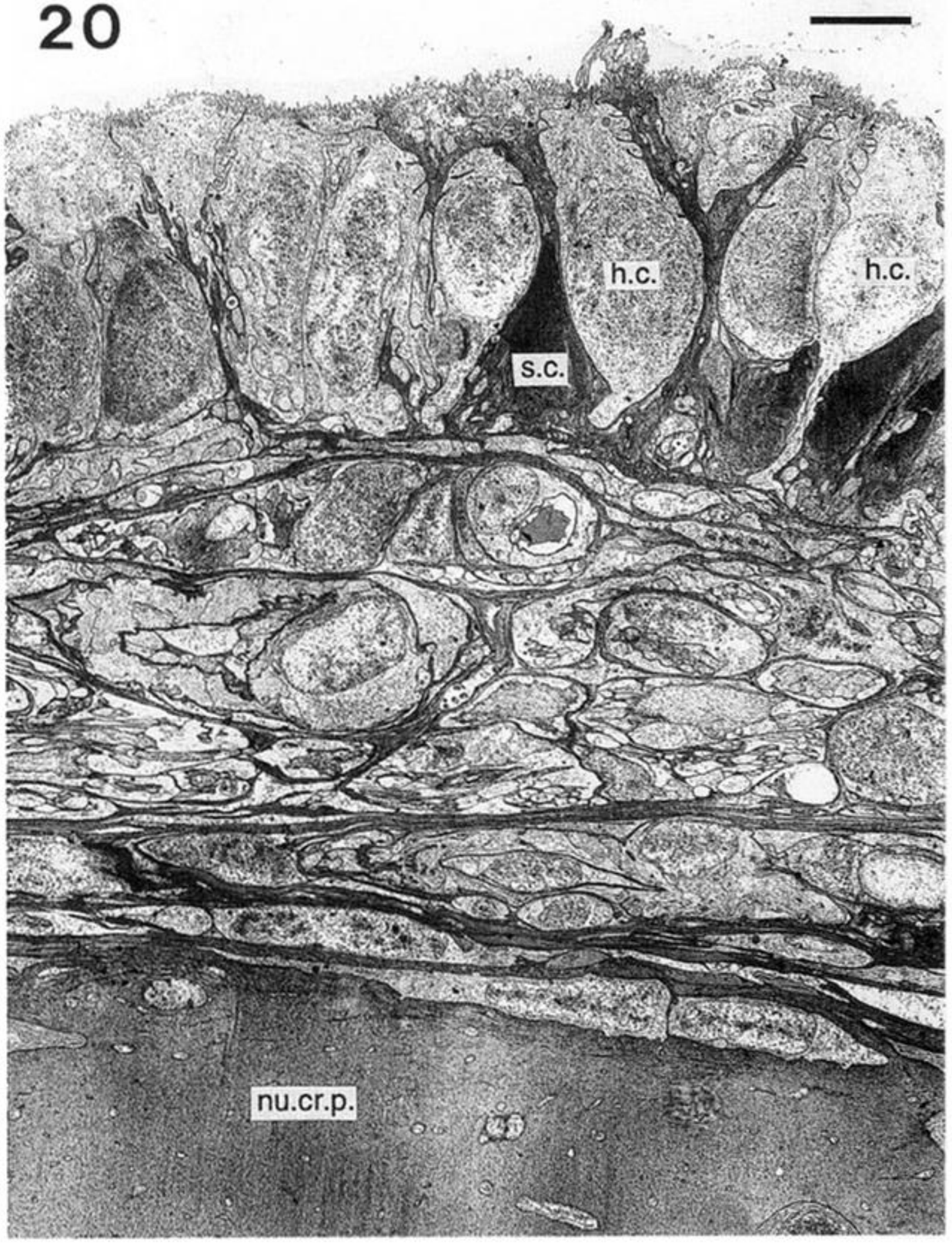

Figure 19. Transverse section through the epidermis of the anterior hair cell group, showing the epithelium with hair cells, mucus cells and supporting cells. Note the thick layers of connective tissue and muscle fibres below the epithelium. Scale bar 5 µm.

Figure 20. Transverse section through the epidermis of the posterior hair cell group, showing the epithelium with hair cells and supporting cells. Note the cartilage of the nuchal crest plate below the epithelium. Scale bar 10 µm.

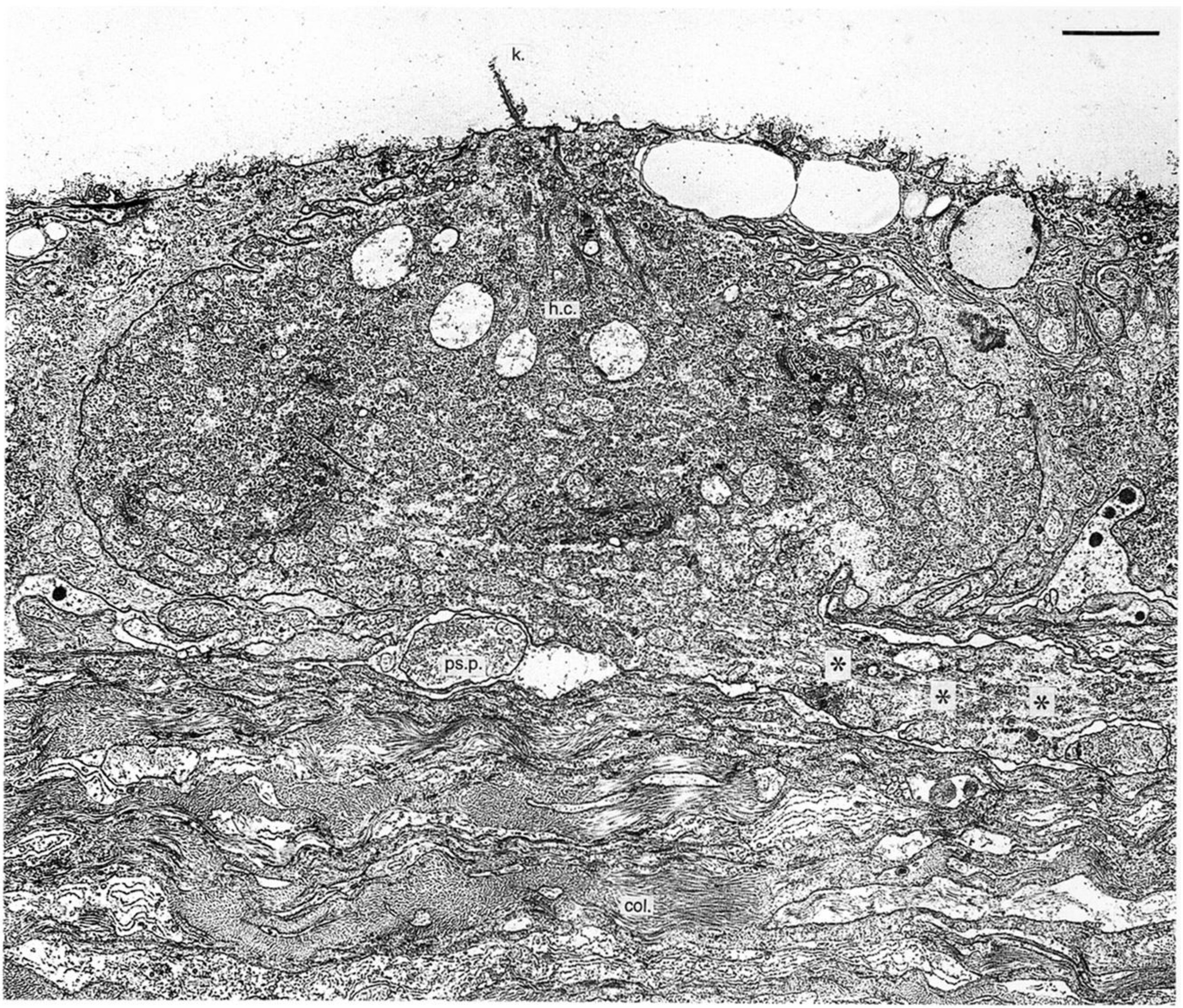

Figure 21. Transverse section through a hair cell of the anterior hair cell group. Note the axon leaving the hair cell (asterisks) and a large presynaptic profile below the hair cell. Scale bar 3 μm.

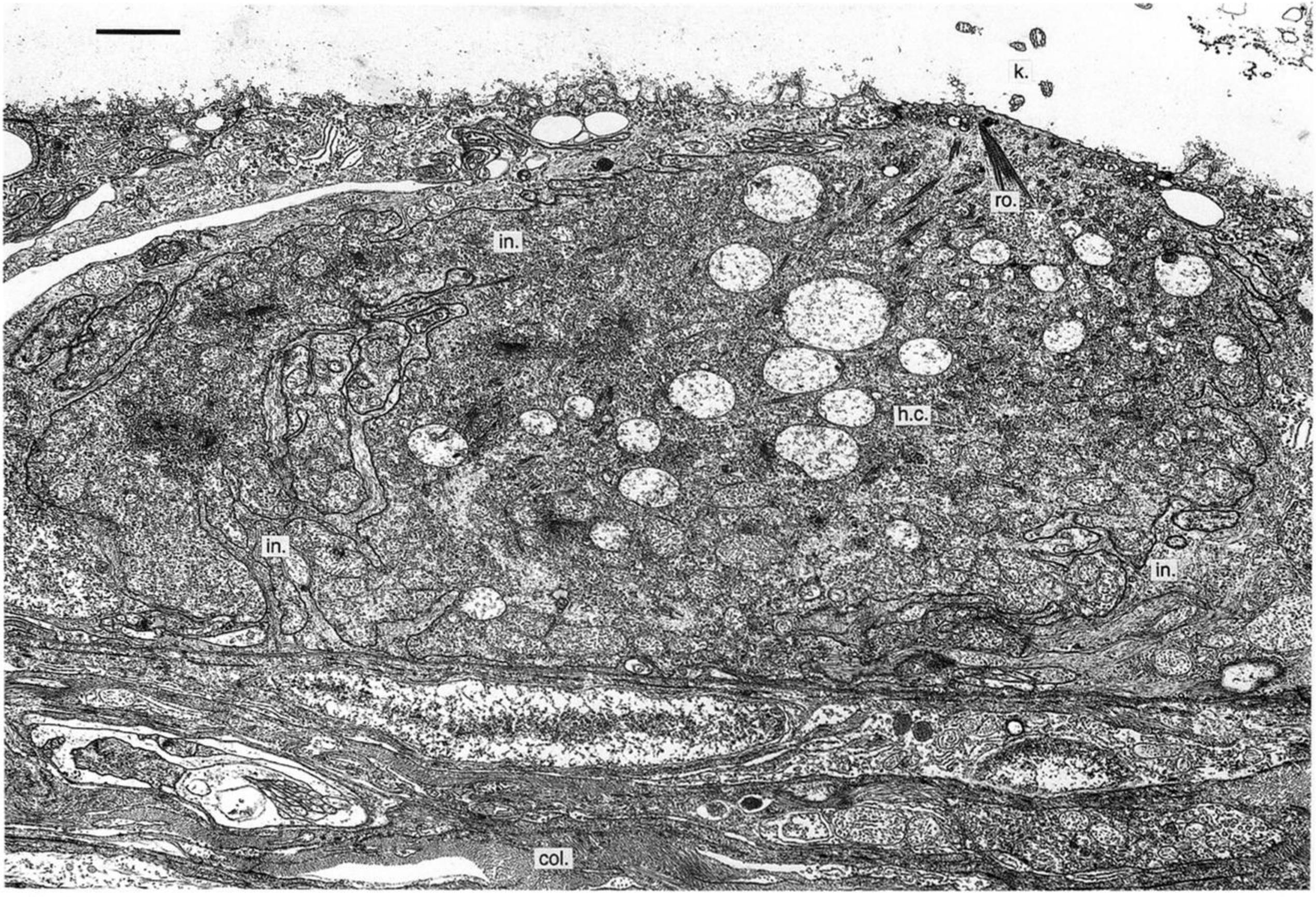

Figure 22. Transverse section through a hair cell of the anterior hair cell group, showing the well-developed interdigitations with the neighbouring supporting cells. Scale bar 2 μm.

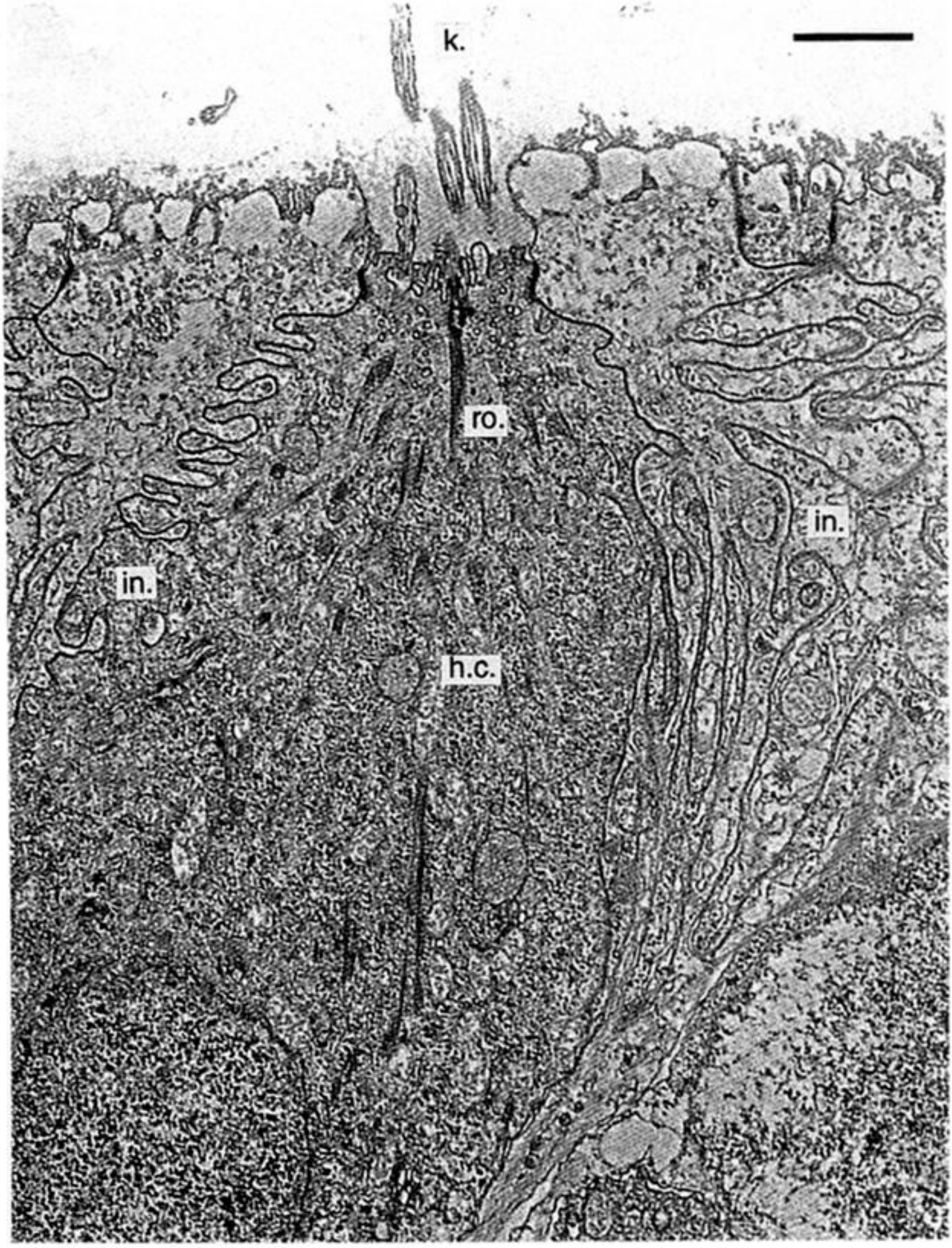

Figure 23. Transverse section through the distal parts of hair and supporting cells of the posterior hair cell group, showing their heavy interdigitations. Scale bar 1 μm.

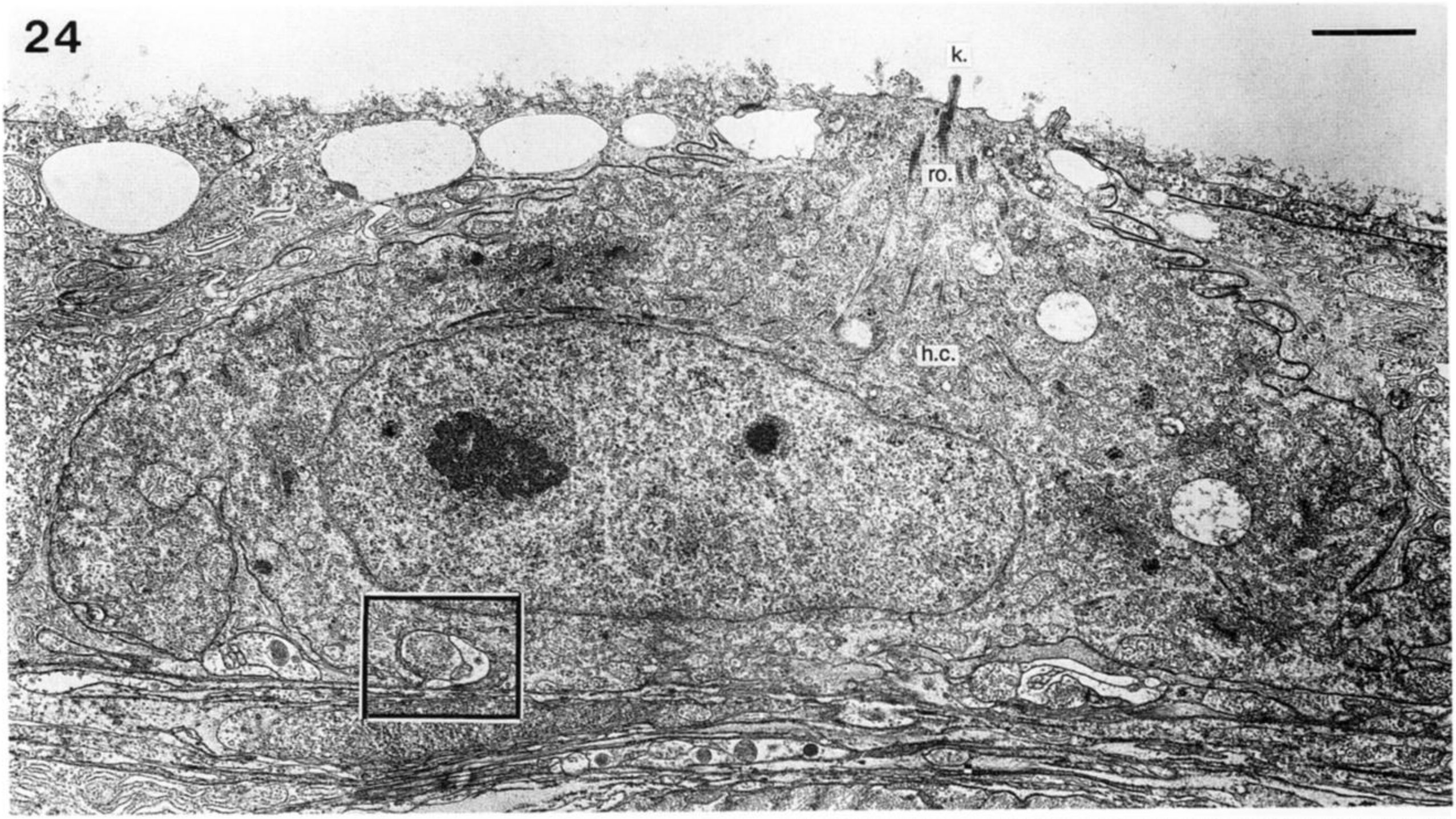

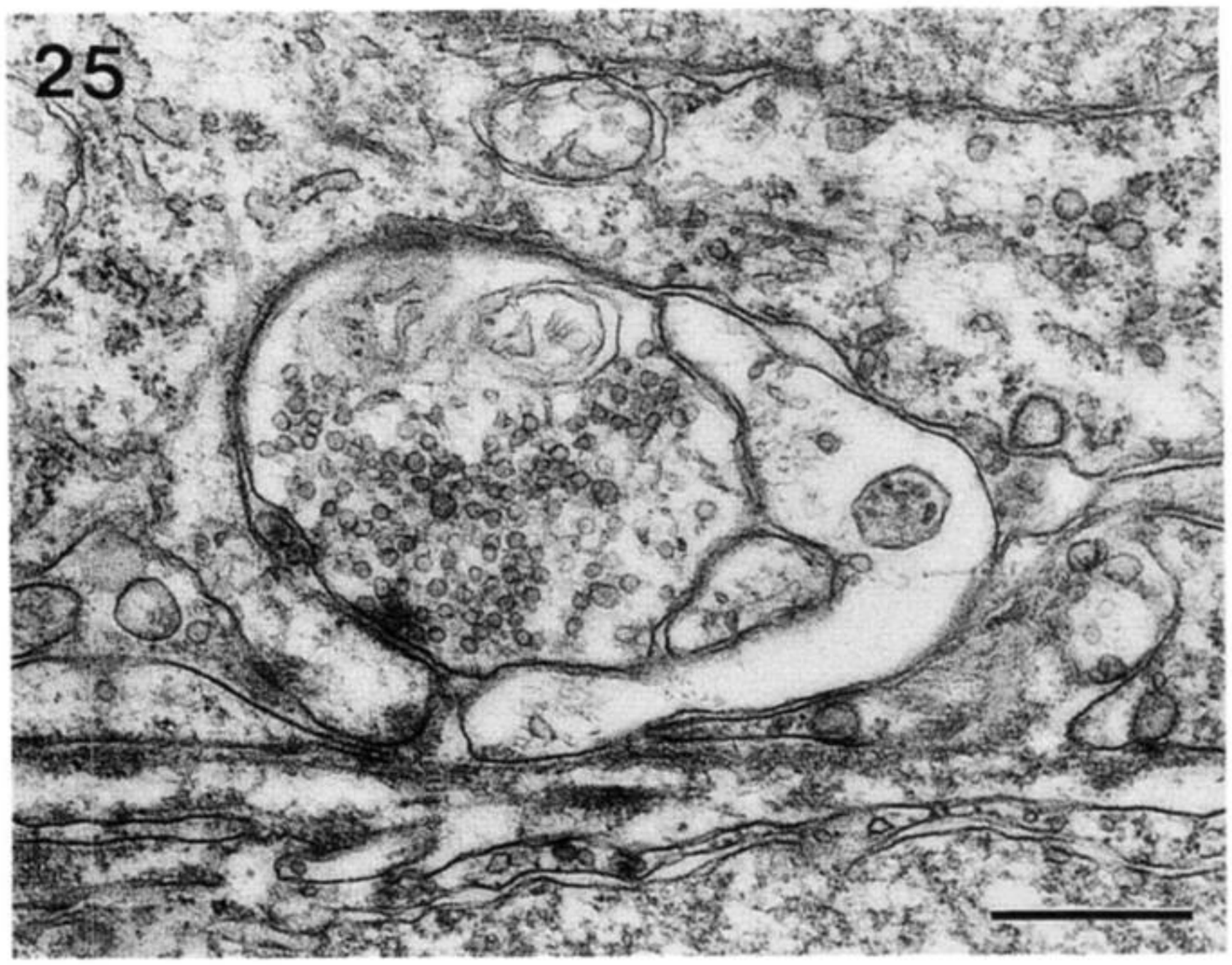

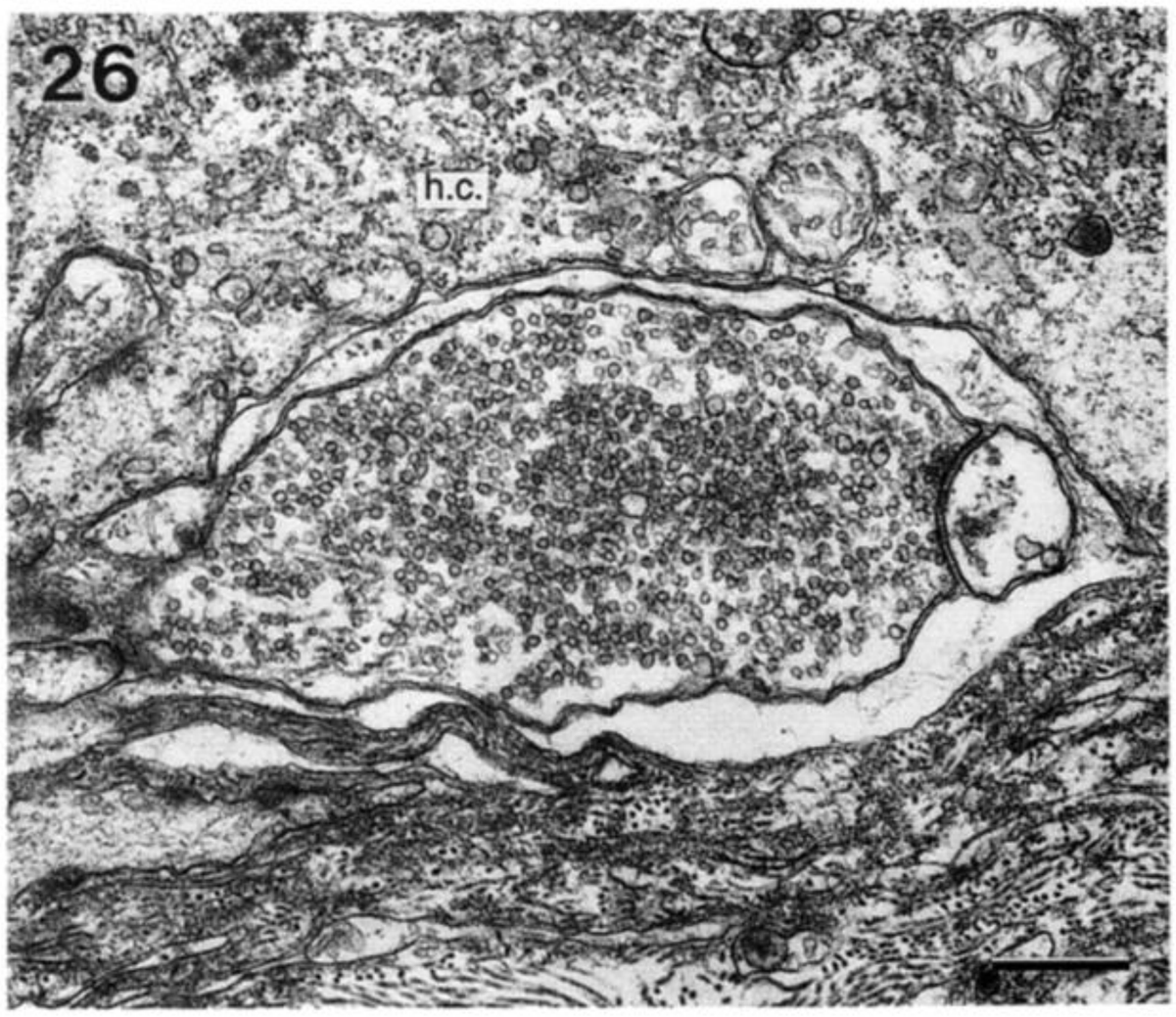

Figures 24–26. Efferent innervation of the hair cells of the neck receptor organ. Transverse section through a hair cell of the anterior hair cell group (figure 24), with a vesicle-filled efferent profile at its base that makes synaptic contact with the hair cell (figure 25; higher magnification of the area outline in figure 24). Figure 26 shows a large efferent profile with a uniform population of small, clear synaptic vesicles. Scale bars 2 μm (figure 24) and 0.5 μm (figures 25 and 26).

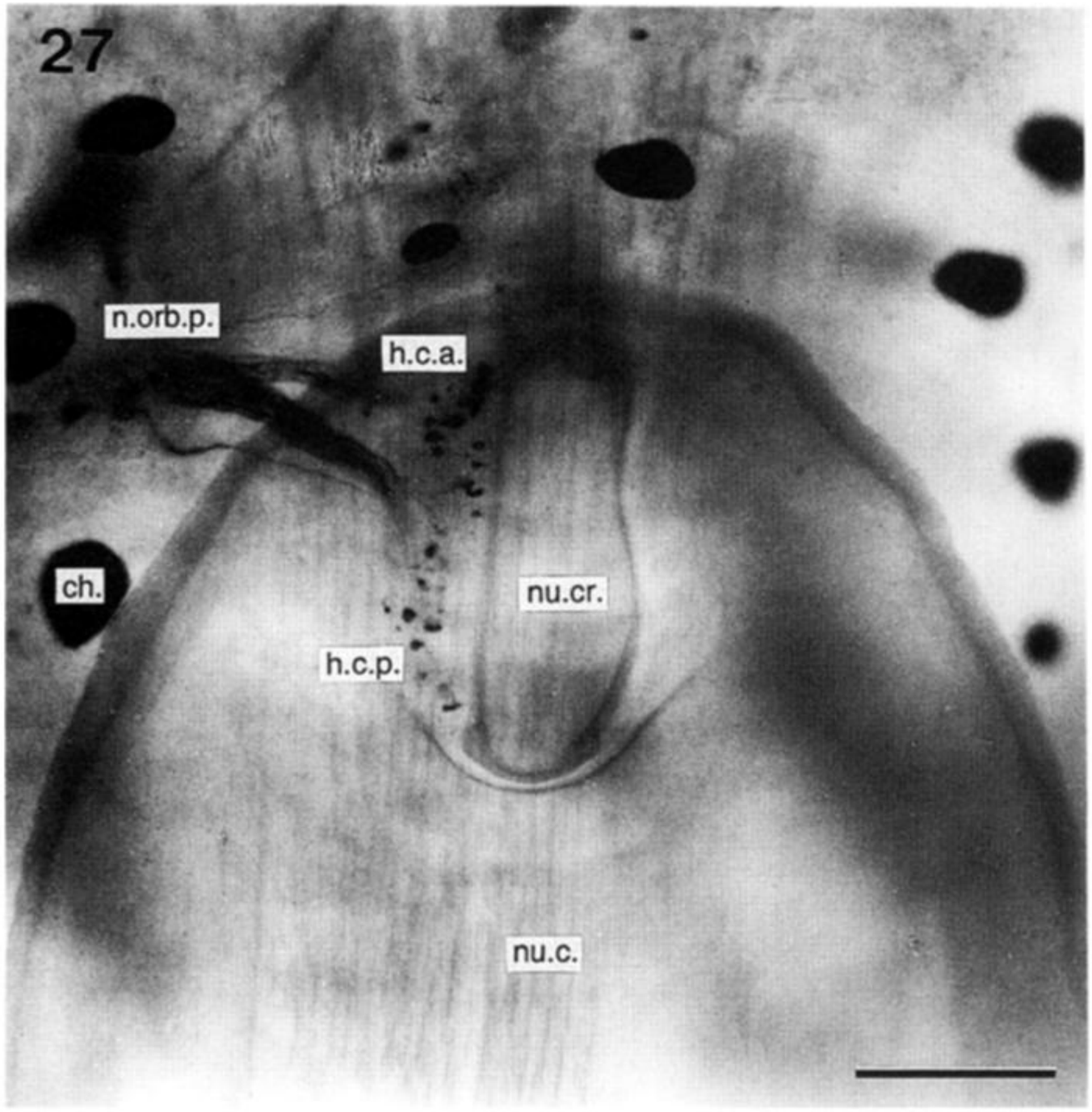

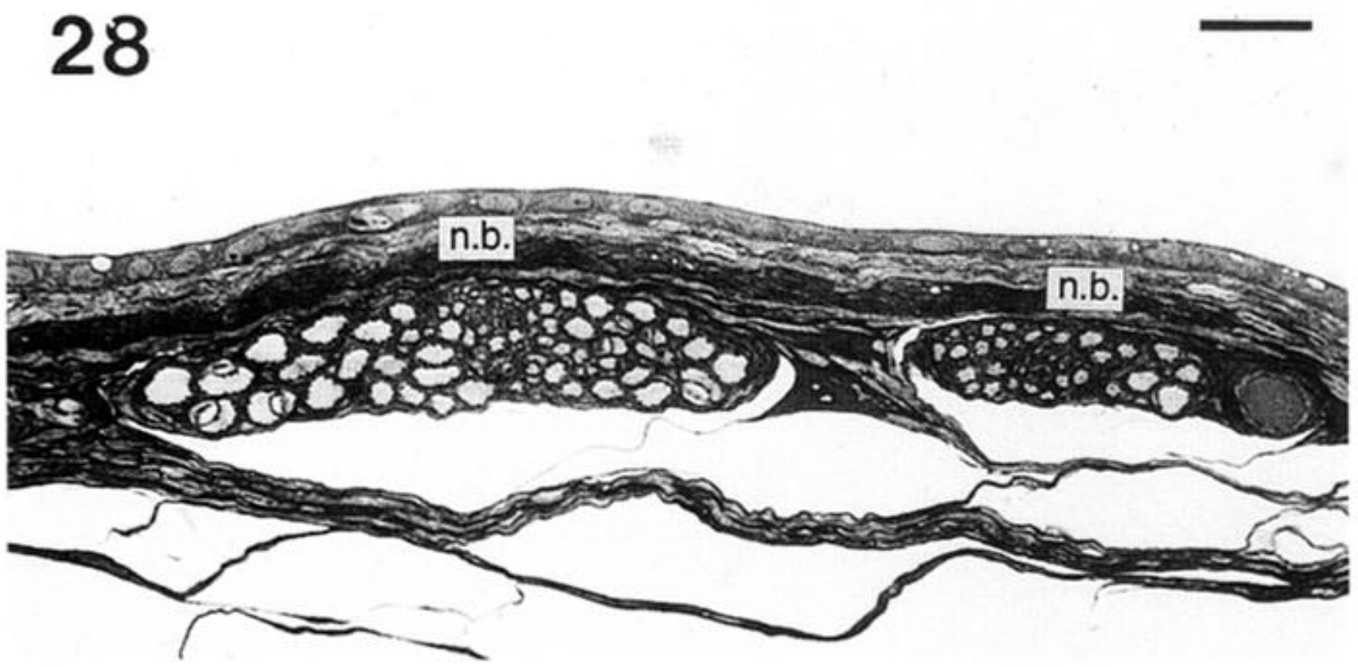

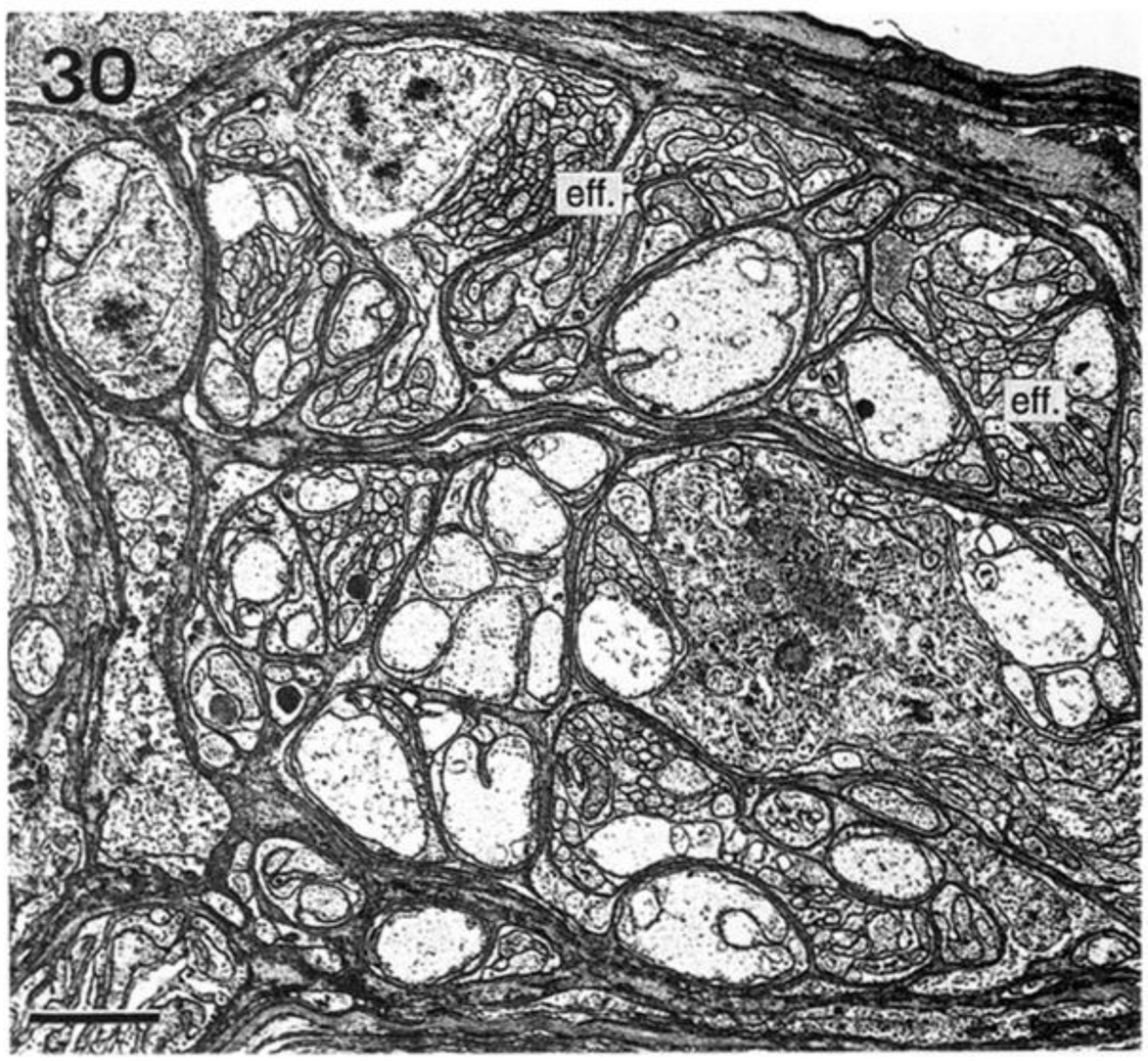

Figure 27. Innervation of the neck hair cells of the neck receptor organ. Dorsal view of the neck region after centrifugal cobalt staining of the left postorbital nerve. The branch that innervates the hair cells divides into two smaller bundles: one innervates the cells of the anterior hair cell groups, and the other those of the posterior groups. Whole mount preparation; anterior is top of page. Scale bar 100 μm.

Figures 28–30. Cross sections at light (figure 28) and electron microscopical level (figures 29 and 30) of the branch of the postorbital nerve that innervates the neck hair cells. Sections were taken at the point where the branch has separated into two smaller bundles. Note the bundles of fine, presumably efferent, fibres (figure 30). Scale bars 20 μm (figure 28) and 2 μm (figures 29 and 30).

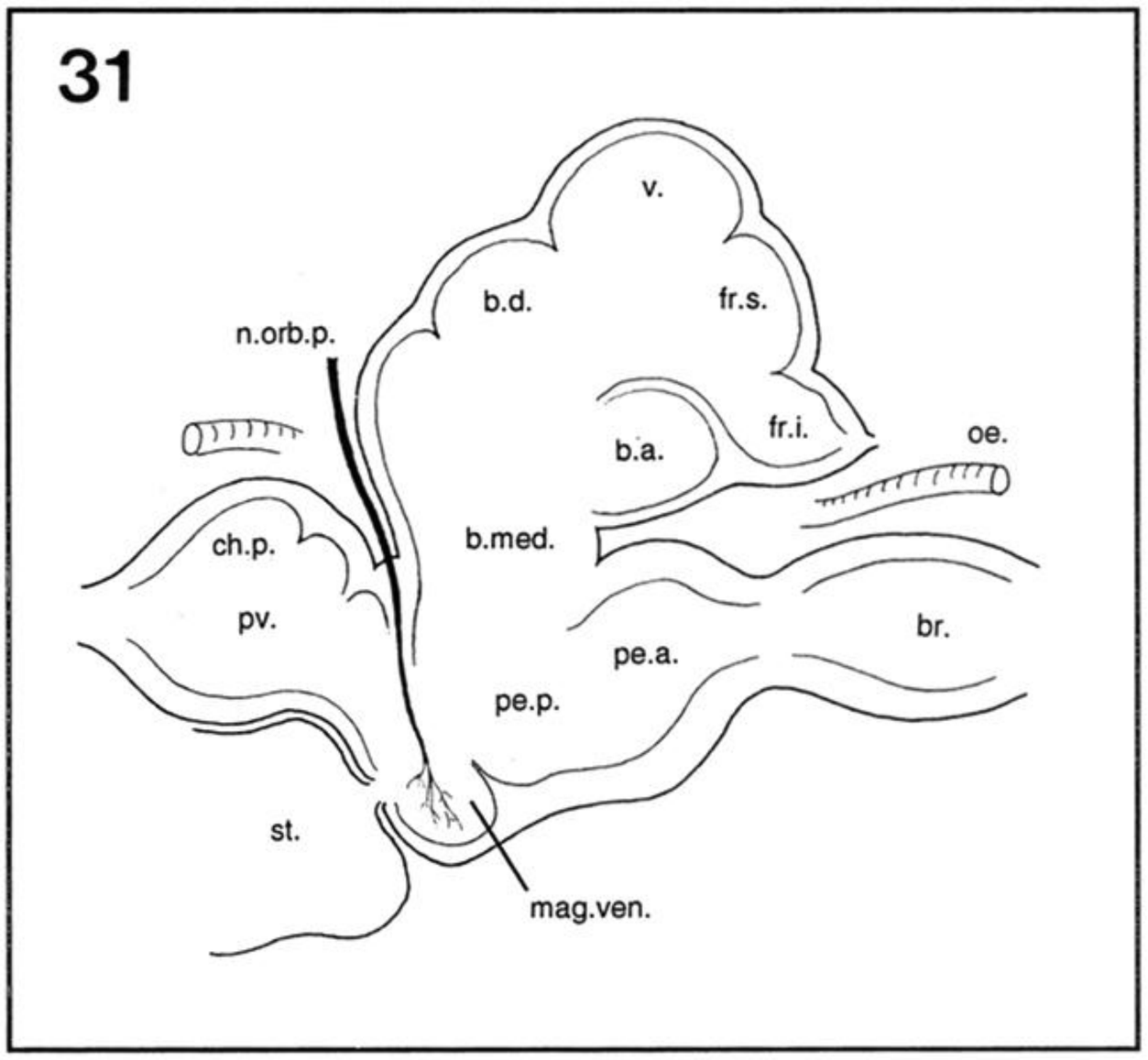

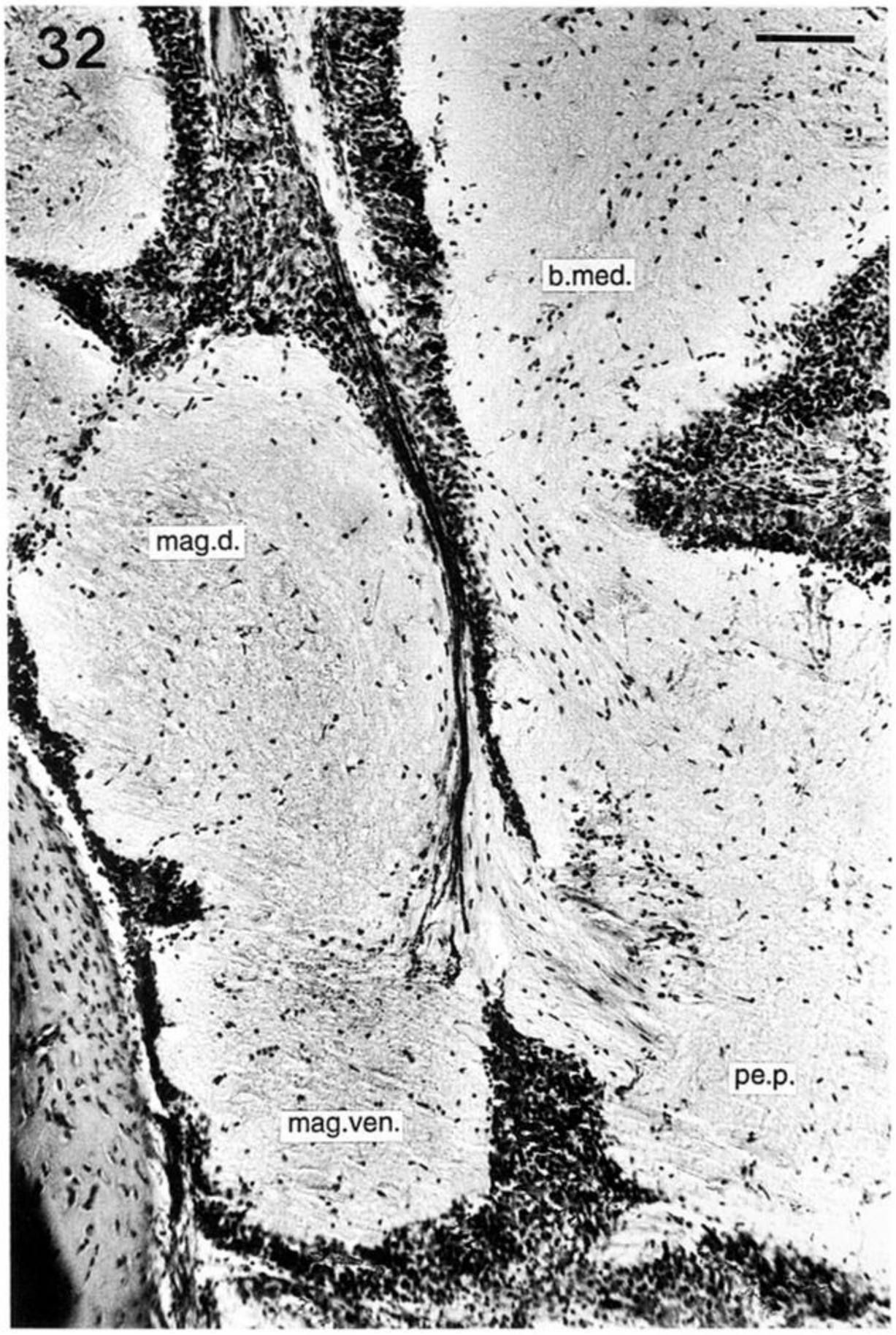

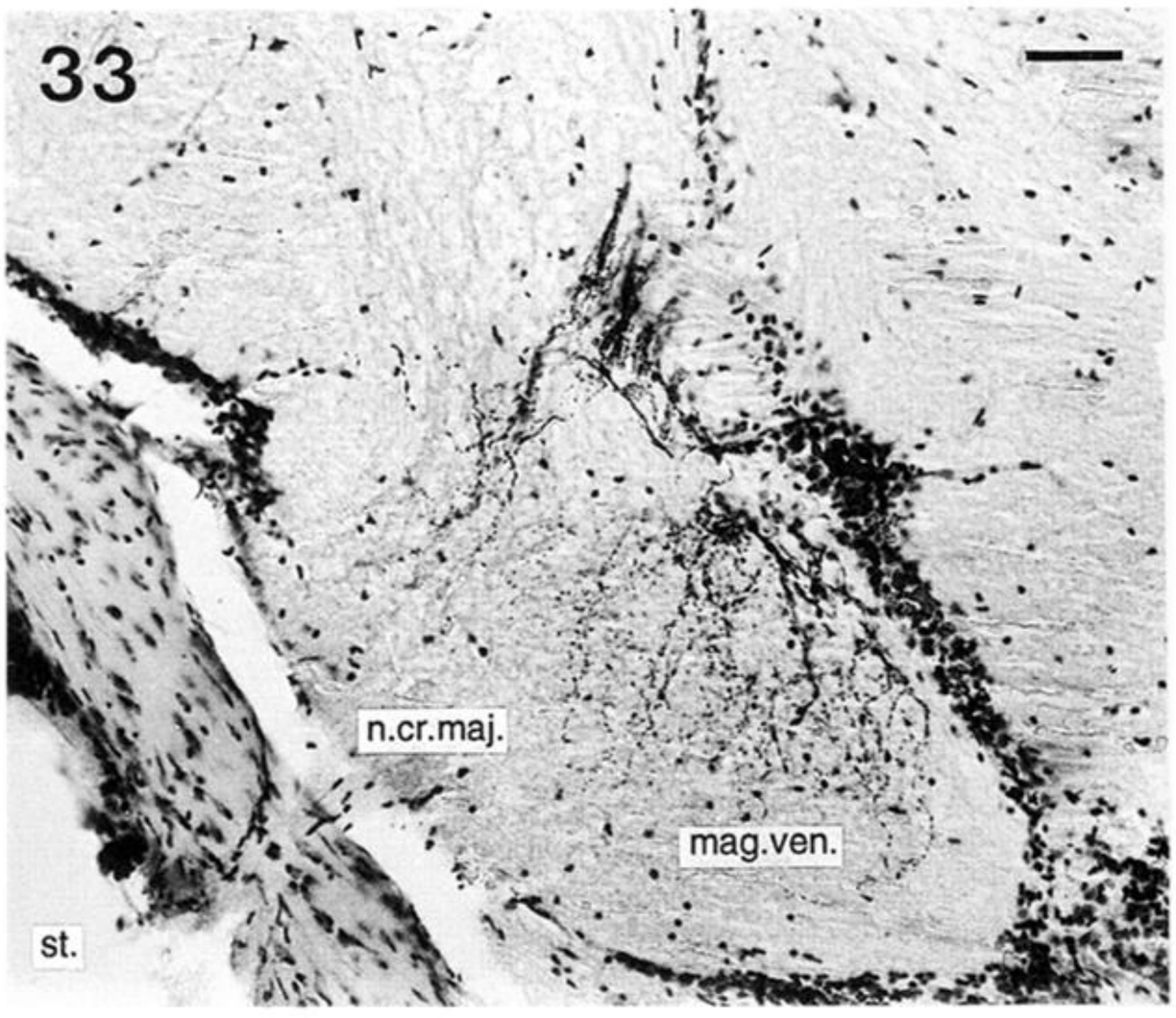

Figure 31. Central projection of the hair cells of the neck receptor organ. Diagram of a sagittal section of the brain of *Lolliguncula brevis*, illustrating the pathway of the hair cells' afferent fibres. The origin of the efferent fibres is still unknown.

Figures 32 and 33. Centripetal cobalt fillings of the branch of the postorbital nerve that innervates the hair cells of the neck receptor organ. Sagittal section of the part of the ventral sub-oesophageal lobes, showing fine afferent fibres running to, and terminating in, the ventral magnocellular lobe. Note the entry of the large crista nerve of the statocyst into that lobe. Scale bars 100 μm (figure 32) and 50 μm (figure 33).